

NITRIC OXIDE INHIBITION OF PLATELET  
DEPOSITION ON BIOMATERIALS

By

ANAND RAMAMURTHI

Bachelor of Engineering  
Bangalore University  
Bangalore, India  
1994

Master of Science  
Oklahoma State University  
Stillwater, Oklahoma  
1996

Submitted to the Faculty of the  
Graduate College of the  
Oklahoma State University  
in partial fulfillment of  
the requirements for  
the Degree of  
DOCTOR OF PHILOSOPHY  
July, 1999

NITRIC OXIDE INHIBITION OF PLATELET  
DEPOSITION ON BIOMATERIALS

Thesis Approved:

*Randy S. Lewis*

Thesis Adviser

*Douglas J. ...*

*Kevin A. ...*

*K. D. Berlin*

*Wayne B. Powell*

Dean of the Graduate College

## ACKNOWLEDGEMENTS

My humble salutations and surrender to God Almighty for showering me with abundant happiness in life, for giving me good judgement, and blessing me with a wonderful family. This dissertation is dedicated to my family- my parents Meena and V. Ramamurthi, my brother Raj, and my sister-in-law Priya. None of this work would have been even remotely possible, but for their boundless love, guidance, and support over the years. Their constant encouragement has been my principal motivation towards completion of this degree. I would like to profoundly thank my advisor, Dr. Randy S. Lewis for providing me the very best education a student could aspire for. He has been a tremendous inspiration and a role model for aspiring Ph.Ds like myself. I thank him for his mentoring, encouragement, for all the professional opportunities he provided me. I thank him and the Department of Chemical Engineering for financially supporting me during the course of my doctoral degree. I am grateful to Drs. Karen A. High, Gary L. Foutch, and K. Darrell Berlin for serving on my dissertation committee, and for their interest in my research. I would also like to acknowledge Mr. Charles Baker and the staff of Chemical Engineering for their help over the years.

Alice Briggs, Mary Stollings, Pat Elsener, Pam Ledford, and Tommy Mrosek at the Student Health Center have been wonderful friends who often selflessly volunteered blood samples for use in my research. I shall ever be grateful to them. I would like to acknowledge Dr. Robert P. Wettemann and LaRuth Mackey at the Department of Animal Sciences for their help and for the use of their facilities. I am sincerely appreciative of Dr. Simon Robson at Harvard Medical School, and Dr. David Janero at NitroMed, Inc.,

both at Boston, MA, for their mentoring, professional and personal advice, as well as for serving as my references.

Finally, I would like to thank my friends Mahesh, Shankar, Rajesh, Rajesh Kumar, Shravan, Amit, Sheetal, Ravi, Partha, Usha, Mohini, Siva, and Lakshminarayanan for their affection and steadfast support. Their frequent calls and mails often bolstered me during my bleakest moments. Mahendra, Xunbao, Srinivasan, and Chun will be fondly remembered as great friends and co-workers. I am hugely indebted to all my blood donors without whose selfless help, progress on my research would have been impossible.

## TABLE OF CONTENTS

Chapter	Page
1. INTRODUCTION.....	1
1.1 <i>In vivo</i> anti-thrombotic mechanisms.....	3
1.1.1 Mechanism I: Endothelium-derived relaxing factor/Nitric oxide.....	4
1.1.2 Mechanism II: Ecto-nucleotidases.....	6
1.1.3 Mechanism III: Eicosanoids.....	6
1.2 Physiological roles of NO.....	8
1.2.1 Role of NO in inhibition of platelet aggregation.....	9
1.2.2 Role of NO in vascular regulation.....	9
1.2.3 Role of NO as a neurotransmitter.....	10
1.2.4 Role of NO in immune response mechanisms.....	10
1.2.5 Role of NO in the endocrine system.....	11
1.3 Pathophysiological roles of NO.....	11
1.3.1 Effects of excess NO production.....	12
1.3.1.1 Sepsis/hypotension.....	12
1.3.1.2 Rheumatoid arthritis.....	12
1.3.1.3 Insulin-dependent diabetes mellitus.....	12
1.3.1.4 Tissue damage associated inflammation.....	13
1.3.2 Effects of NO deficiency.....	13
1.3.2.1 Atherosclerosis.....	13
1.3.2.2 Pulmonary hypertension.....	14
1.4 Reactivity and cytotoxicity of NO.....	14
1.4.1 Reaction of NO with O <sub>2</sub> .....	15
1.4.2 Reaction of NO with superoxide.....	16
1.4.3 Reaction of NO with transition metals /metal groups.....	16
1.5 Methods of NO delivery.....	17
1.5.1 Physical method.....	18
1.5.2 Chemical method.....	18
1.6 Nitric oxide inhibition of platelet adhesion and aggregation.....	19
1.7 Thesis objectives.....	20
2. DELIVERY DEVICE DEVELOPMENT AND MODELING.....	22
2.1 Systems for study of platelet-surface interactions.....	22
2.2 Delivery device requirements.....	24

Chapter	Page
2.2.1 Wall shear rates: Physiological implications.....	24
2.3 Description of NO delivery device.....	26
2.4 Nitric oxide delivery model.....	28
2.4.1 Objective.....	28
2.4.2 Continuity equation.....	29
2.4.3 Boundary conditions.....	30
2.4.4 Non-dimensionalization.....	32
2.4.5 Model parameters.....	33
2.4.5.1 Determination of membrane mass transfer coefficient ....	34
2.4.6 MATLAB specifications.....	37
2.4.7 Prediction of bulk aqueous NO concentration at slit exit.....	40
2.5 Experimental methods for measurement of aqueous NO concentration.....	43
2.5.1 Reagents.....	43
2.5.2 Experimental protocol.....	43
2.6 Results.....	46
2.6.1 Model validation.....	46
2.6.2 Spatial NO concentration and flux profiles.....	50
2.7 Conclusions.....	53
3. EFFECT OF NO EXPOSURE ON PLATELET DEPOSITION.....	57
3.1 Introduction.....	57
3.1.1 Platelet perfusates: whole blood, plasma , and platelet suspensions.....	58
3.2 Qualitative studies.....	59
3.2.1 Objectives.....	60
3.2.2 Reagents.....	60
3.2.3 Preparation of platelet suspension.....	60
3.2.4 Platelet counts.....	62
3.2.5 Fluorescent labeling of platelet.....	64
3.2.6 Collagen preparation and coating.....	65
3.3 Experimental setup.....	66
3.4 Protocol for fluorescent studies.....	68
3.4.1 Perfusion steps.....	68
3.4.2 Fluorescence microscopy.....	69
3.5 Results.....	71
3.6 Quantitative platelet deposition studies.....	72
3.6.1 Objectives.....	72
3.6.2 Platelet labeling.....	75
3.6.3 Selection of radiotracer: Chromium-51 vs. Indium-111.....	76
3.6.4 Preparation of <sup>51</sup> CrO <sub>4</sub> -labeled platelet suspensions.....	77
3.7 Experimental protocol.....	79
3.7.1 Analysis method.....	80

Chapter	Page
3.8 Results.....	82
3.9 Interpretation of results.....	82
3.10 Conclusions.....	85
4. SHEAR RATE, AGONIST, AND PERFUSION TIME EFFECTS.....	89
4.1 Introduction.....	89
4.2 Factors affecting platelet-surface interactions.....	91
4.2.1 Platelet agonists.....	91
4.2.1.1 Plasma proteins.....	91
4.2.1.2 Components of vessel wall.....	95
4.2.1.3 Selection of agonists.....	95
4.2.2 Shear rate.....	96
4.2.2.1 Selection of shear rates.....	97
4.2.3 Perfusion time and other parameters.....	98
4.3 Objectives.....	99
4.4 Experimental methods.....	100
4.4.1 Reagents.....	100
4.4.2 Platelet perfusates.....	100
4.4.3 Experimental setup.....	101
4.4.4 Preparation and coating of agonists.....	101
4.4.5 Experimental protocol.....	102
4.5 Results.....	104
4.6 Interpretation of results.....	112
4.7 Physiological relevance.....	116
4.8 Conclusions.....	117
5. SYNERGISTIC INHIBITION BY APYRASE AND NITRIC OXIDE.....	118
5.1 Introduction.....	118
5.2 Objectives.....	119
5.3 Materials and methods.....	120
5.3.1 Reagents.....	120
5.3.2 Selection of enzyme.....	120
5.3.3 Preparation of enzyme and platelet perfusate.....	122
5.3.4 General experimental methods.....	123
5.3.5 Non-synergistic studies.....	124
5.3.5.1 Nitric oxide.....	125
5.3.5.2 Apyrase.....	126
5.3.6 Synergistic studies.....	126
5.3.6.1 Nitric oxide and aspirin.....	126
5.3.6.2 Apyrase and aspirin.....	126
5.3.6.3 Nitric oxide and apyrase.....	126

Chapter	Page
5.3.6.4 Nitric oxide, apyrase, and aspirin.....	128
5.3.7 Methods of analysis.....	128
5.3.8 Statistical methods.....	129
5.4 Results.....	129
5.4.1 Non-synergistic studies.....	129
5.4.1.1 Nitric oxide.....	129
5.4.1.2 Apyrase studies.....	131
5.4.2 Synergy studies.....	133
5.4.2.1 Nitric oxide and aspirin .....	133
5.4.2.2 Apyrase and aspirin .....	133
5.4.2.3 Nitric oxide and apyrase .....	137
5.4.2.4 Nitric oxide, apyrase, and aspirin.....	140
5.5 Discussion.....	142
5.6 Conclusions.....	143
6. CONCLUSIONS.....	145
6.1 Summary of study.....	145
6.2 Inferences.....	146
6.3 Further studies.....	148
7. REFERENCES.....	150
IRB APPROVAL FORM.....	163



## LIST OF TABLES

Table	Page
3.1 Platelet inhibition at various NO exposures.....	84
4.1 Major protein components of plasma.....	93
4.2 Platelet counts per unit area of upstream membrane section of control .....	105
4.3 Nitric oxide inhibition of agonist-induced platelet deposition.....	110

## LIST OF FIGURES

Figure	Page
1.1 <i>In vivo</i> mechanism of thromboregulation via endothelial NO release.....	5
1.2 <i>In vivo</i> mechanism of thromboregulation via endothelial release of ectonucleotidases.....	7
2.1 NO delivery device.....	27
2.2 Porous block region of the flow slit with dimensions and boundary conditions .....	31
2.3 NO delivery apparatus for determination of mass transfer coefficient ( $k_m$ ).....	35
2.4a Dialog box within boundary mode of MATLAB for boundary condition specs.....	39
2.4b PDE specification box showing the generic parabolic equation and parameters.....	39
2.4c Specification of solve parameters in the solve mode.....	42
2.4d Plot solution dialog box .....	42
2.5 Experimental setup for NO and NO <sub>2</sub> <sup>-</sup> analysis.....	45
2.6 Dimensionless bulk aqueous NO concentration exiting original device at various wall shear rates.....	48
2.7 Dimensionless bulk aqueous NO concentration exiting modified device at various wall shear rates.....	49
2.8 Nitric oxide concentration and flux profiles at flow slit outlet as a function of wall shear rate and slit height for porous hole device.....	51
2.9 Nitric oxide concentration and flux profiles at flow slit outlet as a function of wall shear rate and slit height for parallel slit device.....	52

Figure	Page
2.10 Nitric oxide concentration and flux profiles at NO delivery surface as a function of wall shear rate and length of exposure for porous hole device.....	54
2.11 Nitric oxide concentration and flux profiles at NO delivery surface as a function of wall shear rate and length of exposure for parallel slit device.....	55
3.1 Schematic for preparation of washed platelet suspensions with desired platelet counts.....	61
3.2 Experimental setup for delivery of NO to the platelet suspension.....	67
3.3 Spectral characteristics of fluorescent dye mepacrine.....	70
3.4 Platelet deposition on membrane in control chamber.....	73
3.5 Platelet deposition on membrane in NO-exposure chamber.....	74
3.6 Preparation of <sup>51</sup> Cr-labeled platelet suspension.....	78
3.7 Inhibition of platelet deposition at various NO exposures.....	83
3.8 Nitric oxide concentration and flux profiles across slit height at exit of flow slit for NO exposures of 0.1 and 0.02 ppm.....	86
3.9 Nitric oxide concentration and flux profiles across length for NO exposures of 0.1 and 0.02 ppm.....	87
4.1 Scheme of platelet activation by adhesion to fibrinogen-coated surfaces.....	94
4.2 Percentage inhibition of collagen-stimulated platelet deposition upon exposure to 0.1 and 0.02 ppm of gaseous NO.....	107
4.3 Percentage inhibition of fibrinogen-stimulated platelet deposition upon exposure to 0.1 and 0.01 ppm of gaseous NO.....	108
4.4 Percentage inhibition of IgG-stimulated platelet deposition upon exposure to 0.1 and 0.02 ppm of gaseous NO.....	109
4.5 Percentage inhibition of collagen-stimulated platelet deposition upon exposure to 0.1 and 0.02 ppm of NO as a function of perfusion time.....	111
4.6 Nitric oxide inhibition of collagen-stimulated platelet deposition as a function of wall shear rate.....	113

Figure	Page
4.7 Nitric oxide inhibition of fibrinogen-stimulated platelet deposition as a function of wall shear rate.....	114
5.1 Platelet inhibition as a function of NO exposure.....	130
5.2 Inhibition of platelet deposition by potato apyrase.....	132
5.3 Effect of shear rate on apyrase inhibitory potency.....	134
5.4 Effect of aspirin on platelet inhibitory potency of nitric oxide.....	135
5.5 Effect of aspirin on platelet inhibition by potato apyrase.....	136
5.6 Synergy between NO and apyrase.....	138
5.7 Synergy between apyrase and NO as a function of shear rate.....	139
5.8 Effect of aspirin on synergy between NO and apyrase.....	141

## NOMENCLATURE

$\theta$	Dimensionless NO concentration
$\gamma$	Wall shear rate ( $\text{s}^{-1}$ )
$\lambda$	Wavelength of light (nm)
$\theta_b$	Dimensionless bulk aqueous NO concentration (M)
$A$	Membrane surface area for mass transfer ( $\text{cm}^2$ )
$b$	Half-thickness of flow slit (cm)
$C$	Aqueous NO concentration (M)
$C'$	NO concentration in outlet $\text{N}_2$ stream (M)
$c, q, g$	MATLAB parameters for Neumann boundary conditions
$C_0$	Saturated aqueous NO concentration in equilibrium with NO gas (M)
$C_b$	Velocity-weighted bulk aqueous NO concentration (M)
$C_g$	NO concentration in the $\text{NO}/\text{N}_2$ mixture (M)
$C_i$	Aqueous NO concentration at the inlet into the porous block region (M)
$D$	Aqueous diffusivity ( $\text{cm}^2 \text{s}^{-1}$ )
$f, a, c, d$	MATLAB parameters for generic parabolic PDEs
$h$	Thickness of flow slit (cm)
$h, r$	MATLAB parameters for Dirichlet boundary conditions
$k_m$	Membrane mass transfer coefficient ( $\text{cm s}^{-1}$ )
$L_e$	Equivalent length of flow path over which NO exposure occurs (cm)

$M$	Molar (Moles/liter)
$n$	Number of trials
$\hat{n}$	Unit vector
$N_{Shw}$	Wall Sherwood number
$p$	Probability of the existence of significant difference between two sets of results
$Q$	Volumetric flow rate ( $\text{cc s}^{-1}$ )
$Q'$	Volumetric flow rate of the $\text{N}_2$ stream ( $\text{cc s}^{-1}$ )
$\tau$	Residence time (s)
$v$	Average velocity ( $\text{cm s}^{-1}$ )
$v_y$	Local velocity of flow ( $\text{cm s}^{-1}$ )
$W$	Width of flow slit (cm)
$X$	Dimensionless spatial coordinate along width of flow slit
$x$	Spatial coordinate along width the of slit
$Y$	Dimensionless spatial coordinate perpendicular to direction of flow
$y$	Spatial coordinate perpendicular to the direction of flow
$Z$	Dimensionless spatial coordinate along direction of flow
$z$	Spatial coordinates along the direction of flow

## CHAPTER 1

### INTRODUCTION

Platelet adhesion and aggregation on blood vessel walls is a major contributor to the occurrence of cardiovascular diseases where fibrosis occurs on the inner layers of the arterial wall (*atherosclerosis*). Constriction of arteries due to platelet deposits also often occurs subsequent to surgical intervention (*restenosis*). Although numerous factors may simultaneously or individually enhance platelet deposition on luminal walls, the net consequence is a gradual reduction in the cross-sectional area of the lumen through which blood flows. Physical manifestations of intense vascular thrombosis include an increase in systemic or pulmonary blood pressure (*hypertension*) and more dangerously the formation of circulating platelet aggregates (*emboli*) broken off from the deposition surface. Emboli may cause clogging and rupture of smaller blood capillaries causing hemorrhage. Continuous surface thrombosis can also result in depletion of blood platelet counts (*thrombocytopenia*) and consequent impairment of normal blood coagulative processes (*hemophilia*).

Platelet-surface interactions also restrict the clinical applicability of *in vitro* and *ex-vivo* blood-flow devices, or *in vivo* implants. Nose *et al.* (1996) identified the two major considerations in the design of vascular prosthesis to be (i) the avoidance of blood stagnant pockets, and (ii) the use of biomaterials suitably compatible with blood. During the perfusion of whole or reconstituted blood across a bioartificial surface, plasma

proteins deposit on the biomaterial [Ku *et al.*, 1995]. Depending on the nature of the material, this may render the surface highly thrombogenic or more rarely result in surface passivation [Lyman *et al.*, 1974; Hoffman, 1982]. In medical devices, such as oxygenators incorporating blood-biomaterial contact over extended periods, surface thrombi may impede the transport species such as O<sub>2</sub> across the biomaterial. Additionally, thrombocytopenia and embolism are also encountered in a manner similar to vascular thrombosis.

Platelet deposition in extracorporeal devices may be attenuated or even avoided altogether via either of two different approaches. The first approach involves selection of alternate less thrombogenic materials. However, the use of such materials with enhanced hemocompatibility may be constrained by lack of properties, such as strength, essential to the specific application. A second approach involves modifying the existing material either structurally or via chemical means to prevent deposition of plasma proteins and subsequent thrombus formation. Platelet-antagonists may also be delivered at biomaterial surfaces to prevent platelet deposition. However, local delivery of such agents must be controlled to avoid potential toxic reactions or poisoning. Therefore, knowledge of the minimal surface concentrations and fluxes of anti-aggregative agents required for significant platelet inhibition, is beneficial.

Previous research has widely elucidated the pathways involved in platelet-biomaterial and platelet-platelet interactions. A number of platelet antagonists have been evaluated including prostacyclins, adenosine, dextrans, heparin, and apyrases [Rosenberg *et al.*, 1975] under non-flow shear or non-shear conditions. Currently platelet antagonists like heparin are added to blood-based perfusates to reduce thrombogenicity. Studies, such as



that of Larm *et al.* (1983) obtained blood compatibility through heparin bonding to different surfaces. However, heparin loses its anti-coagulant activity over time, and also orchestrates the denaturation of coagulation factors in the plasma [Larsson *et al.*, 1987]. Aspirin, which is currently the most widely accepted antithrombotic agent, has been shown to be less than optimal for preventing new thrombi on blood vessel walls [Antiplatelet Trialists Collaboration, 1994a, b]. The therapeutic low-dose regimes currently in use are too low because erythrocytes overcome aspirin inhibition of platelet reactivity with time [Valles *et al.*, 1993]. Thus effective, less toxic, and inexpensive anti-thrombogenic agents need to be identified. A good approach is to identify *in vivo* mechanisms by which platelets deposition on luminal walls is inhibited. These anti-thrombotic agents may be isolated and delivered from biomaterial surfaces *in vitro* or *in vivo* to attenuate platelet-biomaterial interactions.

### **1.1 *In vivo* anti-thrombotic mechanisms.**

Endothelial cells lining blood vessels have long been implicated in maintaining the platelet-free nature of blood vessel walls. At sites of damage to the endothelial layer, platelets adhere rapidly to the traumatized exposed sub-endothelium, thereby confirming the role of the endothelium in thromboregulation [Marcus *et al.*, 1993; Ruggeri, 1993]. At present, clinical studies provide evidence for the existence of three thromboregulatory systems in human endothelial cells- (a) Endothelium derived relaxing factor/nitric oxide, (b) Ecto-nucleotidases, and (c) Eicosanoids [Marcus *et al.*, 1995]. Presently, it is not known if these three mechanisms are merely complementary or synergistic in their

action. The current research study investigates the applicability of nitric oxide and ectonucleotidases as agents for inhibiting platelet-biomaterial interactions.

### *1.1.1 Mechanism I: Endothelium-derived relaxing factor/Nitric oxide*

In vivo, in response to physical (*e.g.*, shear) or chemical (*e.g.*, acetylcholine) perturbation, vascular endothelium releases Endothelium-Derived Relaxing Factor (EDRF). Investigation has shown that the biological activity of EDRF is mainly accounted for by nitric oxide (NO) [Ignarro *et al.*, 1993]. Figure 1 shows the mechanism via which NO release from endothelial cells reduces platelet deposition on luminal walls. NO generated by the endothelium activates soluble guanylate cyclase (sGC) in smooth muscle cells and platelets. This in turn induces elevation of intraplatelet cyclic guanosine monophosphate (cGMP) which blocks platelet reactivity via a decrease in intracellular ionized calcium levels (indicated by the negative sign)[Hall *et al.*, 1994]. At sites of destruction of the vascular endothelium, platelets are exposed to the exposed basement membrane of the vascular wall. The basement membrane is made up of numerous thrombogenic proteins, mainly collagen. These promote platelet reactivity and adherence by raising intraplatelet  $Ca^{2+}$  levels thereby enhancing platelet reactivity [Radomski *et al.*, 1996] and inducing intracellular generation of NO from L-arginine. Released NO reduces platelet reactivity in a manner similar to the endothelial NO. The impairment of NO activity due to destruction of the endothelium has been postulated to play a role in pathogenesis in cardiovascular disease [Bassenge *et al.*, 1992; Busse *et al.*, 1993]. NO activity may serve to reinforce thromboregulation when prostaglandin production is insufficient or has been eliminated by therapy with aspirin.

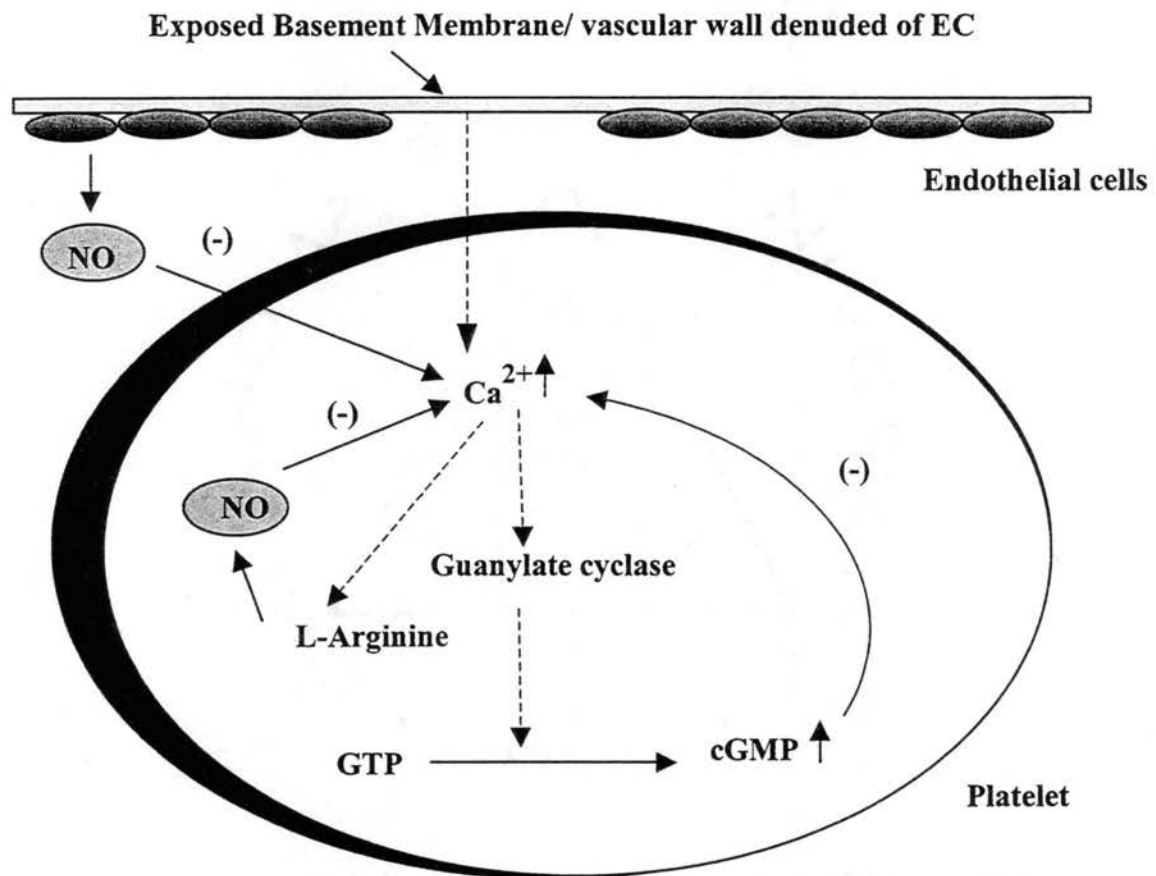


Figure 1.1 *In vivo* mechanism of thromboregulation via endothelial NO release.

### 1.1.2 Mechanism II: Ecto-nucleotidases.

Ecto-nucleotidases form one of three complementary and possibly synergistic mechanisms in human endothelial cells to attenuate surface platelet deposition. Ecto-nucleotidases (also called ecto-ADPases) are aspirin-insensitive anti-thrombogenic agents. Release of nucleotides is in response to cell-injury or other stimuli (e.g., shearing due to blood flow and receptors such as acetylcholine) [Coade *et al.*, 1989; Gordon *et al.*, 1989]. The enzyme is a phosphodiesterase, and acts as a catalyst for the hydrolysis of adenosine triphosphate (ATP) and adenosine diphosphate (ADP) to adenosine monophosphate (AMP) and orthophosphate, as shown in Figure 2. Both ATP and ADP are released by platelets upon activation by basement membrane platelet agonists such as collagen, and are necessary for the aggregation process (indicated by the plus sign in Figure 2). Metabolic studies by Marcus *et al.* (1995) have shown that the enzyme inhibits (indicated as negative signs) by way of two mechanisms- (i) scavenging of necessary ATP, ADP, and (ii) formation of the anti-aggregatory metabolite adenosine [Marcus *et al.*, 1991]. Ecto-ADPases serve as important regulators for maintenance of blood fluidity.

### 1.1.2 Mechanism III: Eicosanoids.

Eicosanoids released by endothelial cells fulfill their thromboregulatory function via inhibition of or reduction in, intraplatelet cyclooxygenase levels [Marcus, A.J., 1990; Serhan, C.N., 1991]. This in turn blocks platelet endoperoxide production necessary for the ultimate production of thromboxanes, which are not agonistic towards platelets. This mechanism is aspirin-sensitive [Petrono *et al.*, 1989].

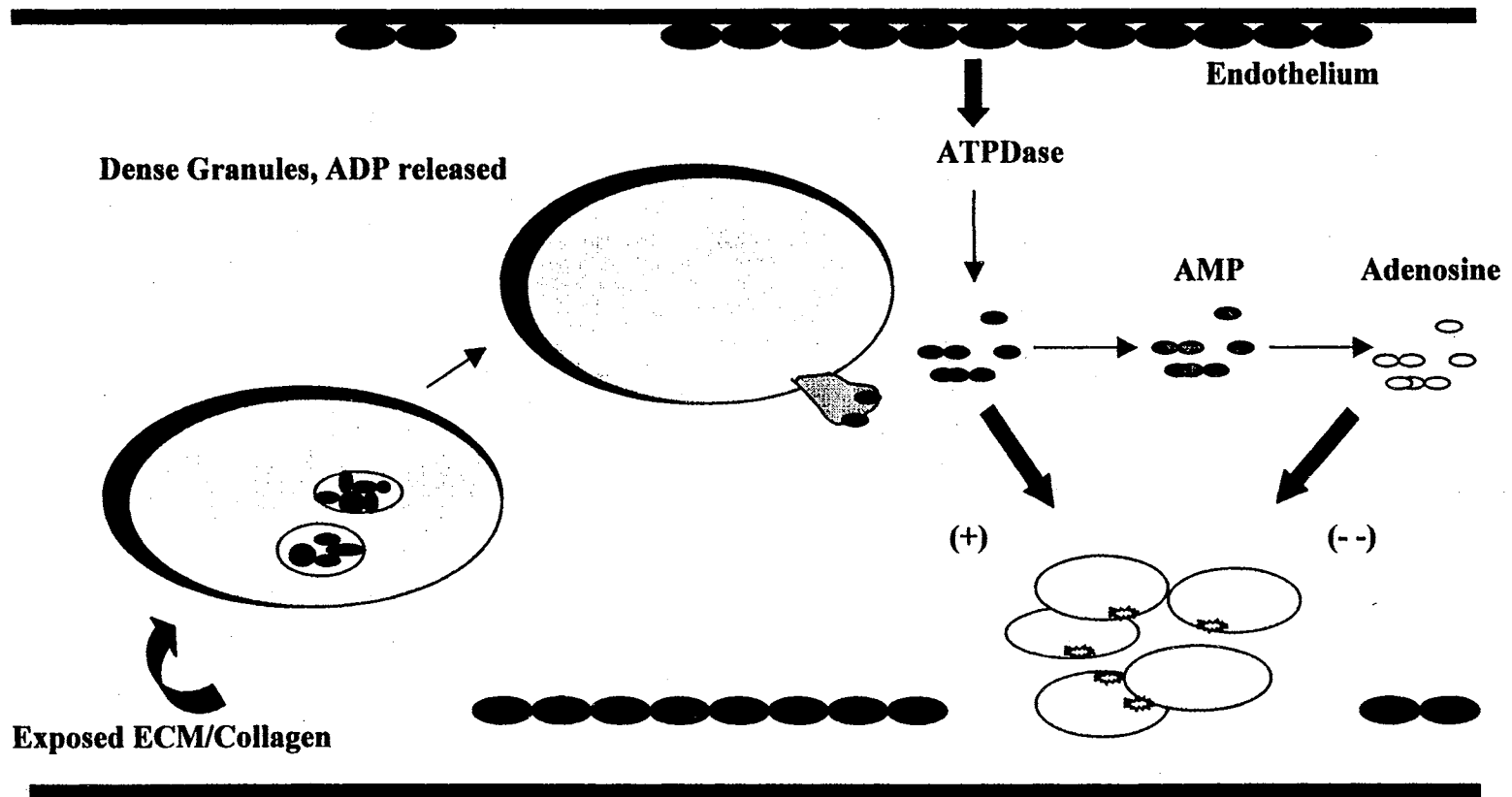


Figure 2.2 *In vivo* mechanism of thromboregulation via endothelial release of ecto-nucleotidases.

## 1.2 Physiological roles of nitric oxide.

Nitric oxide is a colorless, odorless gaseous species. Although initially identified as an atmospheric pollutant, NO is also a biological signal molecule with numerous physiological and pathophysiological roles. The biological roles of NO may be attributed to its small-sized free radical structure, high diffusivity, and high reactivity [Garthwaite, 1991; Wood *et al.*, 1994; Kerwin *et al.*, 1995].

In mammals, NO is generated endogenously by different cell types including macrophages, endothelial cells, neutrophils, and hepatocytes. Nitric oxide is synthesized from the amino acid L-arginine via the mediation of the nitric oxide synthase enzyme (NOS). NOS are of three predominant types [Kelly *et al.*, 1996]. Constitutive NOS (cNOS) is generally localized in platelets, cardiac myocytes, and vascular smooth muscle cells and release picomolar ( $10^{-12}$  M) levels of NO in response to increased intracellular  $\text{Ca}^{2+}$ -calmodulin concentrations induced by physical stimuli. Release of NO promoted by constitutive enzymes predominantly fulfills roles as biological messengers, as in blood pressure regulation. Inducible NOS (iNOS) is localized in cell types such as neutrophils and macrophages, and induces NO release when stimulated by compounds such as cytokines [Fostermann *et al.*, 1991]. Nanomolar concentrations of NO are released over extended periods of time. The large amount of NO released is toxic towards foreign microorganisms and tumor cells and may also contribute to tissue damage and local hypotensive effects at injury sites [Moncada *et al.*, 1994; Calver *et al.*, 1993]. The third form of nitric oxide synthase is of neuronal origin (nNOS). It is predominantly associated with the cranial cells, certain epithelial cells, and skeletal muscle [Fostermann,

1994; Bredt *et al.*, 1994]. Expression and activity of nNOS is also associated with smooth muscle relaxation [Andersson *et al.*, 1994].

Analogues of L-arginine, which act as stereospecific inhibitors of NO synthase, have been used *in vivo* and *in vitro* to identify physiological and pathophysiological roles of NO [Calver *et al.*, 1993; Funder *et al.*, 1995].

### *1.2.1 Role of NO in inhibition of platelet aggregation.*

Loss of blood at sites of injury is prevented by rapid local blood coagulating processes which result in the formation of a 'hemostatic plug' [Radomski *et al.*, 1996]. However, abnormal aggregation of platelets and neutrophils, and consequent clotting of blood in blood vessels is a major contributor to the occurrence of myocardial infarction (heart attack) due to hampered blood supply [Pabla *et al.*, 1996]. NO released from the vascular endothelium lining blood vessels, or released from platelets themselves, has been previously shown to inhibit potentially dangerous platelet aggregation in non-injury regions. The mechanism of action will be discussed later in this chapter.

### *1.2.2 Role of NO in vascular regulation.*

Several endothelium-dependent vasodilators (e.g., acetylcholine) induce an increase in intra-endothelial calcium levels thereby stimulating NO release. NO diffuses from endothelial cells to the adjacent vascular smooth muscle causing muscle relaxation and vasodilatation [Kerwin *et al.*, 1995]. Mechanical stimuli such as shear stress can also evoke changes in intracellular calcium and NO synthesis leading to local systemic vasculature dilation [Rubanyi, 1991; Butler and Williams, 1993].

### *1.2.3 Role of NO as a neurotransmitter.*

Neurotransmitters are chemical agents that enable transmission of nerve impulses across the gaps (synapses) between nerve cells. Previous studies have demonstrated that NO is a major mediator of retrograde neurotransmission in non-cholinergic (NANC) nerves which via their stimulation induce muscle relaxation [Rand *et al.*, 1992]. NANC derived NO also evokes smooth muscle relaxation, supporting the physiological role of NO in the stomach and gastrointestinal system [Tottrup *et al.*, 1991]. NO has also been suggested to play an important role in blood supply within the brain and has a long-term effect on brain development, learning and memory [Toda *et al.*, 1993]. This latter role of NO is being researched as a means of treatment for certain neurodegenerative diseases [Moncada *et al.*, 1993].

### *1.2.4 Role of NO in immune response mechanisms.*

Constitutive NOS in macrophages release NO upon stimulation, a mechanism via which invading microbes and foreign cells are destroyed. Response of the macrophages to microbes is enabled by the presence of chemical mediators called cytokines. Released NO plays an important role in the rejection of transplanted tissues [Southan *et al.*, 1993]. Several reactive intermediates are formed by NO which are potently cytotoxic to the invading cells [Butler and Williams, 1993]. However, NO released during the reperfusion phase of transplantation has been determined to mediate the survival and preservation of graft tissue [Mueller *et al.*, 1994].



### 1.2.5 Role of NO in the endocrine system.

Preliminary findings indicate that NO plays a significant role in the regulation of renin production and sodium homeostasis within the kidney. Shear stress across the endothelial cell surface occurs due to enhanced renal blood flow. The stress activates the eNOS to synthesize NO, which in turn inhibits release of renin [Vallance and Collier, 1994]. A NOS isolated in the adrenal gland has been identified to play a modulatory role in the control of the synthesis and secretion of hormones by the adrenal gland [Palacios *et al.*, 1989; O'Sullivan and Burgoyne, 1990].

### 1.3 Pathophysiological roles of NO.

*In vivo*, NO may be either beneficial or may act as a cytotoxic agent depending upon its concentration or time of exposure. NO release mediated by cNOS (as in endothelial cells) typically generates picomolar concentrations of NO while that mediated by iNOS (via macrophages) generates nanomolar levels. At sites of injury, or due to the presence or absence of other physiological species vital for NO generation by cells, overproduction or deficiency of NO may result. Abnormal *in vivo* NO concentrations can result in certain pathophysiological disorders. Scavenging the excess NO or generating NO using NO-donor drugs may reverse these conditions.

### ***1.3.1 Effects of excess NO production.***

#### ***1.3.1.1 Sepsis/ hypotension.***

Macrophages mobilize at sites of injury to counteract foreign microorganisms via the release of NO. However, this beneficial aspect is often eclipsed by adverse reactions caused by excessive localized NO generation. These effects include substantial vasodilatation and subsequent drop in local or systemic blood pressure [Wright *et al.*, 1992] resulting in sepsis (endotoxic shock). Reduced blood pressure and vasodilatation accompanying liver failure is due to the increased production of cytokines which induce NO synthesis [Vallance and Moncada, 1991].

#### ***1.3.1.2 Rheumatoid arthritis.***

The onset of rheumatoid arthritis is accompanied by local inflammation at the synovial joints. The prime function of NO and its oxidation products released by infiltrating leukocytes upon cytokine stimulation is to induce microbial cytotoxicity [Laskin *et al.*, 1994]. The high levels of NO released can also alter physiological functions in host tissues. The primary effects are local vasodilatation, edema, and erythema that further arthritic symptoms. NO and its oxidation products are commonly found in tissue samples isolated from chronically arthritic tissues [Evans *et al.*, 1995].

#### ***1.3.1.3 Insulin-dependent diabetes mellitus.***

Insulin-dependent diabetes mellitus (IDDM) is an autoimmune disease characterized by specific destruction of pancreatic islet beta cells. The destruction is brought about by infiltrating lymphocytes which release cytokines such as interleukin-1 $\beta$  [Bendtzen *et al.*,

1986; Comens *et al.*, 1987]. Cytokines may destroy beta cell function via the mediation of high levels of nitric oxide released upon stimulation of iNOS in host cells [Corbett *et al.*, 1991, 1993].

#### *1.3.1.4 Tissue damage associated inflammation.*

Nitric oxide is produced upon activation of immune cells following stimulation by bacterial endotoxin or inflammatory mediators such cytokines [Vallance and Collier, 1994]. Tissue damage may occur due to increased vascular perfusion or by reaction of NO with superoxide to produce peroxynitrite which can promote cell lipid oxidation and DNA damage [Kerwin *et al.*, 1995].

#### *1.3.2 Effects of NO deficiency.*

##### *1.3.2.1 Atherosclerosis.*

A slight imbalance in NO production by the vascular endothelium can contribute to atherogenesis [Minor *et al.*, 1990]. Although the adhesion of macrophages to the damaged endothelium stimulates greater NO production locally, there is a concomitant depletion of NO [Minor *et al.*, 1990; Nakai *et al.*, 1995; Hackman *et al.*, 1996]. Products of increased NO degradation can contribute to cellular damage. Decreased availability of NO can also result in the insufficient capacity to scavenge superoxide present at atherosclerotic lesions [Beckman *et al.*, 1990; Mehta *et al.*, 1990]. Increased superoxide levels account for diminished sGC responsiveness, impairing vasodilatory and anti-aggregative responses via endothelial NO release [Cannon, R.O., 1998].

### 1.3.2.2 Pulmonary hypertension.

In the lung, NO is generated from cNOS in pulmonary arterial and venous endothelial cells [Adnot *et al.*, 1995]. The release is stimulated upon activation by shear forces due to circulating blood as well as receptor-based mechanisms. NO protects from thrombosis in pulmonary vessels and simultaneously regulates vasodilatation. Stimuli such as hypoxia or/and endothelin can deplete NO production levels and contribute to pulmonary hypertension [Adnot *et al.*, 1991; Carville *et al.*, 1993]. The results include gradual increase in pulmonary vascular tone, formation and migration of surface thrombi, decreased blood oxygenation levels, and increased smooth muscle cell proliferation. Thus, deficient NO availability in lungs can cause accelerated vascular remodeling [Gibbons and Dzau, 1994].

## 1.4 Reactivity and Cytotoxicity of NO.

NO serves as a biological molecule involved in the regulation of several vital physiological processes as outlined in section 1.2. Contrary to these roles is the detrimental aspect of NO. The specific properties of the NO molecule including its small size and high diffusivity result in its high reactivity in oxygenated biological systems. In such a system, NO undergoes a series of complex and sequential reactions. The chemical biology of NO may be categorized into direct effects and indirect effects. Direct effects are due to NO alone or from the reactions between NO and specific biological molecules (O<sub>2</sub>, thiols etc.). Indirect effects are produced upon further reaction of reactive nitrogen oxide species (RNOS; *e.g.*, peroxynitrite) which may be derived from NO autoxidation with various biological targets [Wink *et al.*, 1996]. As an example, at sites of

inflammation, macrophages generate NO which is cytotoxic towards foreign microbes thus serving as an immune defense mechanism. However, in parallel, healthy host tissue cells may also be a target of the cytotoxicity of NO [Evans *et al.*, 1995]. Mutagenicity and apoptosis of healthy DNA can occur following excessive exposure to NO or its active reaction intermediates [Tamir *et al.*, 1996].

#### 1.4.1 Reaction of NO with O<sub>2</sub>.

Nitric oxide reacts rapidly with oxygen as per the reaction



Nitrous anhydride (N<sub>2</sub>O<sub>3</sub>) disassociates in aqueous media to yield nitrite (NO<sub>2</sub><sup>-</sup>) [Lewis *et al.*, 1994].



DNA may be damaged by N<sub>2</sub>O<sub>3</sub> via two different pathways. The first pathway is through the nitrosation of secondary amines to form carcinogenic N-Nitrosoamines. In presence of appropriate enzyme systems, these form alkylating electrophiles which react with the nucleophilic sites on the DNA strands leading to indirect DNA damage. A second pathway involves direct DNA destruction through nitrosative deamination of primary amines attached to the DNA bases. This leads to weakening and subsequent breakage of the DNA strands [Nyugen *et al.*, 1992; Tamir *et al.*, 1996].

#### 1.4.2 Reaction with superoxide.

The reaction between NO and superoxide ( $O_2^-$ ) to form peroxynitrite ( $ONOO^-$ ) is of great importance in biological systems as a result of the ability to serve as a detoxification mechanism for reactive oxygen species. The extremely rapid and diffusion controlled reaction is



Peroxynitrite is slowly disseminates in solution to yield nitrite and oxygen. Further reaction of peroxynitrite with NO yields nitrite and nitrate as final products [Koppenol, W.H., 1998]. Peroxynitrite may nitrosate tyrosine in the presence of metal ions [Ischiropoulos *et al.*, 1992], or act as an oxidant of various biological molecules [Pryor, W.A., 1995]. Species formed by further reactions of ( $ONOO^-$ ) are toxic, mutagenic or bacteriocidal, and cause destruction of lipid membranes and DNA. This is the phenomenon of oxidative stress associated with reperfusion injury [Hogg *et al.*, 1992]. Notably however, peroxynitrite reactions are much slower than that of reactive oxygen species such as superoxide with NO [Wink *et al.*, 1996].

#### 1.4.3 Reactions of NO with transition metals/metal groups.

Reaction of NO with metals or metal centers in groups is crucial for the bioregulatory roles of NO. The reaction of NO with metal transition groups results in the formation of metal-nitrosyl adducts. *In vivo*, one of the most common reactions is the reaction of NO with ferrous ion in acidic solution.



Heme-containing proteins are important to the biological actions of NO. Also, the reaction of ferryl heme proteins with NO is important as a mechanism for protection against reactive oxygen species. However, these complexes can also release NO under appropriate biological conditions or can act as nitrosating agents through NO donation. Further, the reversible or irreversible binding of NO to a metal group in an enzyme structure can lead to distortion of the enzyme and subsequent loss or change in functionality. Certain dioxygenated metal groups such as oxyferrohemoglobin can act as scavengers of NO. NO also reacts with deoxyferrohemoglobin to form a nitrosyl complex which can either be carcinogenic or release NO [Kerwin *et al.*, 1995]. NO also inhibits cytochrome P450 under infectious conditions, thereby decreasing drug metabolism in the liver.

### 1.5 Methods of NO delivery.

NO participates in the regulation of beneficial physiological mechanisms, but simultaneously is capable of toxic, mutagenic, and carcinogenic effects by itself or via its reaction products. The mechanisms via which NO interacts with biological systems can be understood through *in vitro* studies with cell cultures or *in vivo* studies through the delivery of NO. To effectively study NO effects, a method is required by which known or predictable quantities or concentrations of NO are delivered to the system under study. A second rationale for delivering NO to physiological systems is for the treatment of certain pathophysiological disorders. It is therefore imperative to develop a suitable NO delivery

system capable of consistent and predictable NO delivery rates. Generally, there are two different approaches.

#### 1.5.1 Physical method.

The physical method involves NO delivery from the gaseous phase, via diffusion through a semi-permeable membrane, to a biological system. This method has been used to determine the influence of delivery rate of NO on the biological effects of several cellular systems [Tamir *et al.*, 1994; Kavdia *et al.*, 1998]. Previously, gaseous NO has also been delivered to biomaterial surfaces to attenuate platelet-biomaterial interactions [Keh *et al.*, 1997; Ramamurthi *et al.*, 1998]. The delivery of NO to an aqueous solution could be regulated by changing parameters such as the partial pressure of the gas and the length or type of the semi-permeable membrane.

#### 1.5.2 Chemical method.

The chemical method involves NO release via gradual dissolution of a NO releasing compound. Several classic nitrovasodilators such as nitroglycerin and isoamyl nitrite act via *in vivo* generation of NO which elevates intracellular cGMP levels and produces vasorelaxation. Glyceryl trinitrate and other nitrovasodilator compounds release NO which helps to counteract the effects of hypertension [Vallance and Collier, 1994]. The mechanism of liberation of NO from NO-donors may be either chemical (*e.g.*, nucleophile-NO adducts) or enzymatic (*e.g.*, nitrosothiols, sodium nitroprusside). A number of NO donors which differ in their properties and NO release characteristics, are available commercially. These include:



- (i) SIN-1: A morpholine based NO donor which releases both NO and O<sub>2</sub><sup>-</sup>.
- (ii) Molsidomine: An orally active NO donor which releases NO in response to specific hepatic metabolic processes.
- (iii) NONOates: Nucleophile/NO adducts which generate NO following pH dependent decomposition.
- (iv) Sodium Nitroprusside (SNP): A NO donor, which is widely used to treat hypertension and reduce blood pressure.

Donor-based delivery of NO may be adopted for the *in vitro* study of specific biological processes or for therapeutic purposes. A wide variety of NO donors are available which incorporate a spectrum of release rates and release mechanisms. Further, the method of NO delivery using NO donors is also dependent on the specific application. Previously, polymer beads containing NONOates were used to obtain effective delivery rates for local delivery of NO *in vivo* [Smith *et al.*, 1996]. Another approach is to immobilize NO donors on tissue or biomaterial surfaces for local NO delivery without the problems associated with infusion into the blood stream. In any case, the kinetics of NO release under the exact conditions of use is essential to avoid toxic effects that may result from excessive or rapid NO release and exposure.

## **1.6 Nitric oxide inhibition of platelet adhesion and aggregation.**

NO is extensively involved in cardiovascular phenomena such as vasodilatation and blood pressure regulation [Moncada *et al.*, 1991]. Endothelial cells lining the arterial lumen release low levels of NO, inhibiting platelet activation and deposition thereby maintaining the integrity of the vessel wall [de Graaf *et al.*, 1992; Radomski *et al.*, 1996; Luscher, 1997].

Several research groups have sought to determine the mechanism(s) underlying the anti-thrombogenic action of NO [Nakashima *et al.*, 1986; Salas *et al.*, 1994] and the inhibition of platelet adhesion by gaseous NO delivered *in vitro* static [Radomski *et al.*, 1987; Gries *et al.*, 1998] and dynamic [de Graaf, 1992; Polanowska and Gear, 1994] systems. Konishi *et al.* (1996) delivered gaseous NO at concentrations up to several hundred *ppms* and demonstrated its effectiveness as an anti-aggregatory agent. Keh *et al.* (1996) reduced platelet trapping in oxygenators via transmembraneous delivery of NO. NO released by donor compounds in a thiolation-independent manner has also been demonstrated to sufficiently inhibit platelet aggregation *in vitro* [Rauli, 1998] and *in vivo* [Smith *et al.*, 1996]. In the study by Smith *et al.* (1996), NO platelet aggregation was inhibited by NO delivered in a controlled manner from polymer-immobilized NO donors. In a study by Samama *et al.* (1995), inhaled NO was used to attenuate platelet aggregation in patients with acute respiratory distress syndrome (ARDS).

A common factor linking these studies is that the actual NO concentrations and fluxes inhibiting platelet activation and recruitment were not determined. Measurement and knowledge of NO concentrations and fluxes is essential to avoid the potential toxicity and mutagenicity associated with excessive NO exposure [Radi, 1996; Tamir *et al.*, 1991]. The requirement for this information forms the basis for the current work.

### **1.7 Thesis Objectives.**

The overall objective of this thesis is to establish valid guidelines for the local delivery of NO to reduce platelet deposition on biomaterials. The overall objective of the thesis is realized by the achievement of the following specific goals, which are discussed as follows:

In Chapter 2, the development of a suitable NO delivery device to study NO inhibition of platelet-biomaterial interactions *in vitro*, is discussed. A mathematical model is formulated to predict aqueous NO concentration and flux profiles generated within the blood-flow slit. Experimental validation of the model is also elaborated upon.

Chapter 3 outlines the experimental determination of the minimal gaseous NO exposures for significant inhibition of platelet deposition. The influence of platelet-agonists, wall shear rates, and gas exposure times on these threshold NO concentrations and fluxes was investigated. The results of this study, detailed in chapter 4, illustrate the generality of the conclusions made in chapter 3.

Ectonucleotidases (apyrases) are potent enzymatic antagonists of platelet adhesion and aggregation. NO and ectonucleotidases are agents released by vascular endothelial cells to inhibit vascular thrombosis. A study was thus carried out to determine if NO and apyrases synergistically inhibit platelet deposition on biomaterial surfaces. The effect of aspirin on synergy between apyrases and NO was also investigated. Synergy studies are elucidated in chapter 5.

In chapter 6, the entire work is reviewed and put into perspective. On the basis of the results discussed in previous chapters, recommendations are made towards the development of novel anti-thrombogenic biomaterials incorporating NO-release.

## CHAPTER 2

### DELIVERY DEVICE DEVELOPMENT AND MODELING

#### 2.1 Systems for study of platelet-surface interactions.

Previously, numerous perfusion devices have been developed for the purpose of studying platelet-surface interactions under flow conditions *in vitro*. Lindon *et al.* (1996) lists eight methods for the *in vitro* study of platelet-surface interactions. In studies by Page *et al.* (1979) and Neumann *et al.* (1980), platelet adhesion to a surface was induced by sedimentation. Didisheim *et al.* (1983) evaluated hemocompatibility of a biomaterial via complete immersion of the material in platelet-rich plasma (PRP) or whole blood. Centrifugation has also been used as a method of inducing platelet adhesion and aggregation on surfaces [Mohammed *et al.*, 1976; Coleman *et al.*, 1982]. The glass or polymer-bead column test introduced by Hellam (1960) and modified by Salzman (1963) assesses platelet adhesion and aggregation on packed beads.

For studies of platelet deposition under flow conditions where more defined shear conditions are required, parallel plate chambers are popular. Parallel plate devices have been used to study platelet interactions with extracellular matrix (ECM) [Sakariassen *et al.*, 1983; Sixma *et al.*, 1987; Fry *et al.*, 1989], or collagen-coated biomaterials [McCollum *et al.*, 1980] in a perfusion system. Alternately, a blood or platelet suspension can be passed through a glass, polymer, or polymer-coated tubing which may be sectioned. Adhesion/aggregation is quantified microscopically or by counting

radiolabeled platelets [Adams and Feuerstein, 1981a, b, c]. The influence of shear in promoting platelet adhesion and aggregation to biomaterial surfaces has been investigated by rotating cylindrical devices (made of the test material) in a platelet suspension [Brash *et al.*, 1977; Herzlinger *et al.*, 1981].

Nitric oxide (NO) inhibition of platelet deposition on biomaterial surfaces has been the focus of several studies. Most of these studies focused upon application of NO therapy to attenuation of platelet deposition in extracorporeal circuits. Mellgren *et al.* (1996) evaluated the effect of NO added to oxygenator sweep gases on extracorporeal life support (ECLS)-induced platelet consumption and activation. NO gas concentrations of between 15 and 75 ppm were exposed to the platelet perfusate in ECLS. In a similar study by Keh *et al.* (1996), gaseous NO (40 ppm) was delivered to a heparin-bonded hollow fiber membrane oxygenator (HFMO) to evaluate anti-platelet aggregating and disaggregating properties of NO. Smith *et al.* (1995) studied NO inhibition of thrombosis on grafts *in vivo* via release of NO from NO donors encapsulated in the polymer coating of the graft. Although the above studies demonstrated that NO therapy is effective in inhibiting platelet-biomaterial interactions, the NO concentrations and fluxes at the deposition surface were not identified. However, the minimal NO concentration and flux for significant inhibition was not quantified. Knowledge of surface NO concentrations and fluxes is vital for the proper design of NO-releasing biomaterials to minimize toxicity due to excess or rapid NO delivery. The major objectives of the current study are to predict aqueous surface NO concentrations and fluxes at the adhesion surface and determine the threshold NO concentration for effective platelet inhibition. A NO delivery device was designed to meet the objectives.

## 2.2 Delivery device requirements.

The delivery device was designed to investigate the inhibition of platelet deposition on biomaterial surfaces under flow conditions via the local delivery of gaseous NO.

Controlled and predictable delivery of NO is essential. One of the primary requirements of the design was limiting the gas exposure area for permeation of gas into the perfusate.

In addition, the width of the flow slit should be exposed to similar concentrations of gas.

The biomaterial to be incorporated into the delivery device should be thin, easily incorporated and removed, resistant to degradation on contact with aqueous buffer, and smooth surfaced (to avoid shear rate variations in the perfusate and excessive aggregation associated with rough surfaces).

Most importantly, in order to deliver NO to the biomaterial surface exposed to platelets, the biomaterial should be selectively permeable to NO. A durable and transparent material of construction would be desirable to easily detect leaks. Finally, the geometry and dimensions of the flow slit for perfusion of the platelet suspension/blood should be designed such that physiological flow conditions are satisfied and shear rates extend over the desired range.

### 2.2.1 *Wall shear rates: Physiological implications.*

For this study, platelet adhesion and aggregation on the biomaterial surface was measured under flow conditions. The flow field, in addition to continuously supplying platelets for formation of thrombi, also removes thrombi via the shear force generated at the blood-polymer interface. Platelet deposition on surfaces is a strong function of wall shear rates [Turitto and Baumgartner, 1979; Turitto *et al.*, 1980]. For specified flow rates, the dimensions of the flow channel determine the shear rate. In human blood

vessels, wall shear rates range from 30-40 s<sup>-1</sup> in major vessels to over 5000 s<sup>-1</sup> in the smallest capillaries. To simulate physiological conditions as closely as possible, shear rates adopted for *in vitro* studies should lie within the ranges specified above.

Theoretical considerations and experimental findings indicate that platelet adhesion and thrombus formation on vessel/channel walls is enhanced with increasing shear rate. Platelet adhesion to surfaces starts to asymptotically level off at a shear rate of 650 s<sup>-1</sup>. Below this shear rate, adhesion is predominantly transport controlled, while at higher shear rates, platelet-surface reactions become controlling. For this study, shear rates were restricted between 125 and 500 s<sup>-1</sup>, in order to minimize surface platelet aggregation and thrombus formation, which are substantially enhanced at higher shear rates.

For laminar flow, the wall shear rate  $\gamma$  (s<sup>-1</sup>) in a slit flow chamber is

$$\gamma = \frac{3}{2} \frac{Q}{60Wb^2} \quad (2.1)$$

where  $Q$  is the volumetric flow rate (cc s<sup>-1</sup>),  $W$  is the slit width (cm), and  $b$  is the half-thickness of the flow slit (cm) [Sakariassen *et al.*, 1989]. Experimental and modeling requirements dictate that the slit width be much larger than the slit thickness. At the solid boundaries of the flow slit, along its width, a parabolic velocity profile (defined later in Eq.2.3) is no longer valid. Therefore, two dimensional modeling based on the incorporation of a defined velocity profile within the flow slit will be appropriate only if such a profile is not affected by the presence of side walls. Accordingly, the flow slit must have a large width to thickness ratio to justify the assumption of a semi-infinitely wide slit. These considerations will be discussed in subsequent sections.

### 2.3 Description of NO delivery device.

A novel NO delivery apparatus was designed to expose a flowing platelet suspension to NO as shown in Figs. 2.1*a* and 2.1*b*. The Plexiglas apparatus is composed of two sections. The lower section (A) contains a very thin flow slit ( $0.20 \pm 0.01$  mm deep, 10 mm wide, 70 mm long) with a perfusate inlet and outlet. The large ratio of the flow slit width to its thickness justifies the assumption of a semi-infinitely wide flow channel, necessary from modeling considerations. Flow rates between 0.5 and 5 cc min<sup>-1</sup> within the flow slit produces shear rates between 125 and 1000 s<sup>-1</sup>. In consideration of the squared dependence of shear rate on slit thickness (see Eq. 2.1), the thickness of the flow slit is machined with very high precision. The perfusion inlet and outlet shafts are inclined at 45° and have a diameter of 3 mm. The openings of the inlet and outlet shafts into the flow slit are located as close as possible to the axial extremities to avoid local pockets of stagnant liquid.

The upper section (B) of the delivery device contains a hollow chamber through which gas flows. The section of (B) extending over the downstream half of the flow slit contains a porous block (3.5 cm long) to allow gas to permeate into the perfusate flowing through the slit. The cylindrical pores in the block are 0.5 mm in diameter and are evenly spaced 1.0 mm apart. A gas-permeable silicone-polycarbonate membrane (38 μm thick, 15 mm wide, 75 mm long) (MEM-213, Membrane Products, Albany, NY) is uniformly attached to the lower surface of (B) using a spray adhesive. Perfusate in the upstream half of the flow slit is not exposed to gas. Analysis of the upstream membrane sections is therefore a logical means for establishing a common basis for comparing agonist-stimulated platelet deposition in control (N<sub>2</sub> exposure) and non-control (NO exposure)



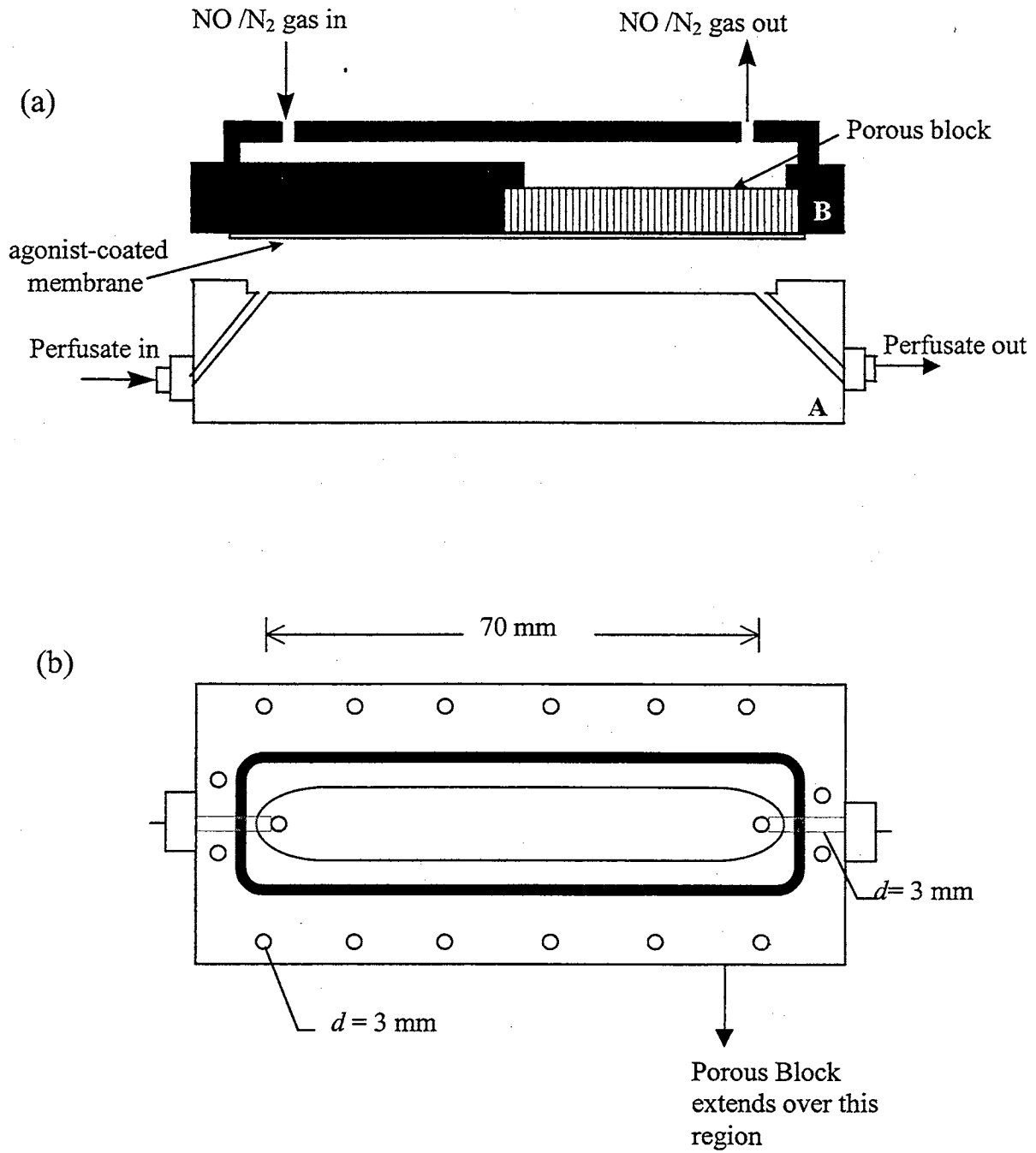


Figure 2.1. NO delivery device. (a) side view of upper (A) and lower (B) chambers. (b) top view of the lower block B containing the flow slit.

chambers. Sections A and B are attached with screws following the application of a thin coating of a platelet agonist to the membrane to enhance platelet deposition. Pharmed<sup>®</sup> tubing (i.d. = 3 mm) is connected to the perfusate inlet and outlet via polypropylene luer fittings. A dual syringe pump (Model 74900-10, Cole Parmer Instrument Co., Vernon Hills, IL) connected to the inlet was used for all perfusion studies.

In the device described above, NO gas was delivered to the perfusate in the downstream half of the flow slit via cylindrical pores placed in a staggered configuration. However, the size and configuration of the pores allowed gas delivery to the perfusate effectively over only 60 % of the slit width with the intermittent spaces between pores devoid of NO delivery. This design does not allow satisfaction of the necessary condition for uniform delivery of NO to liquid at all points along the slit width. The downstream porous region of block B was therefore later modified as a series of 20 parallel slits (0.5 mm wide) extending over the entire width of the flow slit (1 cm). The slits were spaced such that the last slit extended just over the opening of the outlet shaft into the flow slit (see Fig. 2.1b). The modified design ensures uniform gas delivery to the perfusate at all points along the slit width.

## **2.4 Nitric oxide delivery model.**

### *2.4.1 Objective*

Previous research on inhibition of platelet adhesion resulting from exposure to NO has focused upon quantifying concentrations of NO-donor compounds inhibiting adhesion [Groves *et al.*, 1993]. In some instances, gaseous NO or saturated NO solutions have been applied to experimental systems [Keh *et al.*, 1996; Konishi *et al.*, 1996]. However,

in these studies the spatial NO concentration and flux in the solution were not quantified. A knowledge of the NO concentration or flux which minimizes platelet adhesion at the adhesion site and the aqueous NO concentration to which platelets are exposed would be beneficial for the design of NO-releasing biomaterials. A proper design would minimize toxic and/or carcinogenic effects associated with excessive NO fluxes in addition to minimizing platelet adhesion. Therefore, a mathematical model was solved to generate aqueous NO concentration and flux profiles within the flow slit, for a given gaseous NO exposure. The model was experimentally validated prior to interpreting results of NO-platelet inhibition studies on the basis of aqueous NO concentrations and fluxes at the adhesion surface.

#### 2.4.2 Continuity equation.

To predict the aqueous NO concentrations and fluxes within the flow slit beginning at the porous block, the continuity equation for NO was solved for transport between parallel plates. The solution within the flow slit was assumed to be a dilute solution of constant physical properties flowing in fully developed laminar flow. The continuity for laminar flow in a semi-infinitely wide slit is

$$v_y \frac{\partial c}{\partial z} = D \frac{\partial^2 C}{\partial y^2} \quad (2.2)$$

where  $C$  is the aqueous NO concentration (M),  $D$  is the aqueous diffusivity ( $\text{cm}^2 \text{s}^{-1}$ ), and  $y$  and  $z$  are the spatial coordinates perpendicular to and along the direction of flow respectively. The local velocity,  $v_y$ , is represented in terms of the average velocity  $v$  ( $\text{cm s}^{-1}$ ) according to

$$v_y = \frac{3}{2} v \left[ 1 - 4 \left( \frac{y}{h} \right)^2 \right] \quad (2.3)$$

The model is based on steady-state conditions, absence of convection through the wall, negligible axial diffusion, and no reaction. The flow slit is also assumed to be semi-infinitely wide, an assumption justified by the large ratio of the slit width to the height ( $w/h = 50$ ). For flow slit dimensions such as these, concentration and flux profiles within the flow slit are essentially independent of the  $x$  direction (i.e., along the slit width).

#### 2.4.3 Boundary conditions.

Figure 2.2 shows the gas-exposed region of the flow slit depicting symmetry about the centerline ( $y = 0$ ) of the flow slit. The concentration of NO within the fluid is zero for  $z \leq 0$ . At  $z = 0$ , the fluid contacts the permeable membrane through which gaseous NO permeates. Thus,

$$C = 0 \quad \forall y, z = 0 \quad (2.4)$$

At the membrane surface ( $y = h/2$ ), the mass flux into the solution is equal to the mass flux through the membrane resulting in

$$-D \frac{\partial C}{\partial y} = k_m (C - C_0) \quad \forall z, y = h/2 \quad (2.5)$$

The membrane mass transfer coefficient ( $\text{cm s}^{-1}$ ) is  $k_m$  and  $C_0$  is the saturated aqueous NO concentration in equilibrium with the NO gas flowing through the gas chamber.

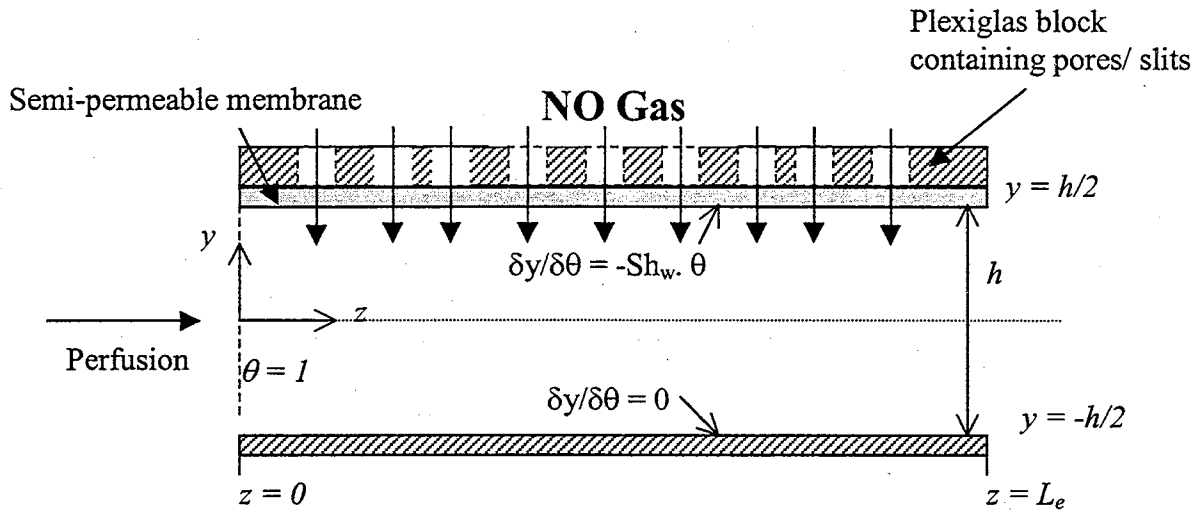


Figure 2.2. Porous block region of the flow slit showing dimensions and boundary conditions.

On the side of the flow slit opposite the membrane, the solid wall prevents any outflux of NO. Accordingly, the boundary condition at this surface is

$$-\frac{\partial C}{\partial y} = 0 \quad \forall z, y = -h/2 \quad (2.6)$$

#### 2.4.4 Non-dimensionalization.

The solution of the continuity equation subject to the boundary conditions above may be vastly simplified by expressing all parameters in terms of dimensionless variables. The dimensionless spatial coordinates are  $X=x/h$ ,  $Y=y/h$ , and  $Z=z/L_e$  where  $h$  (cm) is the thickness of the flow slit and  $L_e$  (cm) is the equivalent length of the flow path over which NO exposure occurs. In the pore/hole device, the equivalent length,  $L_e$ , is approximated as the sum of the porous hole diameters along the length of the porous block. In the redesigned device,  $L_e$  is approximated as the sum of the widths of the parallel slits in the porous block, along the direction of flow. In either case,  $L_e$  is 1.0 cm. Over any cross-section of the flow slit, the  $X$  and  $Y$  axes are along the center line such that  $X$  ranges from  $-25$  to  $25$  and  $Y$  from  $-0.5$  to  $0.5$ .  $Z$  ranges from  $0$  to  $1$ . The dimensionless NO concentration ( $\theta$ ) is given by

$$\theta = \frac{C - C_0}{C_i - C_0} \quad (2.7)$$

where  $C_i$  is the aqueous inlet NO concentration ( $C_i = 0$ ). The dimensionless form of Eq.

2.2 is thus

$$\frac{3}{2} \frac{vh^2}{DL_e} (1 - 4Y^2) \frac{\partial \theta}{\partial Z} = \frac{\partial^2 \theta}{\partial Y^2} \quad (2.8)$$

Correspondingly, the boundary conditions (Eqs. 2.4 - 2.6) are represented as

$$\theta = 1 \quad \forall Y, Z = 0 \quad (2.9)$$

$$\frac{\partial \theta}{\partial Y} = 0 \quad \forall Z, Y = -0.5 \quad (2.10)$$

$$\frac{\partial \theta}{\partial Y} = -N_{Sh_w} \theta \quad \forall Z, Y = 0.5 \quad (2.11)$$

The wall Sherwood number ( $N_{Sh_w}$ ) is a dimensionless grouping ( $k_m h/D$ ) which a measure of the ratio of the mass transfer resistance to gas in the fluid to that in the membrane.

#### 2.4.5 Model parameters.

The diffusivity ( $D$ ) of NO in the platelet suspension/buffer, assumed to be similar to the diffusivity of water, is  $2.7 \times 10^{-5} \text{ cm}^2\text{s}^{-1}$  at 23 °C [Wise and Houghton, 1968].

Knowing the dimensions of the flow slit, the average velocity ( $v$ ) of the perfusate is determined from the volumetric flow rate ( $Q$ ). For a specified gaseous NO exposure, the saturated aqueous NO concentration ( $C_0$ ) is obtained from the NO solubility in water which is  $2.4 \times 10^{-5} \text{ M cm Hg}^{-1}$  [Lange, N.A., *Ed.*, 1967]. A wall Sherwood number of 12.3 was determined using the membrane mass transfer coefficient ( $k_m$ ). For the membrane used in this study, the value of  $k_m$  was experimentally measured to be  $0.017 \text{ cm s}^{-1}$ . The experimental determination of  $k_m$  is detailed in the following section.

As a result of the semi-infinite width assumption, the model assumes that NO permeates entirely across the width of the flow slit resulting in a constant NO

concentration along the slit width at a given height. In the initially designed device, which delivers NO via porous holes, only 60 % of the slit width is exposed to NO. Therefore, the average spatial NO concentration along the slit width is corrected to be 60 % of the model prediction. The re-designed delivery device ensures uniform delivery of NO across the entire slit width, and requires no correction.

The model assumes insignificant NO consumption via reaction with O<sub>2</sub> within the flow slit. This is justified on the basis of the short residence time ( $\tau = 2$  s) of the perfusate in the slit relative to the reaction rate of NO with oxygen [Lewis and Deen, 1994]. However, this was confirmed experimentally, as described later.

#### *2.4.5.1 Determination of membrane mass transfer coefficient ( $k_m$ )*

Although the value for  $k_m$  for NO at 23 °C may be estimated from data provided by the manufacturer, the value was determined experimentally using a NO delivery device previously developed by Kavdia *et al.* (1998).

*Device description.* The device essentially consists of a central block of stainless steel, which incorporates a hollow rectangular slit through which N<sub>2</sub> gas flows as shown in Fig. 2.3. The slit is 15.0 cm long, 0.5 cm wide and 0.3 cm thick. The permeable membrane, gasket, and a peripheral gas-inlet/outlet chamber are bolted on to each side of the central block. The membrane is laminated to each side of the central block using silicone adhesive. The rubber gaskets placed between the central block and the peripheral gas inlet/outlet chambers prevent gas leaks. The peripheral blocks contain hollow chambers (15.0 cm long, 0.5 cm wide, 0.3 cm deep) via which NO/N<sub>2</sub> gas flows. Tube fittings are threaded into the chamber for attachment of gas lines. NO gas flowing



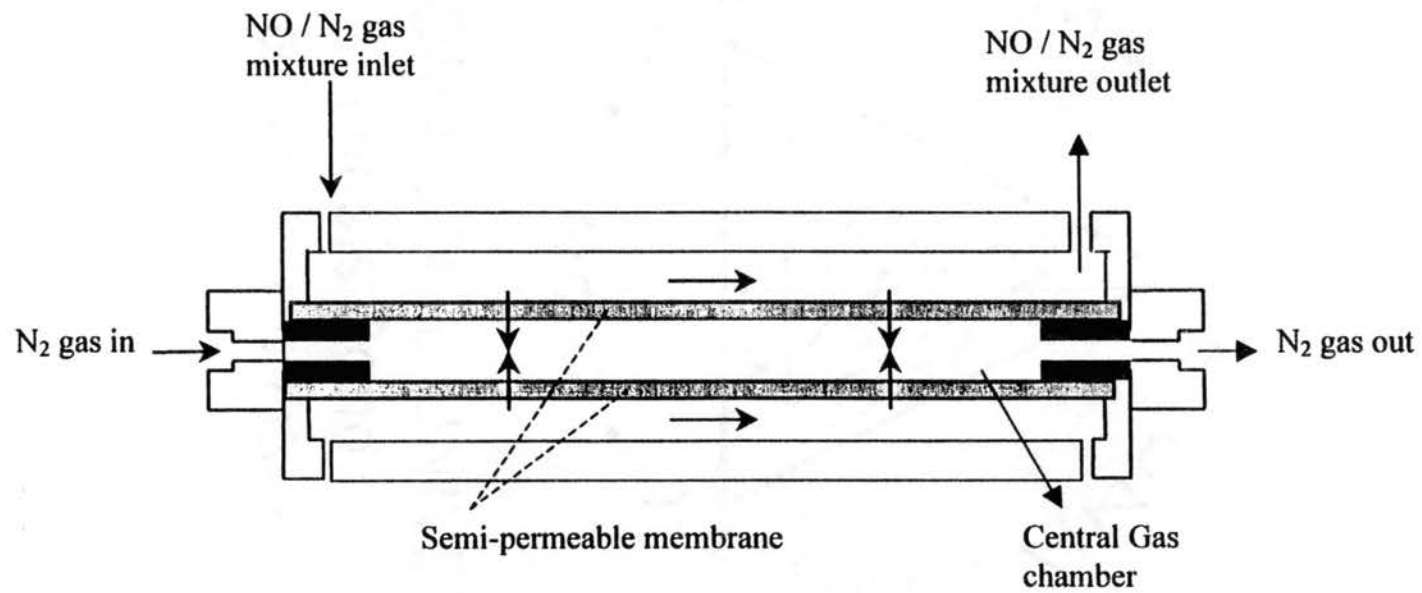


Figure 2.3. NO delivery apparatus for determination of membrane mass transfer coefficient ( $k_m$ ). Figure adapted from Kavdia *et al.* (1998).

through one or both peripheral gas chambers permeate through the membranes and into N<sub>2</sub> gas flowing through the slit in the central section.

*Experimental Protocol.* A NO/ N<sub>2</sub> gas mixture containing 2500 or 5000 ppm of NO continuously flowed through the peripheral sections of the device while N<sub>2</sub> continuously flowed through the central portion, separated from the peripheral section by only the membrane. Thus, NO transported across the membrane into the N<sub>2</sub> stream. The membrane mass transfer coefficient ( $k_m$ ) is determined by

$$k_m A C_g' = Q' C' \quad (2.12)$$

where  $A$  represents the total membrane surface area for mass transfer of NO (15 cm<sup>2</sup>),  $C_g$  is the NO concentration in the NO/N<sub>2</sub> mixture and  $C'$  is the outlet NO concentration in the N<sub>2</sub> stream. The flow rate of the N<sub>2</sub> stream ( $Q'$ ) was maintained at 1000 cc min<sup>-1</sup>, a value high enough so as to ensure that  $C_g' \gg C'$  at all points for Eq. 2.12 to be valid. Since the NO/N<sub>2</sub> flow rate was very high,  $C_g$  was essentially constant along the length of the device. Thus, a constant NO flux existed across the entire length of the membrane. Gas samples were drawn at the NO and N<sub>2</sub> inlet and outlet ports respectively and analyzed for NO concentration using a chemiluminescence detector (NOA 270B, Seivers Instruments, Boulder, CO).

*Results.* The value of  $k_m$  was experimentally measured as  $0.017 \pm 0.002$  cm s<sup>-1</sup> at 23 °C, compared to a suggested value of 0.008 cm s<sup>-1</sup> (MEM-213 Product Information, Membrane Products, Albany, NY). This value was independent of gaseous NO exposure levels as expected.

#### 2.4.6 MATLAB<sup>®</sup> specifications.

Equation 2.8 was solved using the partial differential equation (PDE) toolbox option in MATLAB<sup>®</sup> to obtain  $\theta$ , and thus the spatial NO concentration ( $C$ ) from Eq. 2.7. The PDE solver in MATLAB<sup>®</sup> is based on the *Finite Element Method* (FEM). For solving the problem at hand, the graphical user interface (GUI), 'pdetool' was used.

*Geometry definition.* Initially, a grid was created wherein the x-axis and y-axis grid spacing is defined. The grid spacing and axis limits were based on the ranges of the dimensionless spatial coordinates  $X$  (-25 to 25) and  $Y$  (-0.5 to 0.5). In the *draw mode*, a rectangle was drawn upon the above grid with the coordinates (-25,0.5), (25,0.5), (25,-0.5), and (-25,-0.5) respectively. The rectangle represented the cross-section of the flow slit.

*Boundary Conditions.* Within the boundary mode, the boundary conditions for each of the four boundary segments were specified in the specification dialog box (see Fig. 2.4a). Two different condition types are available in this menu. The first is a generalized Neumann condition where the boundary condition determined by the coefficients  $q$  and  $g$  according to the equation

$$\bar{n} \cdot (c \nabla u) + qu = g \quad (2.13)$$

where  $n$  is a unit vector. The second type of boundary condition is a Dirichlet condition of the form  $hu = r$  wherein  $u$  is specified. For the solution of Eq. 2.8 over the geometry defined above, the boundary conditions at all edges correspond to Neumann conditions.

Comparing with the boundary conditions specified at  $Y = -0.5$  and  $Y = 0.5$  in Eqs. 2.10 and 2.11 respectively, a value of zero was assigned to  $g$ . Parameter  $q$  was assigned a value of 1.0 for the boundary condition at  $Y = -0.5$ , while a value equal to the wall Sherwood number ( $N_{Shw} = 12.3$ ) was specified at  $Y = 0.5$ . As discussed earlier, the velocity profile incorporated in Eq. 2.8 is invalid at the boundaries in the X-direction. Therefore, a semi-infinitely wide slit was assumed. However, one of the disadvantages of MATLAB<sup>®</sup> is that for defining a problem over a geometry as that described above, conditions need to be specified at all boundaries. Hence, although Eq. 2.8 is not strictly applicable at the solid-wall boundaries at  $X = -25$  and  $X = 25$ , conditions of zero flux were specified. Hence, parameters  $q$  and  $g$  are specified as 1.0 and 0 respectively. As will be discussed later in section 2.6.1, this assumption does not significantly affect model predictions over most regions of the flow slit.

*PDE specification.* Upon entering the partial differential equation mode, the PDE is specified in the PDE dialog box (see Fig. 2.4b). MATLAB<sup>®</sup> is capable of handling four kinds of PDEs with different levels of complexity- elliptic, parabolic, and hyperbolic PDEs or eigenvalue problems. Eq. 2.8 corresponds to a generic parabolic PDE of the form

$$d \frac{\partial u}{\partial t} - \nabla \cdot (c \nabla u) + au = f \quad (2.14)$$

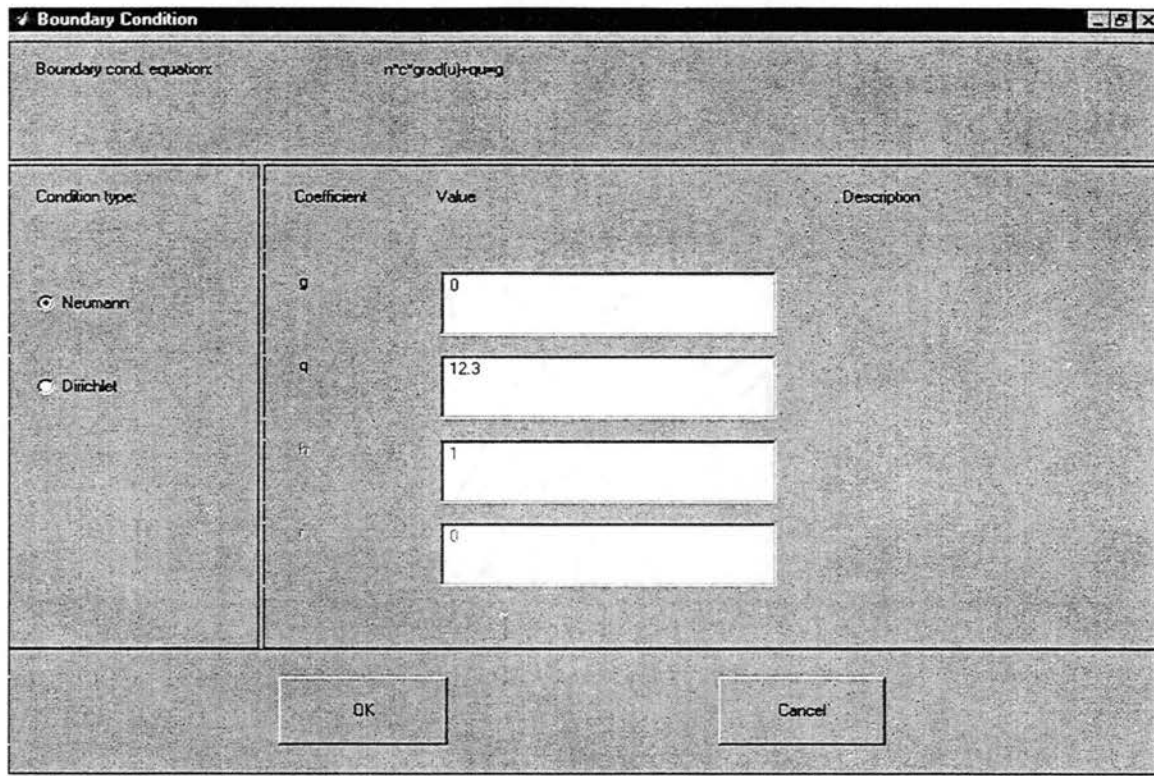


Figure 2.4a. Dialog box within the boundary mode of MATLAB® for specification of boundary conditions. In the above example, the parameters for the boundary condition at  $Y = 0.5$  (NO delivery surface) have been specified.

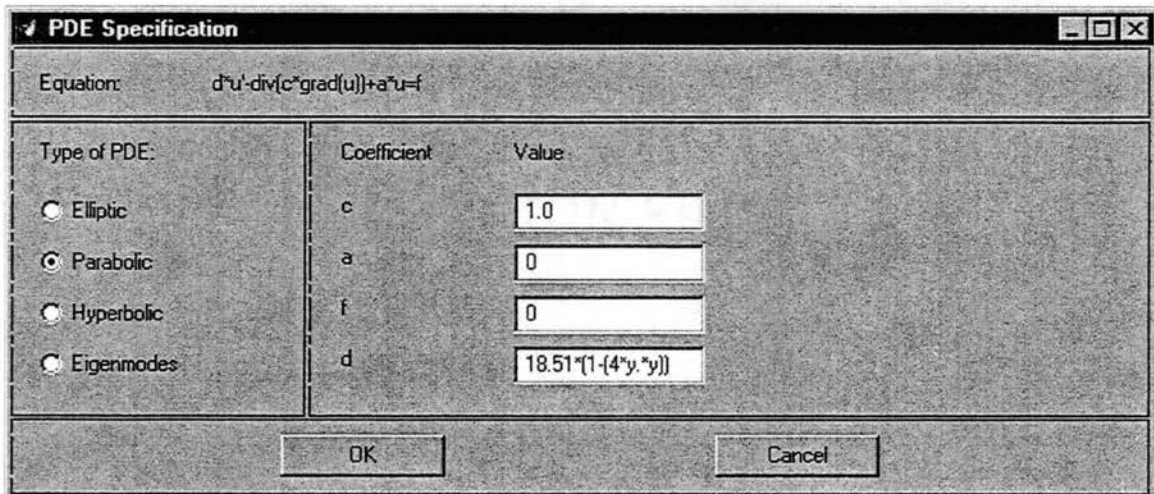


Figure 2.4b. PDE specification dialog box showing the generic parabolic equation and the corresponding parameters of Eq. 2.8 specified.

wherein  $\theta$  and  $t$  correspond to  $u$  and  $Z$  respectively. In Eq. 2.14,  $a = 0$ ,  $f = 0$ , and  $d = vh^2/DL_e [1-4Y^2]$ . The parameters are typed into the PDE specification dialog box as per MATLAB<sup>®</sup> conventions.

*Mesh generation and solving.* In the mesh mode, an initial triangular mesh was created. The mesh size is dependent on the geometry. Selecting the 'refine mesh' option uniformly refines the mesh. In the solve mode, solve parameters are specified. For the solution of Eq. 2.8, a MATLAB vector of distances along the  $Z$  direction (in place of the time parameter) is generated. The length of exposure is specified to range between  $Z = 0$  and  $Z = L_e$  as shown (0:1.0) in the dialog box in Fig. 2.4c. The initial value of the solved parameter  $u$  (i.e.,  $\theta$ ) is also specified [ $u(t0) = 1.0$ ] as per Eq. 2.9. The solution is displayed as a plot as per specifications made in the plot solution dialog box. For display of  $\theta$  values, the property option is set to 'u' as shown in Fig. 2.4d. For calculation of flux values, the generation of the absolute gradient profiles by setting the property option to [ $\text{abs}(\text{grad}(u))$ ] is more useful. Spatial NO fluxes in the  $y$  direction (perpendicular to the membrane surface) may then be obtained by multiplying the NO diffusivity with the concentration gradient in the  $y$  direction according to Fick's law.

#### 2.4.7 Prediction of bulk aqueous NO concentration at slit exit.

Prior to using the model to predict spatial NO concentrations and fluxes within the flow slit and relate them to inhibitory effects of NO on surface platelet deposition, the model must be validated. To validate the model, the velocity-weighted bulk NO concentration ( $C_b$ ) exiting the device was predicted and compared with values measured experimentally. For plug flow, the liquid exits the flow slit at an equal rate, and the

exiting concentration is given by the average of concentrations at each point along the thickness of the flow slit. However, when the velocity profile is parabolic, as is the situation for this study, the bulk aqueous NO concentration exiting the device is a velocity-weighted average determined from

$$C_b(z) = \frac{\int_{-h/2}^{h/2} v_y C(z) dy}{\int_{-h/2}^{h/2} v_y dy} \quad (2.15)$$

This is the aqueous NO concentration that would be measured if the liquid exiting the flow slit were collected in a container and thoroughly mixed [Colton and Lowrie, 1977]. Since the flow slit width is much greater than the slit height, the NO concentration predicted by the model is essentially only a function of  $Y$  and  $Z$  (the dimensionless slit height and length coordinates, respectively). In dimensionless form, eq. 2.15 is represented as

$$\theta_b(z) = \frac{\int_{-1/2}^{1/2} (1 - 4Y^2) \theta(z) dY}{\int_{-1/2}^{1/2} (1 - 4Y^2) dY} \quad (2.16)$$

As mentioned earlier, only 60% of the slit width was exposed to NO gas in the initially designed device. Therefore, the bulk aqueous NO concentration at the slit exit for this design is expected to be 60% of the value determined from Eq. 2.16.

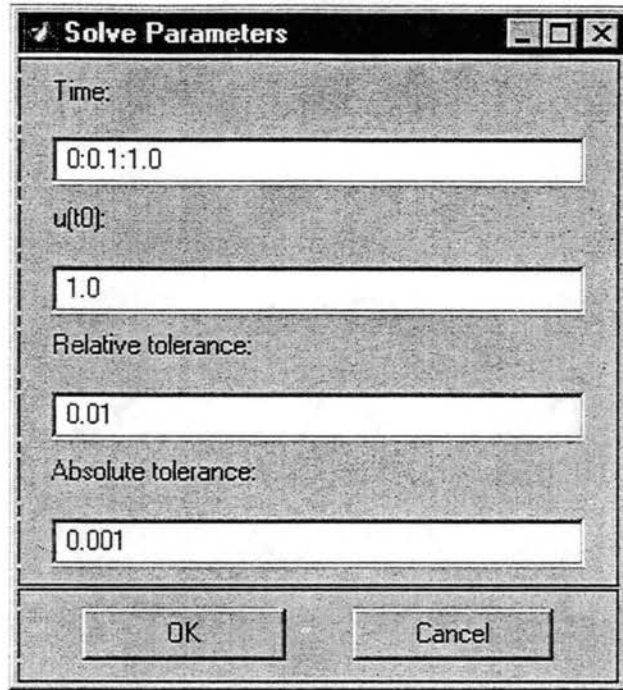


Figure 2.4c. Specification of solve parameters in the solve mode. For the current problem specified by Eq. 2.8, the dimensionless spatial coordinate 'Z' along the length of exposure of NO, is substituted for the time.

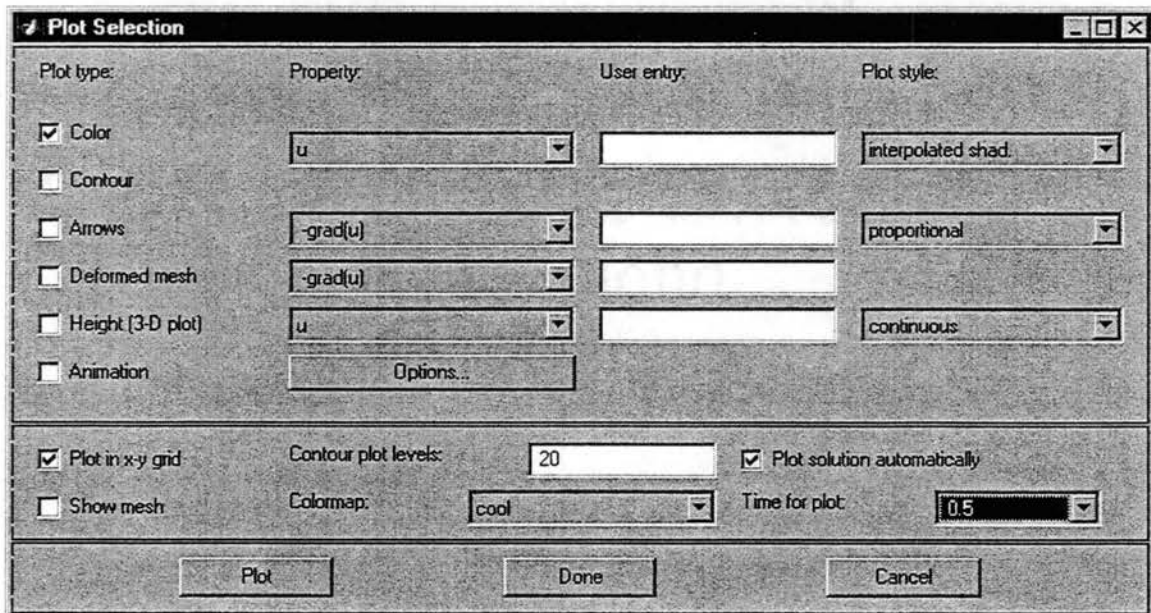


Figure 2.4d. Solutions are displayed as per plot specifications made in the plot solution dialog box. In the above example, the dimensionless concentration ( $\theta$ ) profile over the height of the slit will be displayed as a color-coded plot, at  $Z=0.5$ .



## 2.5 Experimental methods for measurement of aqueous NO concentration.

### 2.5.1 Reagents.

Ultra-high purity nitrogen, following passage through an oxygen trap, was mixed with a mixture of NO and nitrogen using controlled gas-flow meters (Porter Instrument Co., Hatfield, MA) to obtain the desired gaseous NO concentration. All gas mixtures were prepared in a certified hood to avoid the potential toxicity of NO. BSGC buffer (pH 7.3) contained 218 mg  $K_3PO_4$ , 1.2 g  $NaH_2PO_4$ , 7.0 g NaCl, 4.0 g sodium citrate, and 2.0 g of glucose in one liter of deionized water. Nitrite ( $NO_2^-$ ) reducing solution consisted of a mixture of potassium iodide and glacial acetic acid in a 1:3 volumetric ratio. Nitrite standards were prepared using sodium nitrite. Potassium iodide was procured from Fisher Chemicals (Fairlawn, NJ). Glacial acetic acid, glucose, sodium chloride, and sodium nitrite were purchased from Sigma Chemicals (St. Louis, MO). Phosphate salts and sodium citrate were obtained from EM Science (Gibbstown, NJ). Buffered saline (PBS, 1 $\times$ ).

### 2.5.2 Experimental Protocol.

The bulk aqueous NO concentration exiting the NO delivery apparatus was measured to validate the model predicting spatial NO concentrations and fluxes within the flow slit. Model -based predictions for both the original (cylindrical pore) and re-designed (parallel slit) NO delivery devices were validated. Platelet-free BSGC buffer was perfused through the slit at a wall shear rate of  $250 \text{ sec}^{-1}$  (1 cc/min) and at room temperature. Simultaneously, the gas chamber in the delivery device (original or modified) was continuously purged with gaseous NO concentrations of 10,000 ppm ( $C_0 = 18.6 \mu\text{M}$ ). A

high NO concentration was necessary to enhance the detection of NO. In either case, aqueous samples (1 cc) were drawn at the slit outlet into a gas-tight Hamilton® syringe (Hamilton Company, Reno, NV). Care was taken to ensure that the rate of drawing the samples was less than the flow rate through the slit.

The experimental setup for NO analysis is shown in Fig. 2.5. 0.2 ml of the liquid sample was injected into 10 ml of  $\text{NO}_2^-$  reducing solution contained in a glass vial. The reducing solution was continuously stirred with a magnetic stirrer and bubbled with  $\text{N}_2$  at 1 *scfh* to purge NO from the solution. NO transported to the headspace was drawn into a chemiluminescence analyzer (Model NOA 270B, Seivers Corporation, Boulder, CO) via an applied vacuum. Oxygen supplied to the chemiluminescence detector is converted into ozone, which reacts with NO to generate luminescence. The luminescence is proportional to the amount of NO (see Figure 2.5). An acid trap immersed in an ice bath was included in the vacuum line to condense and remove acid vapors from the gas.

The concentration of NO in the sample was obtained by comparison with  $\text{NO}_2^-$  standards since  $\text{NO}_2^-$  is completely converted to NO in the reducing solution. A calibration with  $\text{NO}_2^-$  standards was performed prior to each experiment. Since  $\text{NO}_2^-$  can form via the reaction of NO with  $\text{O}_2$  or  $\text{NO}_2$ , the contribution of  $\text{NO}_2^-$  to the NO assay of the sample was assessed. To assess  $\text{NO}_2^-$  formation within the flow slit, a second sample (1 cc) was drawn at the perfusion outlet. In initial studies, this sample was purged with  $\text{N}_2$  for 45 minutes in an  $\text{O}_2$ -depleted glass vial to remove gas-soluble NO. 0.2 cc of the purged sample was analyzed in the  $\text{NO}_2^-$  reducing solution as described above. The NO concentration in the sample was obtained by subtracting the amount of  $\text{NO}_2^-$  in the sample determined from the earlier NO assay.

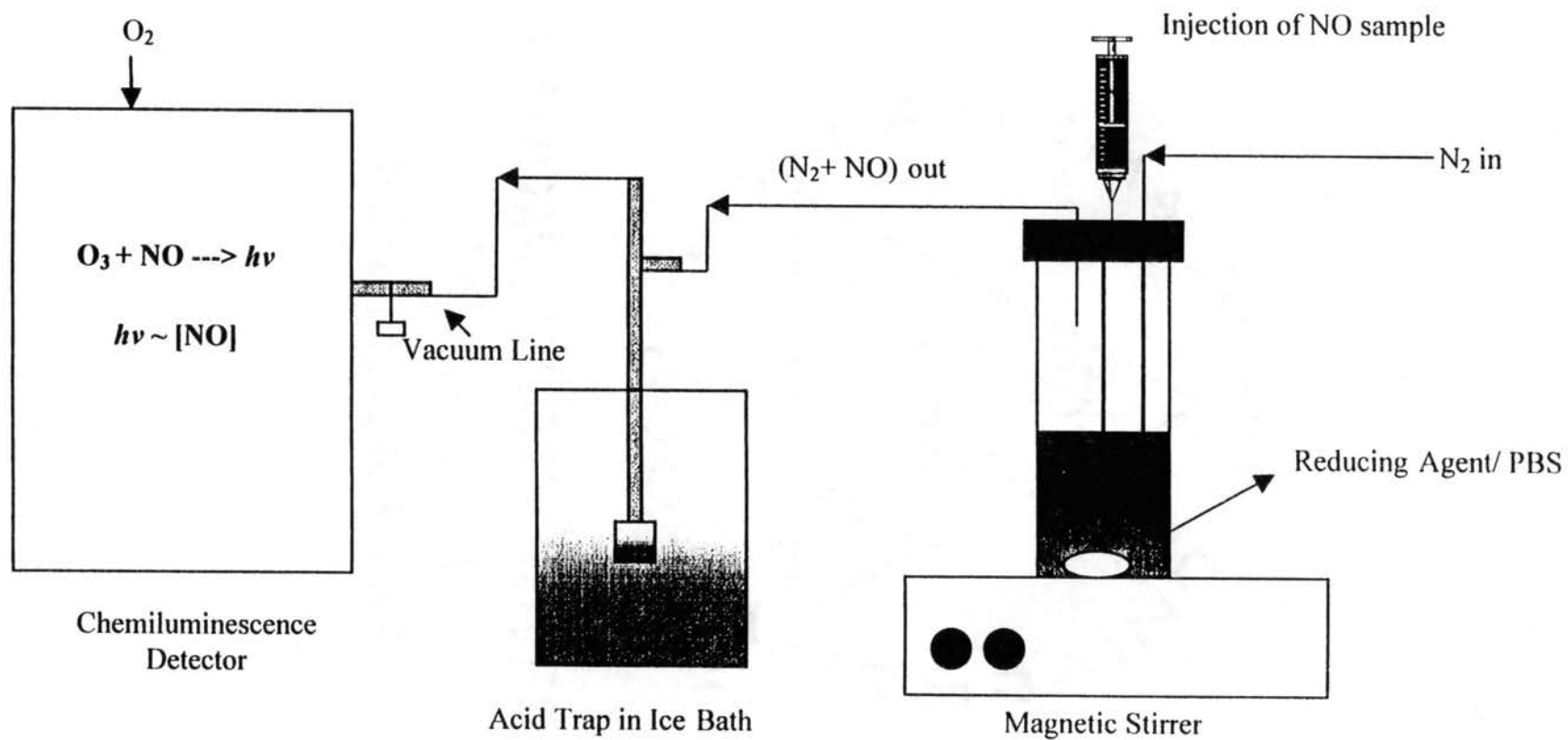


Figure 2.5. Experimental setup for NO and NO<sub>2</sub><sup>-</sup> analysis.

The above method of  $\text{NO}_2^-$  analysis did have certain disadvantages. There was a possibility that  $\text{NO}_2^-$  detected in the sample was formed during the purging with  $\text{N}_2$ , rather than via reaction of NO within the flow slit. In fact, occasionally, detected  $\text{NO}_2^-$  levels were in excess of the maximum  $\text{NO}_2^-$  levels that could theoretically be formed, and predicted on the basis of the second order reaction kinetics of NO with  $\text{O}_2$  [Lewis and Deen, 1994]. To avoid such anomalous situations, the method of  $\text{NO}_2^-$  analysis was modified. Therefore, for  $\text{NO}_2^-$  analysis of the liquid exiting the flow slit, a 1 cc sample was drawn at the slit exit similar to the above case. However, instead of purging the sample as described above, 0.2 cc of the sample was injected directly into the analysis setup containing 10 cc of PBS, rather than  $\text{NO}_2^-$ -reducing solution. In PBS,  $\text{NO}_2^-$  in the injected sample is not reduced to NO. Therefore, only free NO in the sample was detected via chemiluminescence.

## 2.6 Results.

### 2.6.1 Model validation.

Model predictions for NO concentration and flux profiles within the flow slit were predicted and validated following exposure of flowing BSGC buffer to a gas NO concentration of 10,000 ppm. The corresponding saturated aqueous NO concentration ( $C_o$ ) is 18.6  $\mu\text{M}$ , based on a solubility of  $2.4 \times 10^{-5}$  M cm of  $\text{Hg}^{-1}$  in water [Lange, N.A., Ed., 1967]. The NO-exposed fluid at the exit of the flow slit was analyzed by chemiluminescence in both an  $\text{NO}_2^-$ -reducing agent (for measurement of NO and  $\text{NO}_2^-$ ) and in PBS (for measurement of NO alone). The formation of  $\text{NO}_2^-$  indicates a reaction of NO with  $\text{O}_2$ . The possibility of  $\text{NO}_2^-$  formation due to trace impurities of  $\text{NO}_2$  was

eliminated subsequent to analysis of the gas following flow through a soda lime column.

Analysis of the total and unreacted NO concentrations in the fluid exiting the delivery device(s) indicated that NO reacted very sparingly with O<sub>2</sub> (<5 %) within the flow slit, even at high exposures. The dimensionless bulk aqueous NO concentration ( $C_b/C_0$ ) exiting the flow slit was measured as  $0.18 \pm 0.02$ ,  $0.10 \pm 0.01$ , and  $0.07 \pm 0.01$  ( $n = 3$  for all cases) for the porous/holed device at wall shear rates of 125, 250, and 500 s<sup>-1</sup> respectively ( $n = 3$  at each shear rate). Fig. 2.6 shows  $C_b/C_0$  as a function of wall shear rate for this device. The dotted line represents predicted values that are in excellent agreement with experimental results.

The  $C_b/C_0$  ratio was also determined as a function of the wall shear rate, for the parallel-slit device. For this device, the dimensionless bulk aqueous NO concentrations at the slit exit were measured as  $0.30 \pm 0.03$ ,  $0.20 \pm 0.01$ , and  $0.11 \pm 0.01$  at shear rates of 125, 250, and 500 s<sup>-1</sup> respectively ( $n = 3$  at each shear rate). Fig. 2.7 shows that predicted values (dotted line) agree well with experimental results (discrete symbols) when NO is delivered via the parallel-slit chamber. Previous experiments also indicated that the value of  $C_b/C_0$  is independent of the NO gas concentration. A 10% variation in membrane permeability (with or without a simultaneous 10% variation in NO diffusivity) did not influence predictions. Thus, the model can be used to accurately predict NO surface concentrations for the experiments of this study, irrespective of the device used.

Noticeably, in either set of results, increasing shear rates result in a lower value of  $C_b/C_0$ . This is due to a greater deviation in equilibrium between the bulk aqueous NO and the NO in the gas phase. The increased deviation at higher shear (or flow) rates is

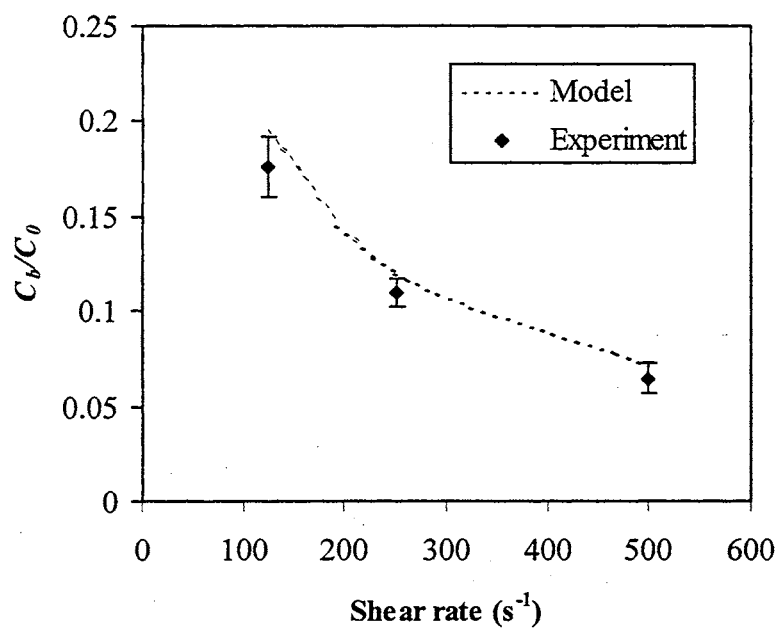


Figure 2.6. Bulk aqueous NO concentration ( $C_b$ ) exiting the originally designed NO delivery apparatus relative to the saturated NO concentration ( $C_0$ ) at various wall shear rates. Symbols represent Means  $\pm$  SD for each shear rate ( $n = 3$ ) at room temperature.

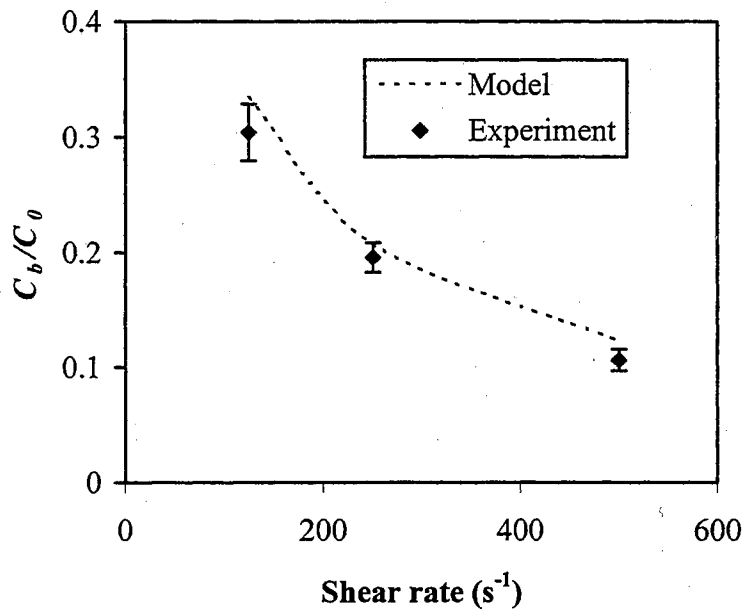


Figure 2.7. Bulk aqueous NO concentration ( $C_b$ ) exiting the modified NO delivery apparatus relative to the saturated NO concentration ( $C_0$ ) at various wall shear rates. Symbols represent Means  $\pm$  SD for each shear rate ( $n=3$ ) at room temperature.

due to reduction in the exposure time of the liquid to the gas and the concomitant reduction in the capacity for the solution to attain equilibrium.

### 2.6.2 Spatial NO concentration and flux profiles.

The velocity-weighted aqueous NO concentrations measured at the exit of the delivery device (with cylindrical holes or parallel slits for gas permeation) were in very good agreement with model predictions. The mathematical model represented by Eq. 2.8 may be reliably used to generate spatial NO concentration and flux profiles. Fig. 2.8 shows the predicted dimensionless NO concentration and flux profiles at the perfusion outlet ( $z = L_e$ ) as a function of the slit height for shear rates of 125, 250, and 500  $s^{-1}$ . The predictions correspond to the porous/holed device.  $C/C_0$  at the membrane surface ( $y/h = 0.5$ ) are 0.51, 0.49, and 0.46 for shear rates of 125, 250, and 500  $s^{-1}$  respectively (see Fig. 2.8a). Fig. 2.9 is a similar plot shown for the parallel-slit NO delivery device. When NO is delivered uniformly over the entire width of the flow slit, the value of  $C/C_0$  at the surface is predicted as 0.88, 0.84, and 0.80 at wall shear rates of 125, 250, and 500  $s^{-1}$  respectively (see Fig. 2.9a). As evident in both Figs. 2.8a and 2.9a, an increase in the shear rate reduces the amount of NO in solution relative to saturation with the gas. This is due to the lower exposure times of the liquid to the gas at higher shear rates.

The flux profiles for the porous/holed and parallel-slit devices are shown in Figs. 2.8b and 2.9b. The fluxes are shown relative to the saturated aqueous NO concentration. In both these flux plots, the flux at the membrane surface increases with increase in shear rate. An increase in shear (or flow) rate causes a reduction in the mass-transfer resistance for NO at the membrane surface. However, the flux across the slit height also depletes



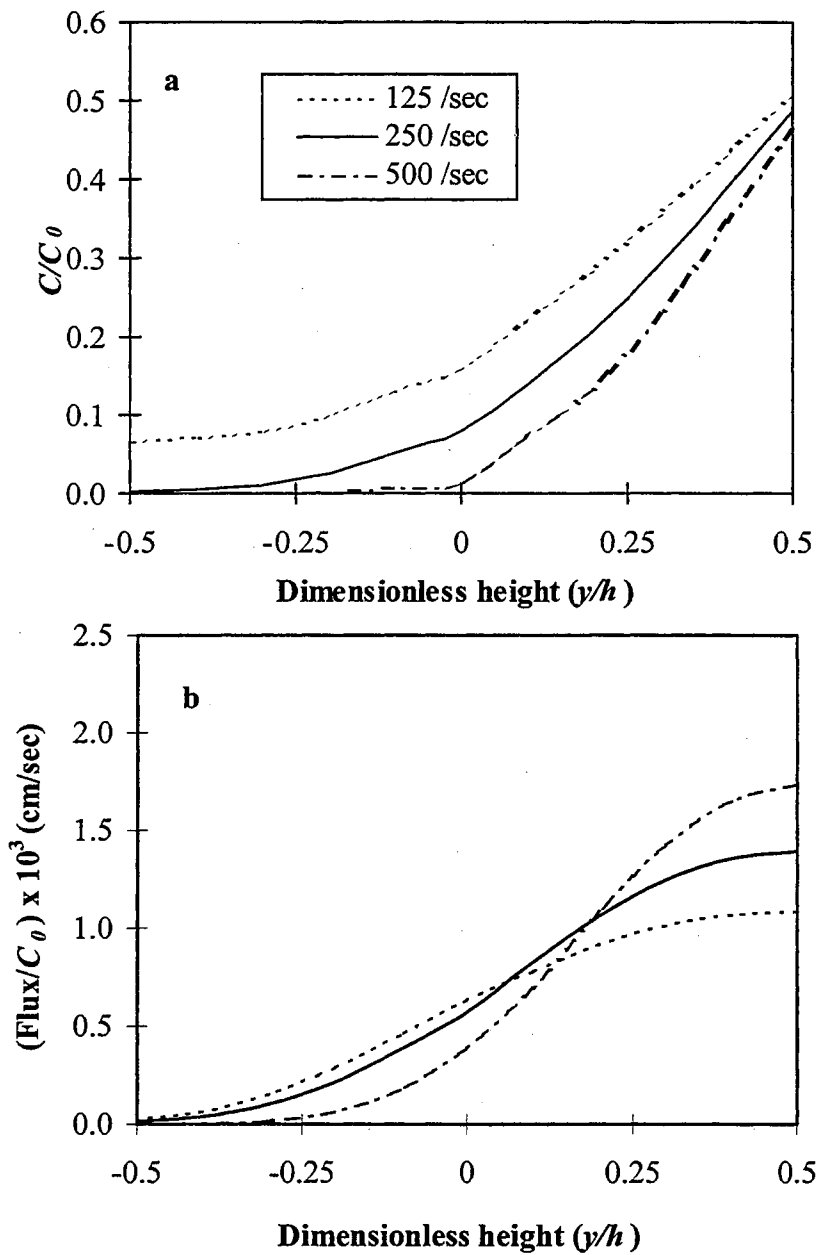


Figure 2.8. Nitric oxide flux and concentration ( $C$ ) at the flow slit outlet as a function of the slit height and wall shear rate and relative to the saturated NO concentration ( $C_0$ ). The profiles were predicted from Eq. 2.8, for the delivery device wherein NO gas was delivered via cylindrical pores.

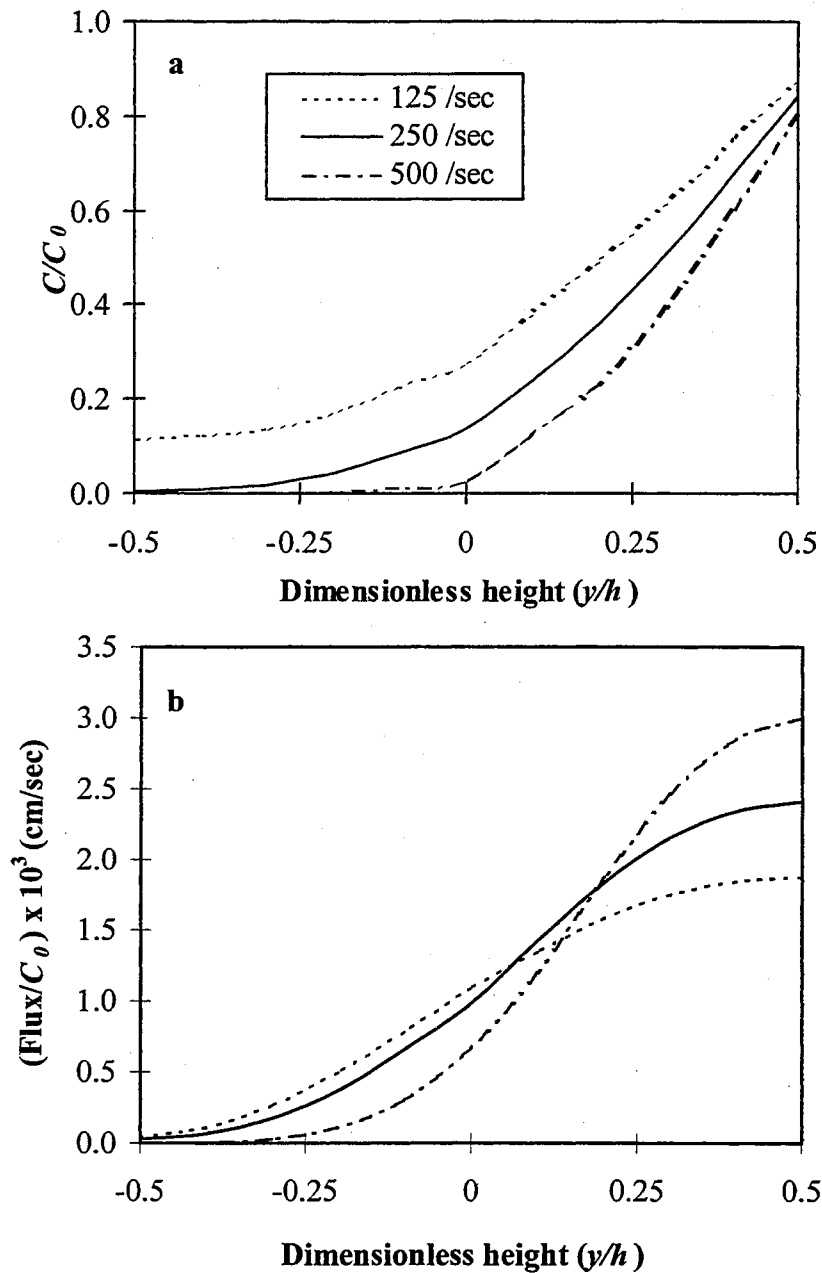


Figure 2.9. Nitric oxide flux and concentration ( $C$ ) at the flow slit outlet as a function of slit height and wall shear rate and relative to the saturated NO concentration ( $C_0$ ). The profiles were predicted from Eq. 2.8, for the delivery device wherein NO gas is uniformly delivered across the slit width via parallel slits.

faster at higher shear rates due to a more rapid depletion of the concentration gradient. At a wall shear rate of  $250 \text{ s}^{-1}$  and for a gas NO exposure of 10,000-ppm ( $C_0 = 18.6 \text{ }\mu\text{M}$ ), the flux at the membrane surface in the porous/holed and parallel-slit delivery devices are 26 and 45 picomoles  $\text{cm}^2 \text{ s}^{-1}$  respectively.

Figures 2.10 and 2.11 show for the original and modified devices the model-predicted dimensionless NO concentration and flux profiles in the flow slit as a function of length of exposure. The profiles are plotted for wall shear rates of 125, 250, and  $500 \text{ s}^{-1}$ . As seen in the dimensionless concentration profiles 2.10*a* and 2.11*a*, the NO concentration at the membrane surface is roughly 35-50% and 60-86% of saturation for the porous/holed and parallel slit devices, respectively. For any given shear rate, the surface NO concentration does not change appreciably along the flow slit length. However, the flux profiles shown in Figs. 2.10*b* and 2.11*b*, deplete much more rapidly (by  $\sim 45\%$  at  $500 \text{ s}^{-1}$  to  $\sim 60\%$  at  $125 \text{ s}^{-1}$ ) along the flow slit length. Along the flow slit length, there is an increase in the bulk aqueous NO concentration that results in a reduced concentration gradient (or flux). At the inlet to the gas exposure region ( $z/L_e = 0$ ), the bulk aqueous NO concentration is zero and hence the flux will be greatest at that point.

## 2.7 Conclusions.

A novel NO-delivery system was developed to study NO inhibition of platelet deposition on biomaterial surfaces. Previous studies involving NO effects on platelet adhesion/aggregation on surfaces have not quantified the spatial NO concentration and flux in solution, especially at the adhesion surface. A model was thus developed to predict spatial NO concentrations and fluxes within the flow slit. The model was

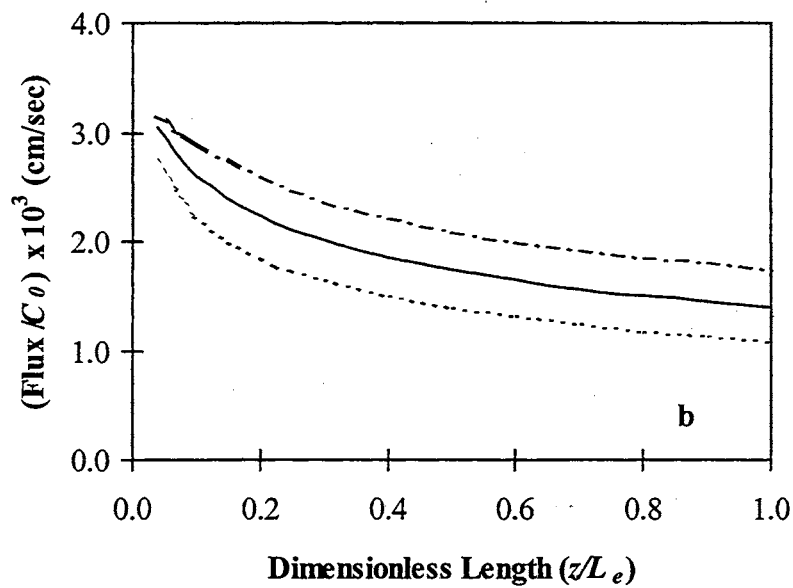
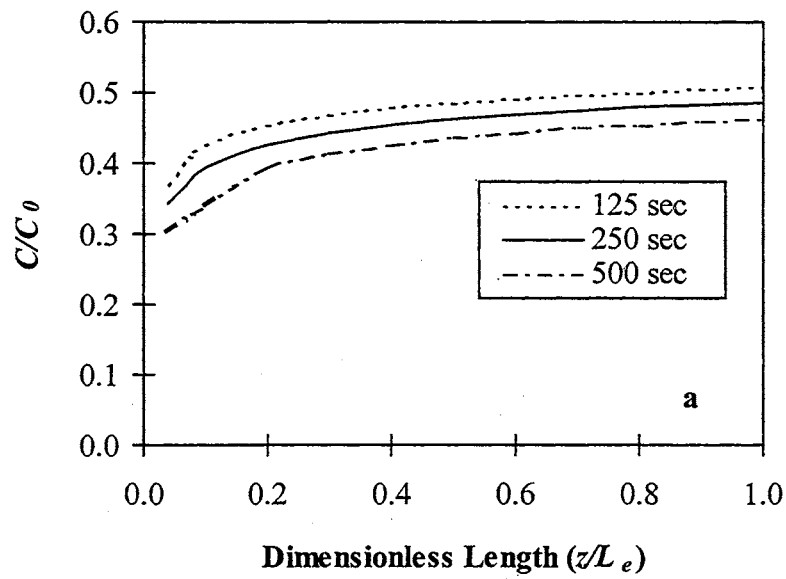


Figure 2.10. Nitric oxide concentration ( $C$ ) and flux profiles at the NO delivery surface shown as a function of dimensionless length of exposure and wall shear rate. Values are shown relative to the saturated aqueous NO concentration ( $C_0$ ). Profiles were predicted from Eq. 2.8 for the device incorporating NO delivery via porous holes.

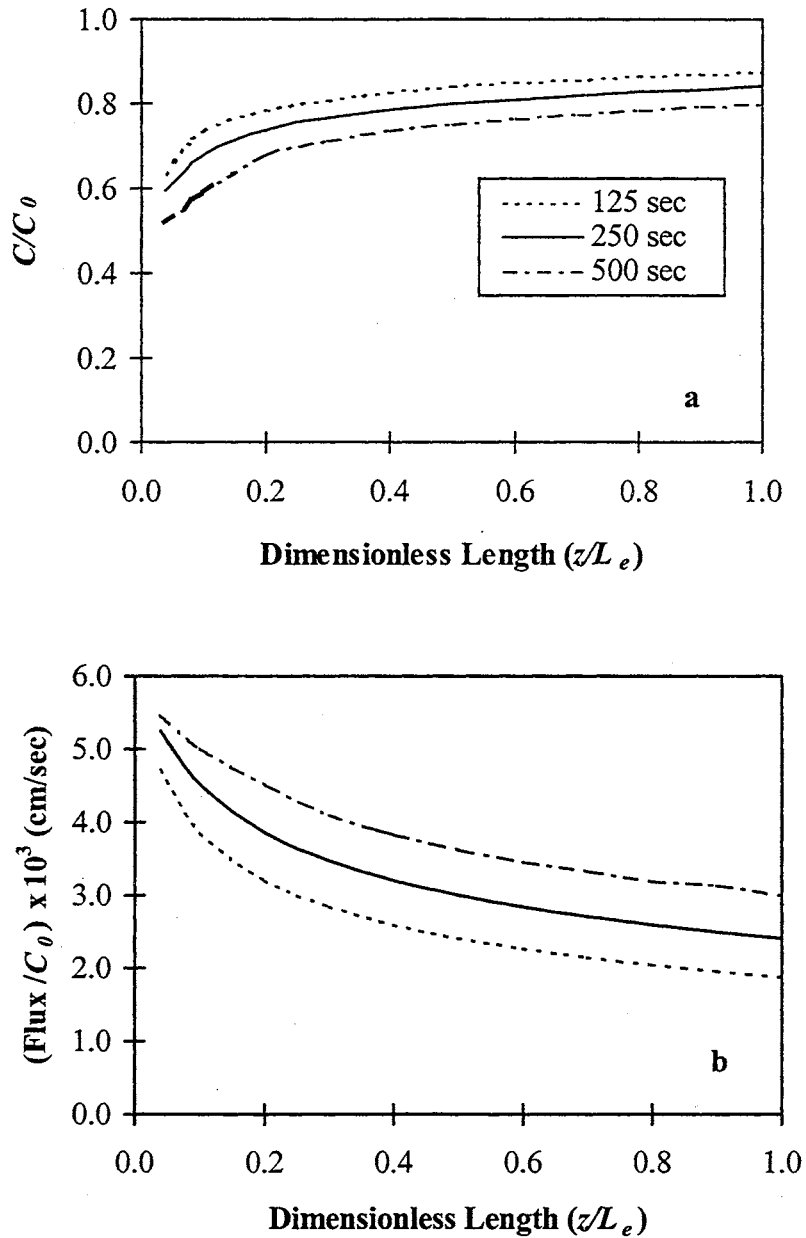


Figure 2.11. Nitric oxide concentration ( $C$ ) and flux profiles at the NO delivery surface shown as a function of dimensionless length of exposure and wall shear rate. Values are shown relative to the saturated aqueous NO concentration ( $C_0$ ). Profiles were predicted from Eq. 2.8 for the device incorporating NO delivery via parallel slits.

successfully validated by experiment. This model may be used to predict spatial NO concentrations and fluxes within a perfusing platelet suspension. Knowledge of these concentrations or fluxes can yield useful information towards the development of novel biomaterials that incorporate and release NO to inhibit surface thrombosis.

## CHAPTER 3

### EFFECT OF NO EXPOSURE ON PLATELET DEPOSITION

#### 3.1 Introduction.

In previous *in vitro* and *in vivo* studies, NO was shown to inhibit platelet adhesion and aggregation. However, the aqueous NO concentrations or fluxes inhibiting platelet deposition at the adhesion surface were not quantified. In some studies, NO gas was demonstrated to attenuate platelet deposition on biomaterial surfaces [Keh *et al.*, 1996]. However, the gas exposures adopted were in far excess of allowable toxic limits (25 ppm) recommended by OSHA. Therefore, the primary objective of the current study is to establish the minimal NO exposure that significantly inhibits platelet deposition on biomaterials.

A novel perfusion/NO delivery device was developed to study NO inhibition of platelet deposition on biomaterials. The biomaterial was coated with collagen, a potent agonist of platelet deposition to simulate the deposition of platelets in response to surface deposition of thrombogenic plasma proteins, or ECM. Collagen is the primary component of ECM. Initially, qualitative experiments were performed to demonstrate the feasibility of the device. Following, quantitative platelet adhesion studies were carried out to determine the minimal NO exposure required for significant inhibition of platelet deposition to a collagen-coated biomaterial. An added objective was to estimate aqueous surface NO concentrations and fluxes which significantly inhibited platelet deposition.

The realization of these objectives would provide quantified guidelines for controlled and safe delivery of NO at biomaterial surfaces to reduce platelet deposition.

### 3.1.1 Platelet perfusates: whole blood, plasma, and platelet suspensions.

For studies investigating hemocompatibility of biomaterials, various perfusates may be used. These include non-anticoagulated blood, anticoagulated blood, plasma, and suspensions of washed platelets in defined buffers. The choice of perfusate depends upon the objective of the investigation. Non-anticoagulated blood was usually drawn from the blood vessel into the perfusion system and was generally used for *ex-vivo* studies. For the current work, anticoagulated (or citrated) blood, platelet rich plasma (PRP) or a washed platelet suspension was used.

Whole blood contains numerous blood factors and components that cannot be replicated in reconstituted media. Therefore, to most closely simulate *in vivo* blood circulation in *in vitro* studies, whole blood should be used. However, to reduce coagulation during handling, whole blood must be citrated immediately following collection. For studies involving fluorescent labeling of blood cells or cell components, use of whole blood is recommended for reduction of reflective effects and to enhance phase contrast during image analysis. However, the limitations imposed by the volume of whole blood that may be collected and the variability in cellular counts restrict its use.

In this study, NO inhibition of platelet deposition was investigated. However, heme in the red blood cells (RBCs) rapidly scavenges NO and may interfere with NO studies. Therefore, PRP was considered for the current study. PRP is whole blood without the red blood cells and contains many factors. However, plasma proteins such as thiols react



with NO, although not as rapidly as RBCs. Perfusates used for NO studies should be free of plasma proteins and components to eliminate such reactions with NO.

For this study, a washed platelet suspension in a physiological buffer was used. The advantage of using a washed platelet suspension is that the composition of the suspension may be altered and the platelet counts may be set at the desired level by volume adjustment. Of particular interest to using a washed platelet suspension is the fact that NO is not depleted in the absence of heme or plasma thiols. However, in contrast, fluorescence from labeled cells is more difficult to detect due to strong reflections in non-colored media. One drawback of washed platelets is that the multiple steps involved in the preparation of platelets can result in platelet activation. This latter phenomenon was avoided in the current study by treating platelets with aspirin prior to preparation of the suspension.

## **3.2 Qualitative studies.**

### *3.2.1 Objectives.*

Prior to performing quantitative platelet inhibition studies, qualitative studies were performed to demonstrate that the perfusion device could be successfully used to study NO inhibition of platelet deposition on biomaterials. The usefulness of coating the membrane with a platelet agonist (collagen) for enhancing platelet deposition was determined. Initial studies were restricted to qualitative analysis to reduce expenses associated with expensive radioactive materials necessary to label and quantify platelet deposition.

### 3.2.2 Reagents.

Ultra-high purity nitrogen (99.999 % v/v) and nitric oxide (as a NO/N<sub>2</sub> mixture containing 10% v/v NO) were procured from Sooner Gas Company (Stillwater, OK). BSGC buffer (pH 7.3) contained 218 mg of K<sub>3</sub>PO<sub>4</sub>, 1.2 g of NaH<sub>2</sub>PO<sub>4</sub>, 7.0 g of NaCl, 4.0 g of sodium citrate, and 2.0 g of glucose in one liter of deionized water. Glucose, ammonium oxalate, glacial acetic acid, acid soluble type-I calfskin collagen, and quinacrine dihydrochloride (mepacrine) were procured from Sigma Chemicals (St. Louis, MO). Sodium phosphates and citrate were obtained from EM Science (Gibbstown, NJ). Phosphate-buffered saline (PBS, 10×) was purchased from Life Technologies (Grand Island, NY). Acetyl salicylic acid (aspirin) was obtained from Sigma (St. Louis, MO).

### 3.2.3 Preparation of platelet suspension.

Methods used in this study were approved by the *Institutional Review Board for Human Research* (IRB) at Oklahoma State University, Stillwater, OK. Blood was solicited from healthy individuals 18 years and older. Human blood (30 cc) was drawn from the forearm by venipuncture and collected into multiple tubes containing trisodium citrate to obtain a 9:1 (v/v) ratio of blood to sodium citrate. Sodium citrate is an anti-coagulant, which, by lowering the pH of the blood, prevents platelet aggregation and activation prior to processing. Precautions were taken to discard the first tube of drawn blood since the initial blood is usually rich in coagulating factors such as thrombin [McNichol, A., 1996].

Blood was processed as detailed in Fig. 3.1. Blood was collected, transferred to two 15 cc centrifuge tubes and centrifuged at 180 × g for ten minutes at room temperature.

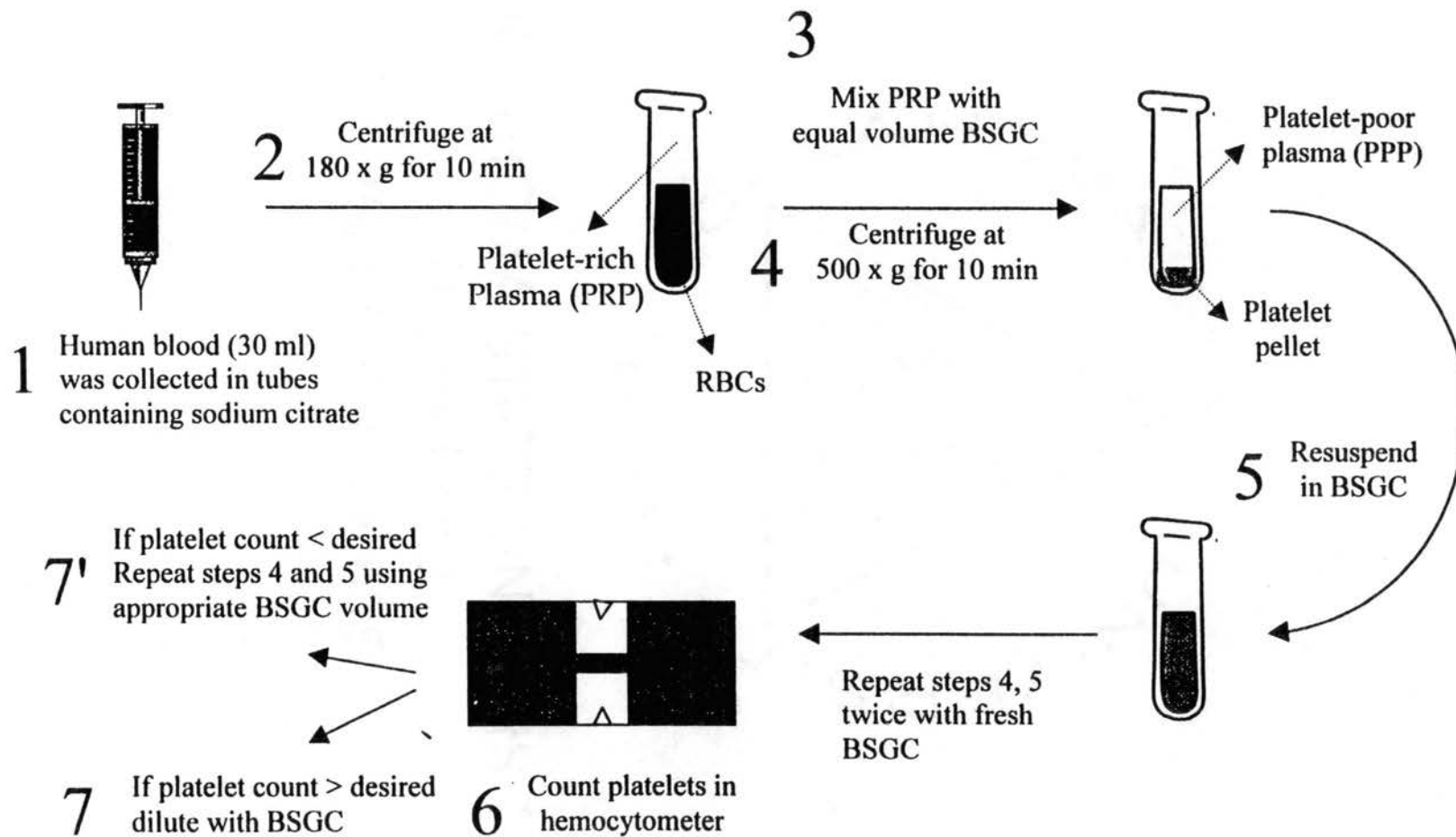


Figure 3.1. Schematic for preparation of washed platelet suspensions with desired platelet counts.

Whole blood was thus separated into a lower layer rich in red blood cells (RBCs) (~45-60% of the total volume) and an overlying layer of PRP. The volume of suspended PRP was measured and removed by pipetting. The PRP was mixed with an equal volume of BSGC buffer, pH 7.3, and gently mixed for 30 seconds. Subsequently, the mixture was recentrifuged at  $500 \times g$  for 10 minutes at room temperature. The platelet-poor plasma (PPP) forming the supernatant was discarded and the platelet pellet at the bottom was resuspended in BSGC buffer to obtain a total volume of 20-24 cc. Centrifugation and resuspension was repeated twice for several reasons including

- (i) Reduction in interference of plasma proteins with NO action.
- (ii) Increased permeabilization of platelets to radiolabels or fluorescent dyes
- (iii) Removal of coagulation-inducing factors such as thrombin.

Platelet counts and preparation of final suspension were performed as described in the next section. Importantly, during the preparation process, some degree of platelet destruction or activation may occur. Therefore, resuspension must be carried out very gently.

#### *3.2.4 Platelet counts.*

Experiments were performed using blood samples drawn from several donors. Since the reactivity of platelets in different individuals may vary, use of random blood samples is beneficial for the generalization of results. As indicated previously, normal platelet counts vary widely between individuals (100,000 – 600,000/ $\mu$ l). To allow for

consistency and provide a common basis for comparison of results between experiments, platelet counts in the final platelet suspension was  $2.0 \times 10^8$  platelets/ ml.

Enumeration of platelets in platelet suspensions may be performed by one of three methods. These are

- (i) *Phase contrast microscopy.* In this method, platelets are counted using a hemocytometer. This is a labor-intensive technique, which is recommended only when other methods are unavailable.
- (ii) *Semi-automated counting.* In this method, platelets are counted using a semi-automated coulter-type counter. The instrument quantifies particles based on impedance or optical density. However, pre-calibration and noise correction are extremely laborious.
- (iii) *Electronic particle analysis.* This method may be used to determine platelet counts from both whole blood and PRP, and requires only minute (50-100 ml) sample volumes. Cells are detected on the basis of optical density. However, since any particle within a given size range is identified as a platelet, overestimation of platelet numbers is possible.

For this study, platelet counting was performed using phase-contrast microscopy due to the non-availability or prohibitive costs of the other methods. In order to keep platelet counting simple, an aliquot of the platelet suspension was diluted a thousand-fold to reduce platelet numbers. A 1% (v/v) ammonium oxalate solution was prepared as recommended by McNichol (1996). 20  $\mu$ l of the platelet suspension was added to 1980  $\mu$ l of ammonium oxalate and well mixed. A 100- $\mu$ l aliquot of this suspension was mixed

with 900  $\mu\text{l}$  of fresh ammonium oxalate. Two-step dilution allowed working with smaller volumes to provide a more consistent dilution. Ammonium oxalate, rather than a buffer medium, was used for dilution since it causes lysis of any erythrocytes remaining in the sampled aliquot of the platelet suspension.

Exactly 20  $\mu\text{l}$  of the platelet suspension was applied to each side of a hemocytometer and incubated at 37 °C for 15 minutes. The hemocytometer was then examined under a phase contrast microscope ( $\times 400$  magnification). Etched on each side of the hemocytometer is a major grid with four minor grids each containing sixteen squares. The number of platelets contained in each of the eight minor grids (four on each side of the hemocytometer) were counted and averaged. The volume of sample contained in the area extending over each minor grid is  $10^{-4}$  cc. Accordingly, the actual platelet count in the undiluted platelet suspension was determined as

$$\text{Platelet count/ml} = \frac{\text{Platelet count/minor grid}}{\text{Sample volume/minor grid (cc)}} \times \text{DilutionFactor} \quad (3.1)$$

Platelet counts in the undiluted platelet suspension volume were set at 200,000 / $\mu\text{l}$  (for fluorescent studies).

### 3.2.5 *Fluorescent labeling of platelets.*

For qualitative platelet deposition studies, platelets were labeled with a fluorescent tracer, quinacrine dihydrochloride (mepacrine), as recommended by Feuerstein and Kush (1983). Mepacrine is a yellow dye that is absorbed by platelets and is stored in their

dense granules. For this study, a 1 millimolar stock solution of mepacrine was prepared. The platelet suspension to be labeled was centrifuged at  $500 \times g$  to pellet out the platelets. An appropriate micro-volume of the stock mepacrine solution was added to the supernatant overlying the platelet pellet to obtain a final mepacrine concentration of 10  $\mu$ molar. The solution was allowed to stand undisturbed for 10-15 minutes. The supernatant was pipetted out and replaced with BSGC buffer. Mepacrine was again added to the suspension in a repeat of the process described above. The multiple-washing process is necessary to (a) label platelets adequately with mepacrine to obtain strong fluorescence, and (b) avoid mepacrine-induced inhibition of certain adhesion and aggregation pathways within platelets [Adams and Feuerstein, 1980; Feuerstein and Kush, 1983]. Subsequent to the second labeling and incubation periods, the platelet pellet was resuspended in fresh BSGC buffer. During this multi-step process, the volume of the suspension/supernatant was maintained so as to keep the platelet count unchanged.

### 3.2.6 *Collagen preparation and coating.*

Collagen is a potent agonist of platelet deposition. In initial non-flow experiments, platelet deposition on a collagen pre-coated membrane surface was enhanced relative to platelet deposition on an uncoated membrane. Therefore, for flow experiments, collagen was utilized as a precoat on the membrane surface. Collagen (type I, from calf skin) was prepared by the method of Cazenave *et al.* (1973). Briefly, 100 mg of collagen was dissolved in 1.2 ml of glacial acetic acid and then diluted with 19.8 ml of deionized water. The mixture was swirled gently for 10 minutes. The mixture was then placed in an ice bath and homogenized for 15 minutes using a Biospec<sup>®</sup> homogenizer (Biospec

Instruments, Bartlesville, OK). The homogenate was centrifuged at  $2500 \times g$  for 15 minutes at room temperature. After removing the white film at the top, 20 ml of deionized water was added and the solution was recentrifuged at  $1000 \times g$  for 10 minutes at room temperature. The supernatant was decanted and stored at  $4\text{ }^{\circ}\text{C}$ . For coating the membrane, approximately 3 cc of the collagen suspension was layered on top of the gas-permeable membrane and incubated in a humidified atmosphere at  $37\text{ }^{\circ}\text{C}$  for two hours prior to the experiment.

### 3.3 Experimental setup.

The experimental setup for delivering NO to the platelet suspension is shown in Fig. 3.2. The setup was designed to vary the range of gaseous NO concentrations and flow rates to adjust the NO delivery rate. All NO gas mixtures were prepared in a certified hood to avoid the potential toxicity of NO. Ultra-high purity  $\text{N}_2$  following passage through an oxygen trap was mixed with NO using mass flow controllers (Porter Instrument Co., Hatfield, MA) (marked as *a* and *b* in Fig. 3.2) to set the mixing ratio of  $\text{NO}/\text{N}_2$  with pure  $\text{N}_2$ . The NO gas supply to the NO flow controller was procured from one of two NO cylinders containing either a 10 or a 1% (v/v) mixture of NO with ultrahigh purity  $\text{N}_2$  by using a two-way valve (*c*).

The  $\text{NO}/\text{N}_2$  mixture was split into two flows by means of a sensitive check valve (*d*) and a similar valve (*e*) on a side exhaust-line. Ultra-high purity  $\text{N}_2$  from a second  $\text{N}_2$  tank, also following passage through an oxygen trap, was bled into the  $\text{NO}/\text{N}_2$  gas mixture. The flow rate of the  $\text{N}_2$  bled into the NO stream was adjusted by means of a needle valve (*f*). Using this setup, a final  $\text{NO}/\text{N}_2$  mixture in the range of 0.1 to 15,000



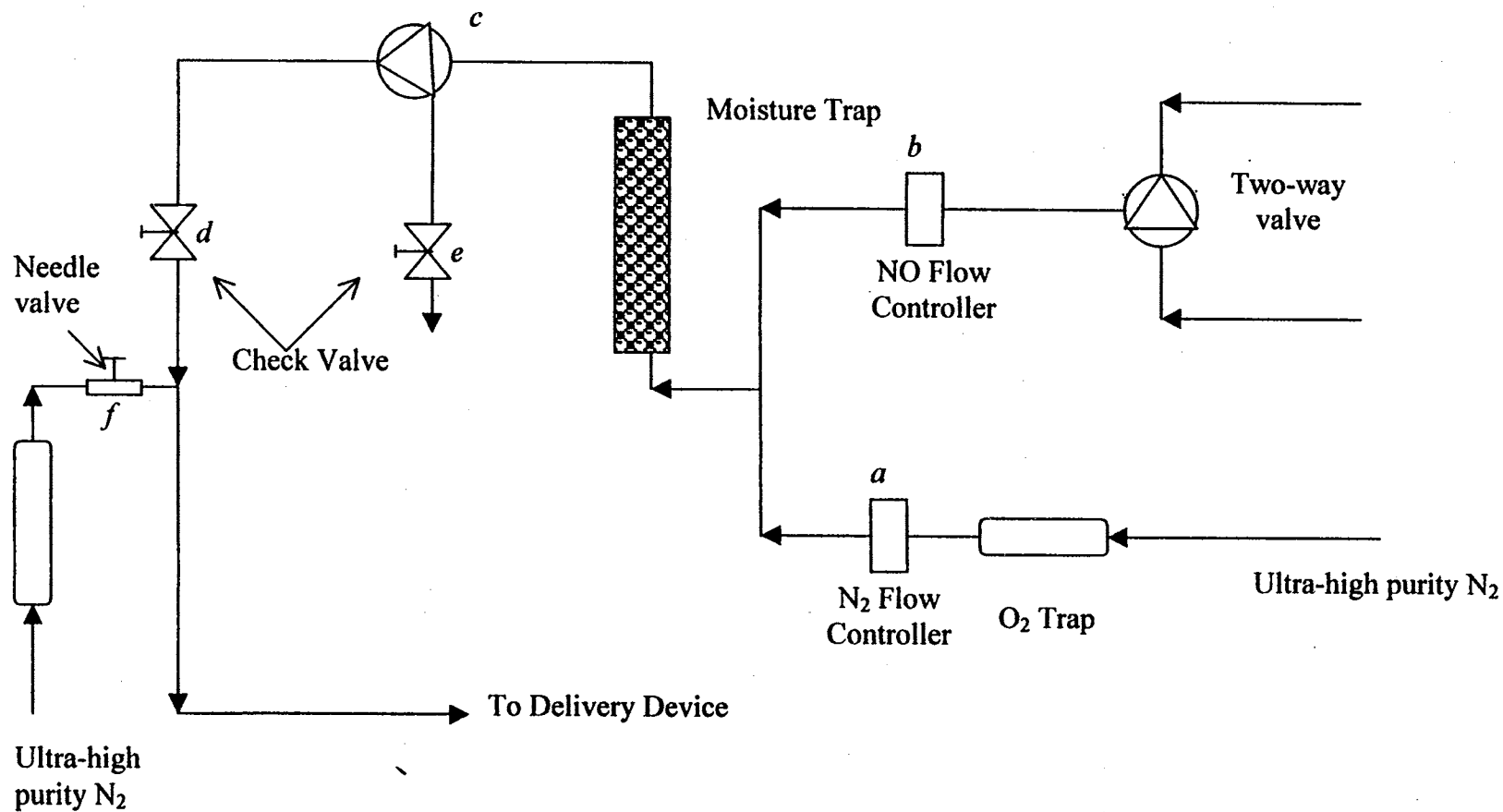


Figure 3.2 Experimental setup for delivery of NO to the platelet suspension.

ppm is obtainable when 10% (v/v) NO is used. When the 1% (v/v) NO is used, gas mixtures as low as 0.01 ppm of NO can be obtained.

### **3.4 Protocol for fluorescent studies.**

#### *3.4.1 Perfusion steps.*

All platelet adhesion experiments were at room temperature (23 °C). In all experiments, the flow shear rate was maintained at 250 s<sup>-1</sup>. In the first step of the experiment, PBS [1% (v/v)] was perfused through the flow slit for 5 minutes prior to perfusion of the platelet suspension. Pre-perfusion with PBS is essential to remove micro air bubbles on the membrane (adhesion) surface which affect platelet adhesion and aggregation characteristics [Sakariassen *et al.*, 1989]. Subsequently, the fluorescent-labeled platelet suspension was perfused through the flow slit for 15 minutes. Simultaneously, N<sub>2</sub> (in controls) or an NO/N<sub>2</sub> gas mixture (in non-controls) was continuously purged through the gas chamber section of the NO delivery device. Platelets in the porous block section of the perfusion device were exposed to 500 ppm, 250 ppm, 100 ppm, or 0 ppm (controls) of NO. Platelet suspension upstream of the porous block region was not exposed to any gas. Subsequent to perfusion of platelet suspension, PBS [1% (v/v)] was again perfused through the flow slit for 5 minutes.

Upon completion of the experiment, the platelet-adhered membrane was carefully removed and transferred to a glass slide. Entrapment of air bubbles between the membrane and the glass was strictly avoided to allow for better focus when viewed under a fluorescence microscope.

### 3.4.2 *Fluorescence microscopy.*

Platelets adhered to the membrane surface were observed under a fluorescent microscope. The principle underlying this method and the specific accessories required are described below.

*Principle.* Fluorescence is the property of some atoms and molecules to absorb light of a particular wavelength and re-transmit light at longer wavelengths, due to excitation via chemical reaction. Each fluorescent molecule (e.g., mepacrine) can absorb only in a specified wavelength range (absorption band) and emit in a narrow wavelength range (emission band). The specific absorption and emission characteristics of the fluorescent dye mepacrine, used in this study, are shown in Fig. 3.3. As shown, mepacrine absorbed into the dense granules of platelets is excited by light in the wavelength range of 420-490 nm (blue excitation region), and emits at higher wavelengths ( $> 510$  nm).

A short pass filter (SP 490) on the microscope generates only blue excitation light by mostly allowing only light of wavelength ( $\lambda$ ) between 420 nm and 490 nm to pass through unattenuated (see Fig. 3.3). This is called the excitation spectrum. The excitation light then hits a dichroic mirror (DM 510) and any light below  $\lambda = 510$  nm is reflected downwards through the objective to the sample (mepacrine-labeled platelets). The fluorescence emitted from platelets then hits the dichroic mirror again, via the objective. The dichroic mirror allows light with  $\lambda > 510$  nm (fluorescence emission) to pass through the mirror while emitted light of lower wavelengths are reflected off. A third filter (long pass-LP 520) allows only wavelengths of 520 nm and above of the fluorescent emission to pass through to the detector, and removes the faint residual light.

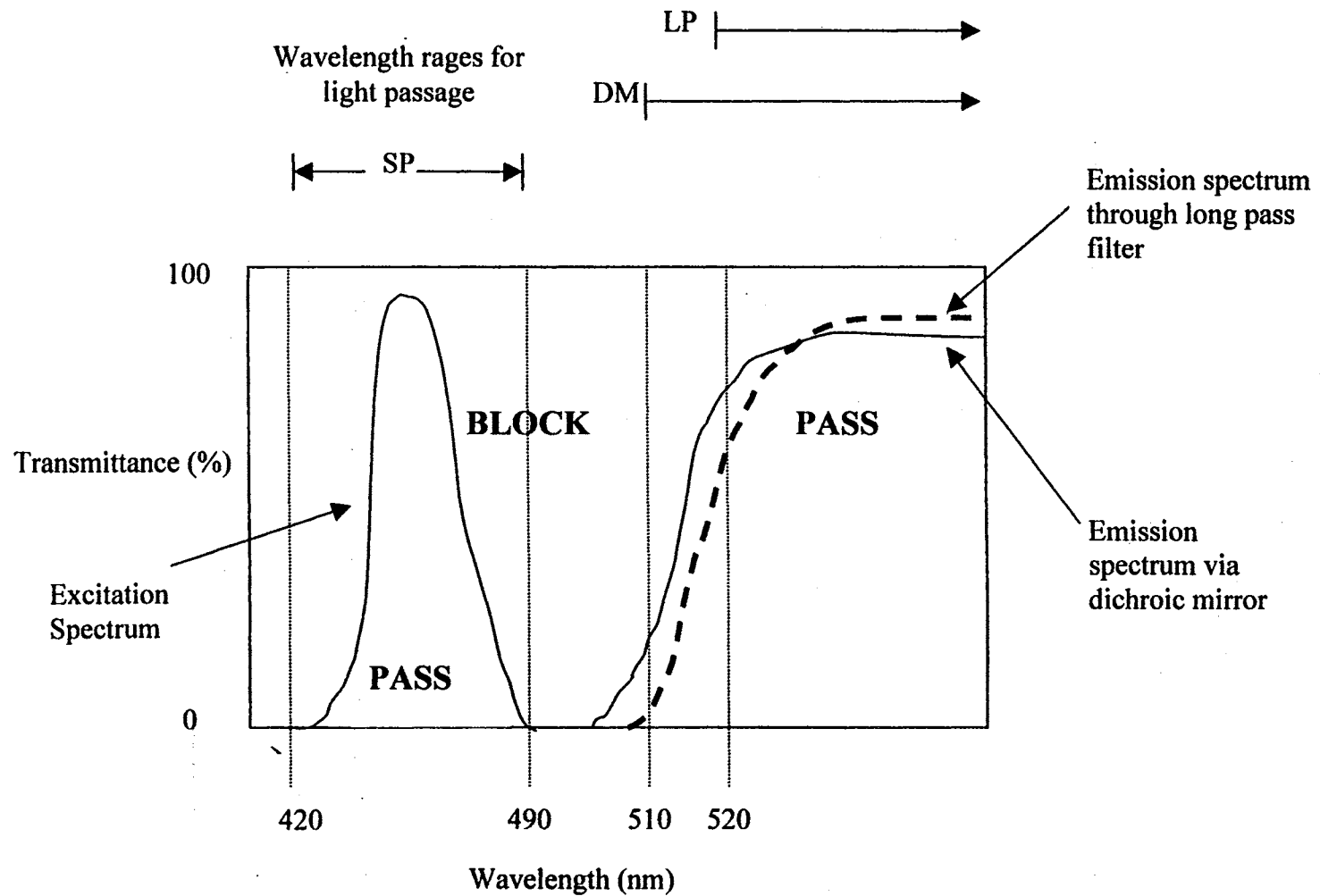


Figure 3.3. Spectral characteristics required for observing platelets labeled with the fluorescent dye mepacrine (quinacrine dihydrochloride). The vertical dotted lines represent cut-off wavelengths for short pass filter (SP), dichroic mirror (DM), and long pass filter (LP) as described in section 3.4.2.

The emerging beam seen by the observer appears as yellow light. The wavelengths included in the observed light beam form the emission spectrum.

Fluorescence microscopy, based on this phenomenon, allows detailed observation of cells and tissues, which are otherwise difficult to observe with the naked eye. The principal components of a fluorescence microscope are (i) excitation light source; (ii) wavelength selection devices (filters); (iii) objectives; (iv) detectors; (v) stages; (vi) camera [Herman, B., 1998]. In any study involving the use of fluorescence microscopy, it is essential to specify the spectral characteristics of the fluorescent dye used and the specifics of necessary microscope accessories. Adherence to specifications is critical for the proper observation of the subject samples. For this study, an epi-fluorescence illumination microscope was used (EFP-3, Nikon Corporation, Melville, NY) which is essentially a reflected-light vertical illumination system. A xenon lamp was used as the excitation light source.

*Procedure.* The microscope was fitted with an EFP-3 filter set (containing the filters mentioned above) for this study. Magnification was set at 200×. Photographs were taken of the membrane surface on the centerline, along its length at 1 cm intervals beginning at the point corresponding to the liquid entry into the flow slit. The photographic exposure time was between 5 and 10 seconds for best clarity and resolution.

### **3.5 Results.**

At all NO exposure levels (500, 250, or 100 ppm), platelet deposition on the downstream NO-exposed section of the collagen-coated membrane was significantly inhibited compared to a similar section of the control membrane (N<sub>2</sub> exposure). Figures

3.4a and 3.5a show an area of  $400\ \mu\text{m} \times 600\ \mu\text{m}$  centered 1 cm from the liquid inlet. Figures 3.4b and 3.5b show a similar area centered 5 cm from the liquid inlet (1.5 cm from the beginning of the porous block). In Fig. 3.4, the downstream section was exposed to  $\text{N}_2$  only. A significant number of platelets are adhered to the upstream (Fig. 3.4a), and the downstream (Fig. 3.4b) sections, although the upstream sections exhibited a slightly greater degree of platelet deposition. Fig. 3.5 shows platelet deposition following perfusion through a chamber in which 100 ppm of NO was delivered to the platelet suspension. Platelet deposition on the downstream surface was significantly inhibited upon exposure to 100 ppm of NO (Fig. 3.5b) compared to the upstream section (Fig. 3.5a). At higher NO exposures platelet deposition was greatly reduced relative to controls.

### **3.6 Quantitative platelet deposition studies.**

#### *3.6.1 Objectives.*

Initial qualitative fluorescent studies indicated that gaseous NO exposures as low as 100 ppm are effective in significantly inhibiting platelet deposition on the biomembrane surface at the experimental flow conditions. The next logical step was to determine if NO exposures lower than 100 ppm would similarly inhibit platelet deposition. The three major objectives to be assessed were:

- (i) Determine the potency of platelet inhibition by NO at successively lower gas NO exposures, below 100 ppm.

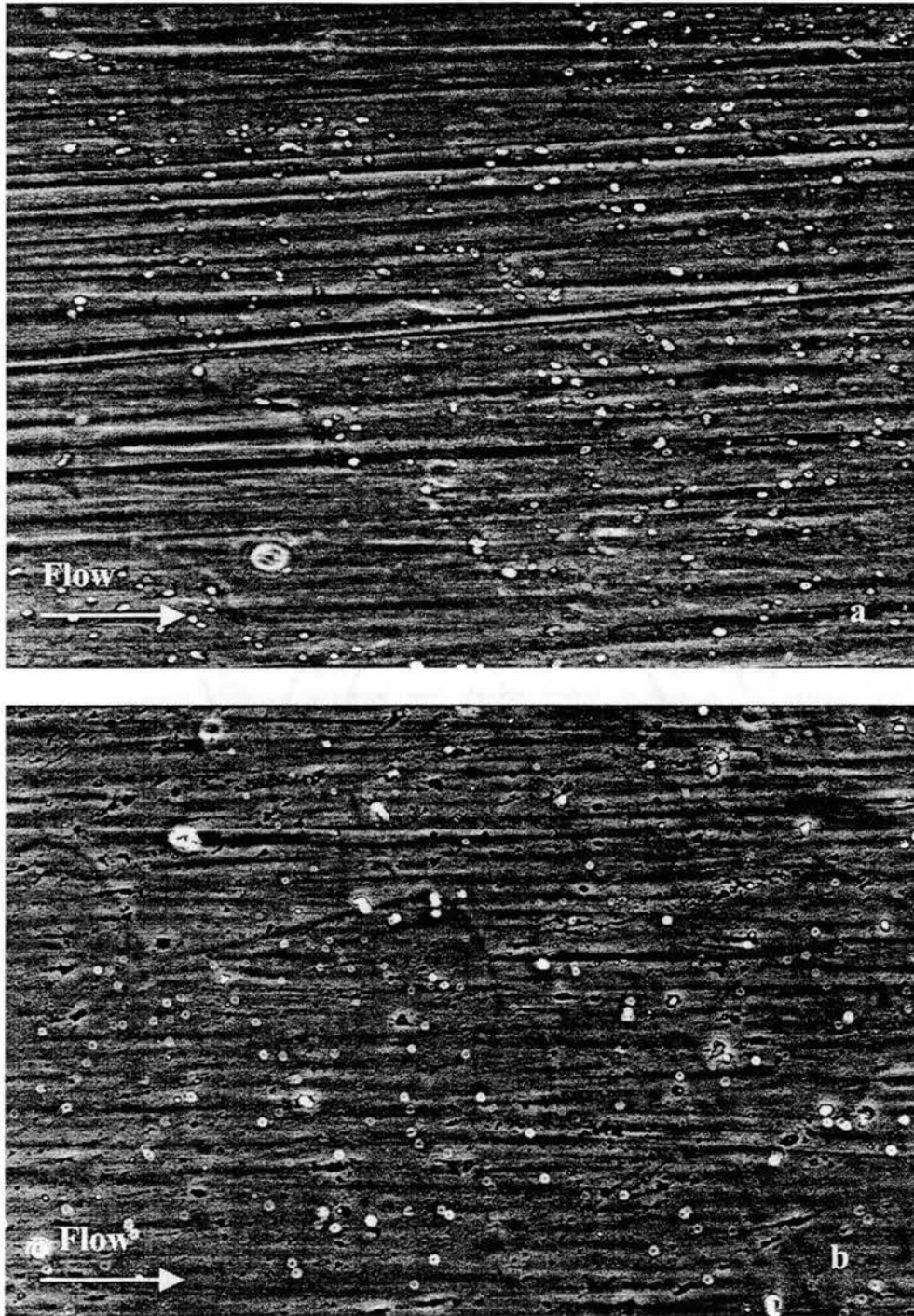


Figure 3.4 Platelet deposition on membrane in control chamber. The top figure represents platelet deposition over an area  $400\ \mu\text{m} \times 600\ \mu\text{m}$  centered at a distance of 1 cm from the liquid inlet into the flow slit. The lower figure shows platelet deposition over a similar area 5 cm downstream from the inlet. Magnification was  $200\times$ .

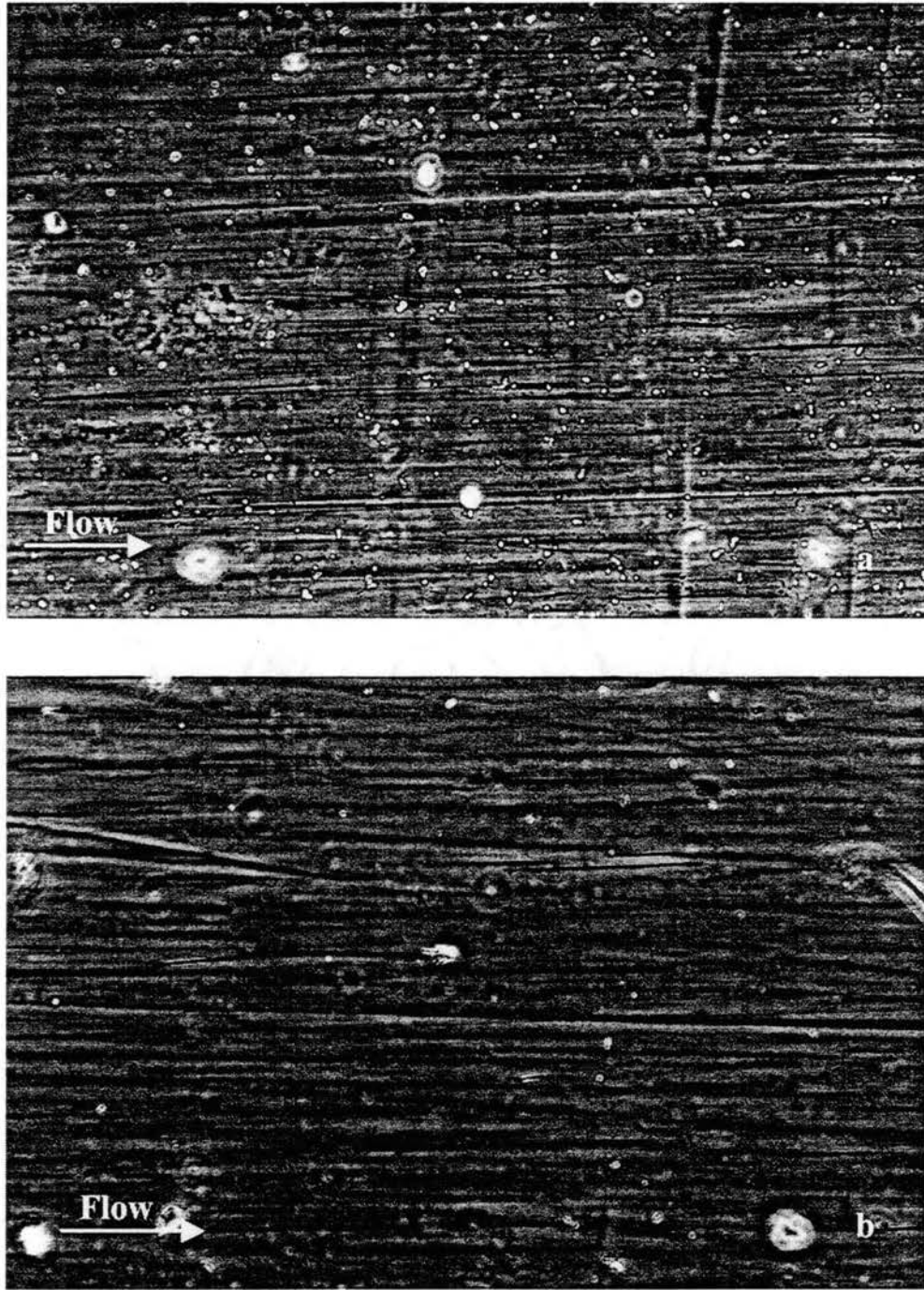


Figure 3.5. Platelet deposition on membrane in NO-exposure chamber. The top figure represents platelet deposition over an area  $400\ \mu\text{m} \times 600\ \mu\text{m}$  centered at a distance of 1 cm from the liquid inlet. The lower figure shows significant platelet inhibition over a similar area 5 cm downstream from the inlet where platelets following exposure to 100 ppm of NO. Magnification was  $200\times$ .



- (ii) Identify the minimal (threshold) NO exposure significantly inhibiting platelet deposition.
- (iii) Enumerate the number of platelets adhered per unit area of the membrane in control and NO exposed sections.

### 3.6.2 *Platelet labeling.*

Fluorescent-labeling and radioactive labeling are two widely adopted techniques for quantitative assessment of platelet deposition on biomaterials. Fluorescent labeling techniques were used for qualitative studies as detailed earlier. However, for quantitative studies the method was not adopted for the following reasons:

- (i) Necessity for redesign of the perfusion device to allow placement on the microscope stage for in-chamber detection of platelets. Membrane removal and transfer as performed previously can potentially remove platelets from the surface or cause damage to the membrane.
- (ii) Requirement of expensive detection equipment including a phototube detector and image-analysis software.
- (iii) Difficulty of quantifying fluorescent-labeled platelets in non-colored solutions or surfaces due to significant light reflection.
- (iv) Difficulty in calibrating photons of light emitted from labeled platelets in terms of actual platelet numbers. Also platelet counts in liquid samples cannot be determined.

The second option is to quantify platelet deposition by labeling platelets with a radioactive tracer. Radiolabeling offers the advantage of being specific for the cell under study (i.e., platelets). In many cases, the method is highly sensitive. Further, radiolabeled cells may be detected in solid or liquid samples and therefore calibration of counts in terms of actual platelet numbers is easy and accurate. A gamma counter for quantifying radioactive platelets was readily available for use. Therefore, for quantitative platelet deposition studies, platelets were radiolabeled.

### 3.6.3 Selection of radiotracer: Chromium-51 vs. Indium-111.

A review of literature shows that radiolabeling of platelets is generally performed with either chromium-51 as  $^{51}\text{CrO}_4$  [Steiner and Baldini, 1970; Tschopp, T.B., 1977] or Indium-111 as an  $^{111}\text{In}$ -oxine complex [Scheffel *et al.*, 1977; Hudson *et al.*, 1981]. The isotope  $^{51}\text{Cr}$  is a gamma ray emitter. The labeling efficiency of chromium-51 is generally low (~10%) and the  $\gamma$ -photon emission (9% at 320 keV) is too low for external detection [Joist *et al.*, 1983; Thakur, M.L., 1983]. Therefore,  $^{51}\text{Cr}$  may not be adequate for labeling platelets for *in vivo* deposition studies. However, platelets labeled with  $^{51}\text{CrO}_4$  can be readily detected and counted *in vitro*. The relatively long half-life of chromium (27 days) ensures that it may be stored over a few weeks without significant depletion. Further, radiolabeled samples may be assessed over a few days without significant change in the radioactive counts. These factors favor the use of  $^{51}\text{Cr}$  as a radiotracer for this study.

$^{111}\text{In}$ -oxine (or 8-hydroxyquinoline) is far more advantageous to use because the labeling efficiency is much higher than  $^{51}\text{Cr}$  (> 90%). The radionuclide does not emit high-energy particulate radiation. Therefore the radionuclide is ideal for use as an *in vivo*

tracer.  $^{111}\text{In}$  is not lost appreciably by labeled platelets when stimulated by strong release-inducing stimuli like collagen, thrombin, or upon prolonged in vitro storage. The disadvantages of using  $^{111}\text{In}$ -oxine as a radiolabel include

- a. A short physical half-life of 2.8 days which precludes storage over periods exceeding one day.
- b. High permeability of all blood cells to the complex (stable above pH 4.0) Separation of platelets from RBCs and leukocytes is therefore necessary to label platelets specifically.
- c. High affinity of  $^{111}\text{In}$ -oxine for plasma proteins like transferrin. Platelets must therefore be isolated from plasma and suspended in some electrolyte solution.
- d. Toxicity associated with labeling with  $^{111}\text{In}$ -oxine above the specified dosage.

After considering the advantages and disadvantages of both  $^{51}\text{Cr}$  and  $^{111}\text{In}$ ,  $^{51}\text{Cr}$  was chosen to radiolabel platelets for this study. Factors in favor of the use of  $^{51}\text{Cr}$  are its specificity for labeling platelets, long half-life, and comparatively low cost.

#### 3.6.4 Preparation of $^{51}\text{CrO}_4$ -labeled platelet suspensions.

**Caution:** All work with radioactive gamma emitters such as  $^{51}\text{Cr}$  was performed behind a 1/3-inch thick lead glass shield. Radioactive monitoring equipment and safety apparel was used and contaminated waste was disposed as per guidelines specified by the *Radiological Safety Office* (RSO) at Oklahoma State University, Stillwater, OK. The protocol for radiolabeling platelets is outlined in Fig. 3.6.

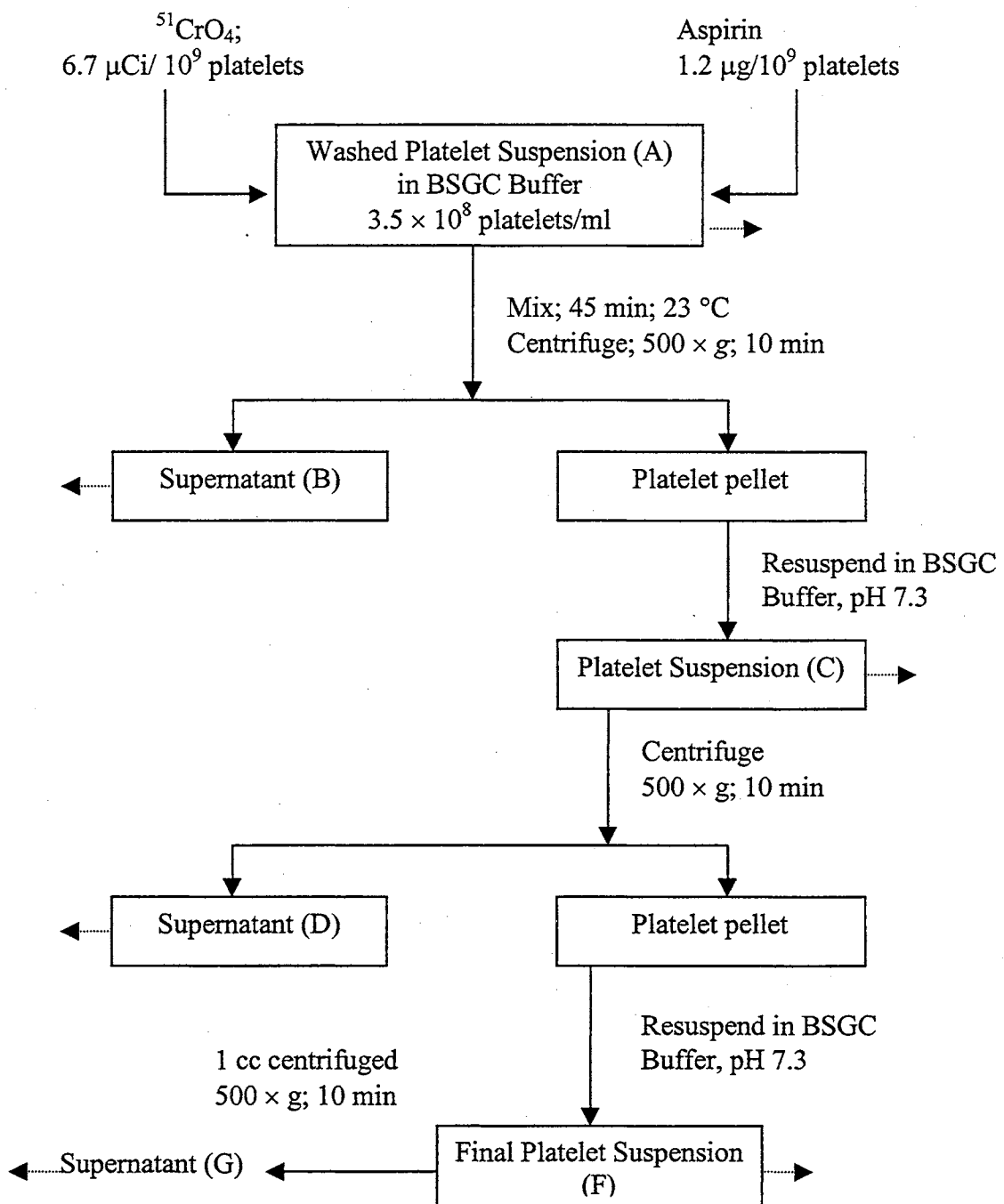


Figure 3.6. Preparation of  $^{51}\text{Cr}$ -labeled platelet suspension. Dotted arrows represent removal of 1 cc aliquots for purposes of calibration and determination of labeling efficiency.

The platelet suspension (A) was prepared as described earlier in sections 3.2.3 and 3.2.4, except that the platelet count was  $3.5 \times 10^8$  platelets/ml. Platelets in this suspension were labeled with 6.7  $\mu\text{Ci}$  of  $^{51}\text{CrO}_4$  per  $10^9$  platelets as recommended by Steiner and Baldini (1970). Aspirin (1.2  $\mu\text{g}$  per  $10^9$  platelets) was also added to the suspension (A) to reduce platelet activation and aggregation during the pre-experiment processing. The platelet suspension was incubated for 45 minutes at room temperature while gently mixed in a Labquake shaker (Barnstead Thermolyne, Dubuque, IA). The suspension was centrifuged at  $500 \times g$  for 10 minutes at room temperature to yield a platelet pellet. The overlying supernatant (B) was discarded. The platelet pellet was gently resuspended in BSGC buffer, pH 7.3 (C), with a Pasteur pipette. The centrifugation and resuspension process was repeated once more to yield supernatant (D) and a final platelet suspension (E). A 1 cc aliquot of the final platelet suspension was centrifuged at  $500 \times g$  and the supernatant (F) was collected. Volumes of BSGC buffer used for resuspension ensured that the platelet count was maintained at  $3.5 \times 10^8$  platelets/ml at all times. After each centrifugation or resuspension step, a 1 cc aliquot of the appropriate supernatant or resuspension was collected and monitored for radioactivity. While the collected aliquots of samples (A) through (D) were used to evaluate labeling efficiencies and the elution of  $^{51}\text{CrO}_4$  from platelets, the aliquots of (E) and (F) were used as calibrants. The method of calibration is detailed in section 3.7.1.

### **3.7. Experimental Protocol.**

The experimental setup for the quantitative platelet inhibition studies was identical to that described earlier in section 3.3. In anticipation of the objective to evaluate inhibition

of platelet deposition on exposure to NO gas exposures lower than 100 ppm, the NO source tank containing 1% (v/v) NO was used to obtain NO gas mixtures as low as 0.01 ppm. The porous/holed NO delivery device was used for all experiments. The membrane surface was precoated with collagen (type I, calf skin) to stimulate platelet deposition, as described in section 3.2.6.

The experimental protocol was similar to that described for the fluorescent studies. Flow shear rate of the perfusate was maintained at  $250 \text{ s}^{-1}$ . All studies were performed at  $23 \text{ }^{\circ}\text{C}$ . PBS [1% (v/v)] was initially perfused for 5 minutes through the flow slit in the perfusion device. This was followed by perfusion of the final radiolabeled platelet suspension for 15 minutes during which time platelets in the porous block region of the flow slit were exposed to an NO/N<sub>2</sub> gas mixture. Platelet inhibition due to NO was evaluated at successively lower NO exposures of 50, 10, 1, 0.1 and 0.02 ppm of NO. Perfusion of platelet suspension was followed by perfusion of 1% (v/v) PBS for five minutes. After the completion of each experiment, platelet deposition on the NO-exposed membrane section was compared to a similar membrane section in a control chamber wherein only N<sub>2</sub> was exposed to platelets. Platelets in the upstream half of the flow slit in either NO exposure or control chambers, which were not exposed to gas, were also quantified for platelet deposition.

### *3.7.1 Analysis method.*

Following each experiment, membranes were sectioned into upstream and downstream halves and the radioactivity due to adhered platelets was counted on an Autogamma Counter (Cobra II, Beckman Instruments, Downers Grove, IL). Samples

were counted over a two-minute period. Longer counting times did not change the number of counts in any significant manner. Radioactivity of the final platelet suspension (E) was used as a calibrant to determine platelet #s/cm<sup>2</sup> of surface. The radioactivity associated with a 1 cc aliquot of this suspension was associated with both the platelets and the suspending medium. Therefore, to obtain counts due to platelets alone, the radioactivity associated with a similar aliquot of the suspending medium alone (F) (obtained by centrifuging 1 cc of suspension E) was subtracted from that of the suspension. Accordingly, the platelet #s/cm<sup>2</sup> of the membrane surface was determined using Eq. 3.2.

$$\text{Platelet \#/cm}^2 = \frac{\text{Counts on membrane section}}{[(\text{Count/cc})_E - (\text{Count/cc})_F]} \times \frac{(\text{Platelet \#/cm}^2)_E}{\text{Area of membrane section (cm}^2)} \quad (3.2)$$

To avoid biasing results due to potential differences in collagen concentrations on control and non-control surfaces, the total platelet counts in the upstream and downstream sections were quantified. The percent inhibition was defined as

$$\% \text{ Inhibition Ratio} = \left( 1 - \frac{(\text{down/up})_{\text{non-control}}}{(\text{down/up})_{\text{control}}} \right) \times 100 \quad (3.3)$$

In Eq. 3.3, the upstream membrane sections in both the NO-exposure and control chambers (N<sub>2</sub> exposure only) were used as a basis for comparison. As mentioned earlier, the upstream membrane sections in both chambers are not exposed to any gas, and should accordingly have similar levels of platelet deposition if surface concentrations of collagen are similar.

### 3.8 Results.

The primary objectives of  $^{51}\text{Cr}$ -labeled platelet studies were to compare the percent inhibition relative to controls at successively lower NO exposures, and to determine the minimal NO exposure level at which platelet inhibition was still significant. Fig. 3.7 shows the percentage inhibition of platelet deposition on the NO-exposed downstream section of the membrane according to Eq. 3.3. NO inhibition of platelet-surface interactions was evaluated at NO gas exposures of 50, 10, 1, 0.1, and 0.02 ppm. At all exposures except the lowest, platelet deposition was inhibited by  $87\% \pm 3\%$  relative to controls. However, exposure to 0.02 ppm of NO inhibited platelet deposition only marginally ( $10\% \pm 8\%$ ). Table 3.1 details the platelet inhibition observed at each NO exposure. Also shown are the platelet counts/cm<sup>2</sup> adhered on the gas-unexposed upstream membrane section on controls. Platelet counts for the controls were  $1.4 \pm 0.9 \times 10^7$  platelets/cm<sup>2</sup>. Platelet counts/cm<sup>2</sup> of a similar section in non-control chambers was identical. Hence, the surface concentration of collagen precoated on the membranes in both chambers was likely similar. Platelet deposition on the control membrane decreased downstream from the liquid inlet. This may be attributed, in part, to distance-related effects on platelet adhesion and aggregation, as described in previous studies [Baumgartner and Sakariassen, 1985].

### 3.9 Interpretation of results.

Results of quantitative platelet deposition studies indicate that NO exposures as low as 0.1 ppm of NO significantly inhibit platelet deposition on a collagen coated membrane. At higher NO exposures, platelet inhibition is almost similar to the inhibition at 0.1 ppm.



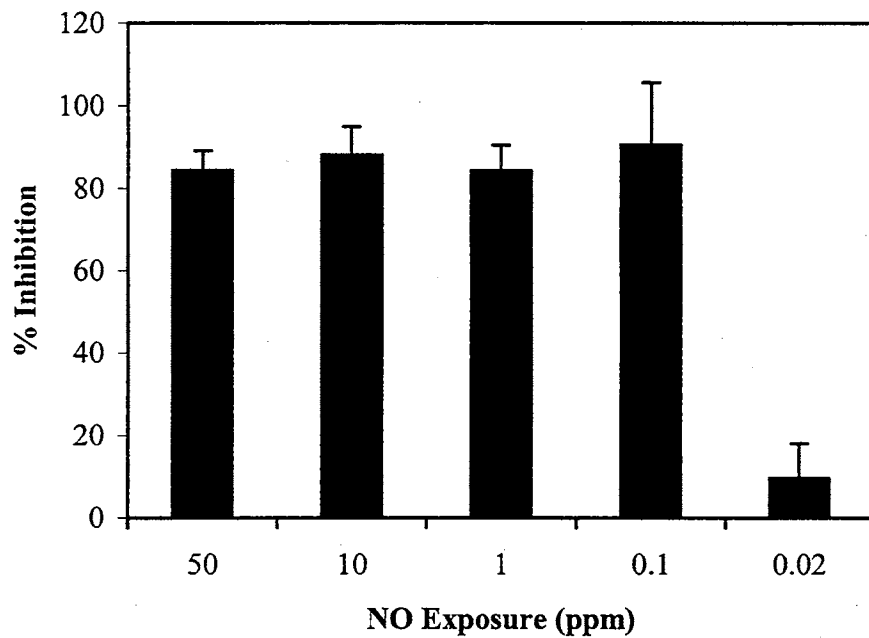


Figure 3.7. Inhibition of platelet deposition at various NO gas exposures ( $n = 3$ ). Platelet deposition was stimulated by a collagen precoat on the membrane.

**Table 3.1**

**Platelet inhibition at various NO exposures.**

NO Exposure (ppm)	<i>n</i>	% Platelet Inhibition	(Platelet count on upstream controls) #/cm <sup>2</sup>
50	3	84.4 ± 4.8	2.58 ± 0.84
10	4	88.1 ± 6.8	2.01 ± 0.92
1	3	84.3 ± 6.2	1.49 ± 0.37
0.1	4	90.6 ± 15.1	0.38 ± 0.12
0.02	3	9.7 ± 8.4	0.56 ± 0.18

The above results can be interpreted in terms of aqueous NO concentrations and fluxes delivered at the membrane (adhesion) surface. Surface NO concentrations and fluxes are predicted using the model represented by Eq. 2.8. Fig. 3.8*a* and *b* show the aqueous NO concentration and flux profiles, respectively, across the slit height at the exit of the flow device, predicted for gaseous NO exposures of 0.1 ppm and 0.02 ppm for a shear rate of  $250 \text{ s}^{-1}$ . For a shear rate of  $250 \text{ s}^{-1}$  and a NO exposure of 0.1 ppm ( $C_0 = 0.18 \text{ nM}$ ), the NO concentration at the adhesion surface ( $y/h = 0.5$ ) underlying the porous block region is  $0.09 \text{ nM}$ . This is the aqueous NO concentration which significantly inhibits platelet deposition on the collagen coated surface. The corresponding surface NO flux significantly inhibiting platelet deposition is  $0.26 \text{ femtomoles cm}^{-2} \text{ s}^{-1}$  (see Fig. 3.8*b*). The surface NO concentration corresponding to an exposure of 0.02 ppm is  $0.02 \text{ nM}$  at  $250 \text{ s}^{-1}$ . As evident in Fig. 3.9*a*, at either exposure platelets are exposed to a fairly constant NO concentration at the surface, along the slit length. For an exposure of 0.1 ppm of NO that was determined to significantly inhibit platelet deposition onto the collagen-coated surface, the NO flux at the surface decreases from 0.6 to  $0.3 \text{ femtomoles cm}^{-2} \text{ s}^{-1}$  at a shear rate of  $250 \text{ s}^{-1}$  (see Fig. 3.9*b*). The above concentration and flux values corresponding to 0.1 ppm NO are therefore representative of the threshold range of aqueous NO concentrations and fluxes causing significant platelet inhibition.

### 3.10 Conclusions.

Qualitative (fluorescence) and quantitative (radiolabeling) platelet deposition studies were performed. The fluorescence studies demonstrated the feasibility of the designed NO-delivery/perfusion device for the study of NO inhibition of platelet deposition on

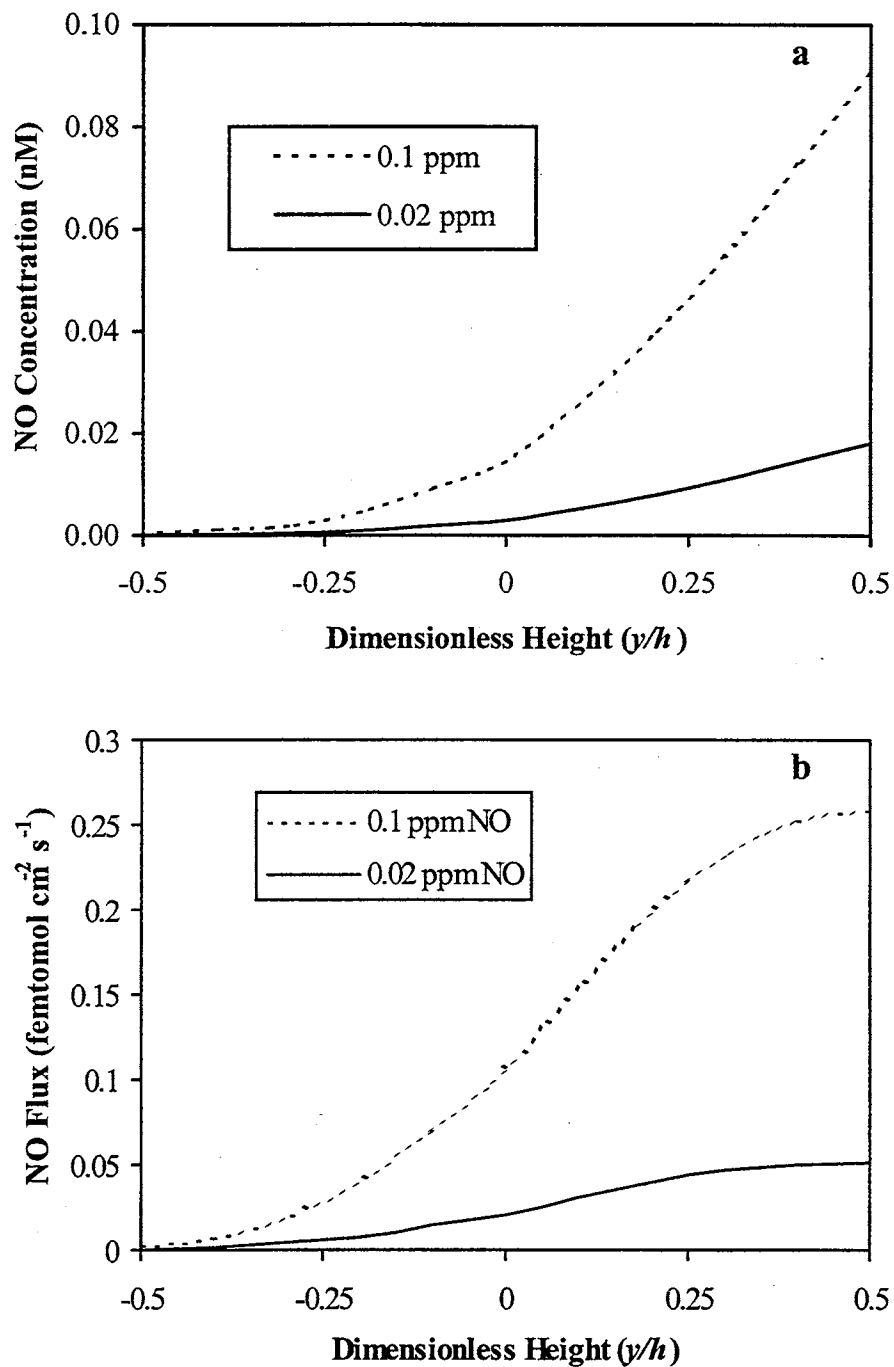


Figure 3.8. NO concentration and flux profiles across the slit height at exit of flow device for NO exposures of 0.1 and 0.02 ppm. Values were predicted for the pore/holed device using the model represented by Eq. 2.8. at a shear rate of  $250 \text{ s}^{-1}$ .

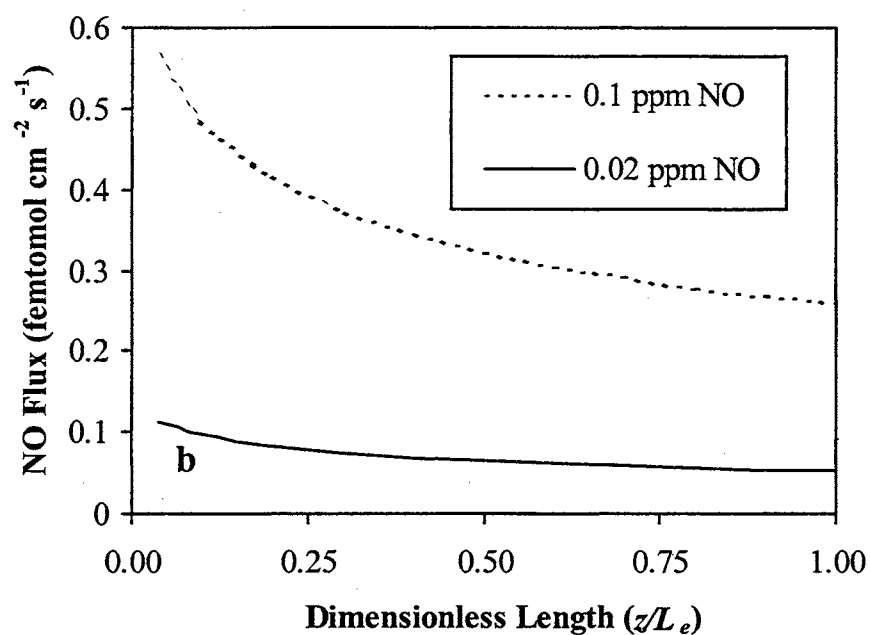
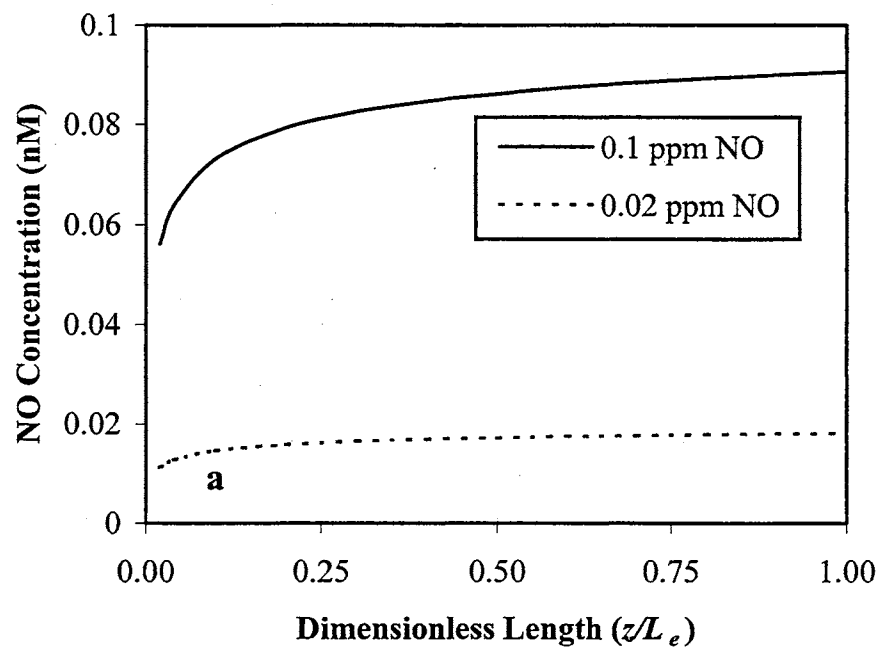


Figure 3.9. NO concentration and flux profiles along the slit length at exposures of 0.1 and 0.02 ppm. Values were predicted for the pore/holed device using the model represented by Eq. 2.8. at a shear rate of  $250 \text{ s}^{-1}$ .

collagen-coated biomaterials. The study also indicated that NO exposures as low as 100 ppm significantly inhibited platelet deposition. Adhesion studies with <sup>51</sup>Cr-labeled platelets determined the minimal NO exposures for significant platelet inhibition. Using the model of chapter 2, the corresponding aqueous NO concentration and flux at the adhesion surface was estimated. These results may be used as a starting point to establish guidelines for delivery of suitable surface NO concentrations and fluxes which would be effective in inhibiting platelet deposition, irrespective of the coated agonist or flow conditions. Knowledge of these fluxes and concentrations is useful towards the better design of biomaterials which incorporate NO to inhibit platelet deposition.

## CHAPTER 4

### AGONIST, SHEAR RATE, AND PERFUSION TIME EFFECTS

#### 4.1 Introduction.

In chapter 3, the minimal aqueous NO concentrations and fluxes required to inhibit platelet deposition on a collagen-coated biomaterial were identified. The NO concentrations and fluxes were predicted using a mathematical model. The results showed that platelet deposition on a collagen-coated membrane was inhibited upon exposure to surface NO concentrations as low as 0.09 nM, at a wall shear rate of 250 s<sup>-1</sup>. The effective NO concentrations and fluxes were, however, specific to the conditions of the study.

Platelet deposition characteristics, including the formation of surface aggregates (thrombi), platelet detachment, and axial distribution, are strong functions of shear and perfusion time [Turitto *et al.*, 1980,1985]. The migration of platelets towards a biomaterial surface is dictated by channel geometry and flow characteristics [Turitto and Baumgartner, 1975]. Additionally, surface-platelet interactions are strongly influenced by the presence of agents (platelet agonists) that stimulate platelet recruitment and adhesion [Tschopp *et al.*, 1974; Weiss *et al.*, 1974; Baumgartner and Haudenschild, 1972]. In physiological systems, blood flow conditions and the presence of platelet agonists are major factors determining localized platelet deposition. The study described

in this chapter thus seeks to establish more generalized guidelines for the local delivery of NO at biomaterial surfaces to inhibit platelet deposition. Such guidelines are imperative for the successful design of biomaterial surfaces incorporating NO that may be effectively used to inhibit surface platelet deposition *in vivo* or *in vitro* under a wide variety of conditions.

The primary objectives of this study are to determine if the minimal surface NO concentrations and fluxes inhibiting platelet deposition are functions of the nature of platelet agonist, flow shear rate, and time period of gas exposure to platelets. Platelet deposition on blood-contacting biomaterials is preceded by deposition of one or more platelet-thrombogenic plasma proteins. These proteins vary in their attachment characteristics and affinities for platelets. Hence, the minimal effective NO concentrations and fluxes for significant platelet inhibition, determined earlier for a collagen-coated surface, may not be as effective for other platelet agonists. Similarly, shear rate may affect the rate of transport of platelets to the surface and also NO concentration and flux distributions. Thus, platelets may not be exposed to the same NO concentrations over most of the flow slit, except perhaps at the adhesion/NO-delivery surface. Accordingly, NO delivery rates may need to be modified to obtain similar levels of platelet inhibition under different flow conditions. The effect of gas exposure time must also be evaluated to determine if continual NO exposure loses its effectiveness over time, and if so, determine the limits for effective platelet inhibition.



## 4.2 Factors affecting platelet-surface interactions.

### 4.2.1 Platelet agonists.

The adhesion of individual platelets to a surface depends on receptor-mediated recognition of specific sites or chemical species on adsorbed proteins [Bartlett and Anderson, 1982]. Platelet deposition on biomaterials incorporated in either *in vivo* or *in vitro* devices is stimulated in the presence of platelet recruiting agents (agonists). Surface irregularities such as non-smooth surfaces promote the formation of a fine network of fibrous blood proteins such as fibrin which entrap platelets. However, smooth surfaces are not immune to platelet deposition due to the presence of platelet agonists at the site of contact. Whether they are blood components or tissue based, platelet agonists must be taken into account for evaluation of biomaterial hemocompatibility. The major sources and types of platelet agonists are detailed below.

#### 4.2.1.1 Plasma proteins.

The first event generally occurring after blood/plasma contacts a polymer surface is the formation of a protein layer at the blood-polymer interface. The formation of this protein layer is followed by the adhesion of platelets, fibrin, and often leukocytes (white blood cells). Further deposition of platelets and entrapment in a fibrin network constitutes thrombus formation. The plasma component of blood, often used in *ex-vivo* or *in vitro* applications, contains a wide spectrum of proteins, numbering more than 5000 [Andrade and Hlady, 1987]. These proteins vary widely in their structures, thrombogenicity, and binding characteristics. Complex multi-component solutions, such

as serum and plasma, thus contain complex proteins all interacting at the biomaterial surface.

Twelve proteins are present in plasma in significant concentrations (>1 mg/ml). These include platelet antagonistic albumin (the most abundant component), and thrombogenic immunoglobulin-G, M, and A (IgG, IgM, IgA), fibrinogen, fibronectin, and transferrin. The properties of these proteins are detailed in Table 4.1. Albumin has a significantly greater diffusivity than other plasma proteins. Protein deposition on surfaces is therefore often dominated by albumin, which keeps vascular surfaces platelet-free. IgG and fibrinogen are the most abundant and platelet-agonistic among the thrombogenic proteins. Long residence times stimulate a great degree of surface immobilization of IgG and fibrinogen [Deboer, J.H., 1968].

*Mechanism.* In spite of the wide variation in anti-thrombogenic mechanisms of platelet adhesion and aggregation, a common feature between plasma proteins is an interaction between the plasma protein, von Willebrand factor (vWF; a component of plasma), and platelet surface protein(s). Fibrinogen concentrations as low as 0.02 mg/ml are sufficient to stimulate platelet aggregation. Figure 4.1 illustrates a typical mechanism of platelet recruitment, shown for aggregation stimulated by fibrinogen-coated surfaces. Briefly, adsorbed fibrinogen interacts with platelet surface receptors of low affinity (GP IIa-IIIb) which elevates cytoplasmic ionized calcium concentration via a multi-step mechanism. This activates glycoprotein receptors of higher affinity on the membrane surface resulting in further fibrinogen binding to platelets and platelet aggregation. The response may be enhanced by ADP secreted from adherent platelets in response to shear or modifications on platelet surfaces [Salzman *et al.*, 1987].

**Table 4.1**

**Major protein components of plasma**

<b>Protein</b>	<b>Plasma Concentration (mg/ml)</b>	<b>Molecular Wt.</b>	<b>Diffusion Coefficient (<math>10^{-7} \text{ cm}^2 \text{ s}^{-1}</math>)</b>	<b>Property</b>
Albumin	40	66,000	6.7	Anti-thrombogenic
IgG	8-17	150,000	4.0	Thrombogenic
LDL	4.0	2,000,000	2.0	Thrombogenic
Transferrin	2.3	77,000	5.0	Thrombogenic
Fibrinogen	2-3	340,000	2	Thrombogenic
IgA	1-4	150,000	4	Thrombogenic
IgM	0.05-2	900,000	2.6	Thrombogenic

Table adapted from Andrade and Hlady, 1987.

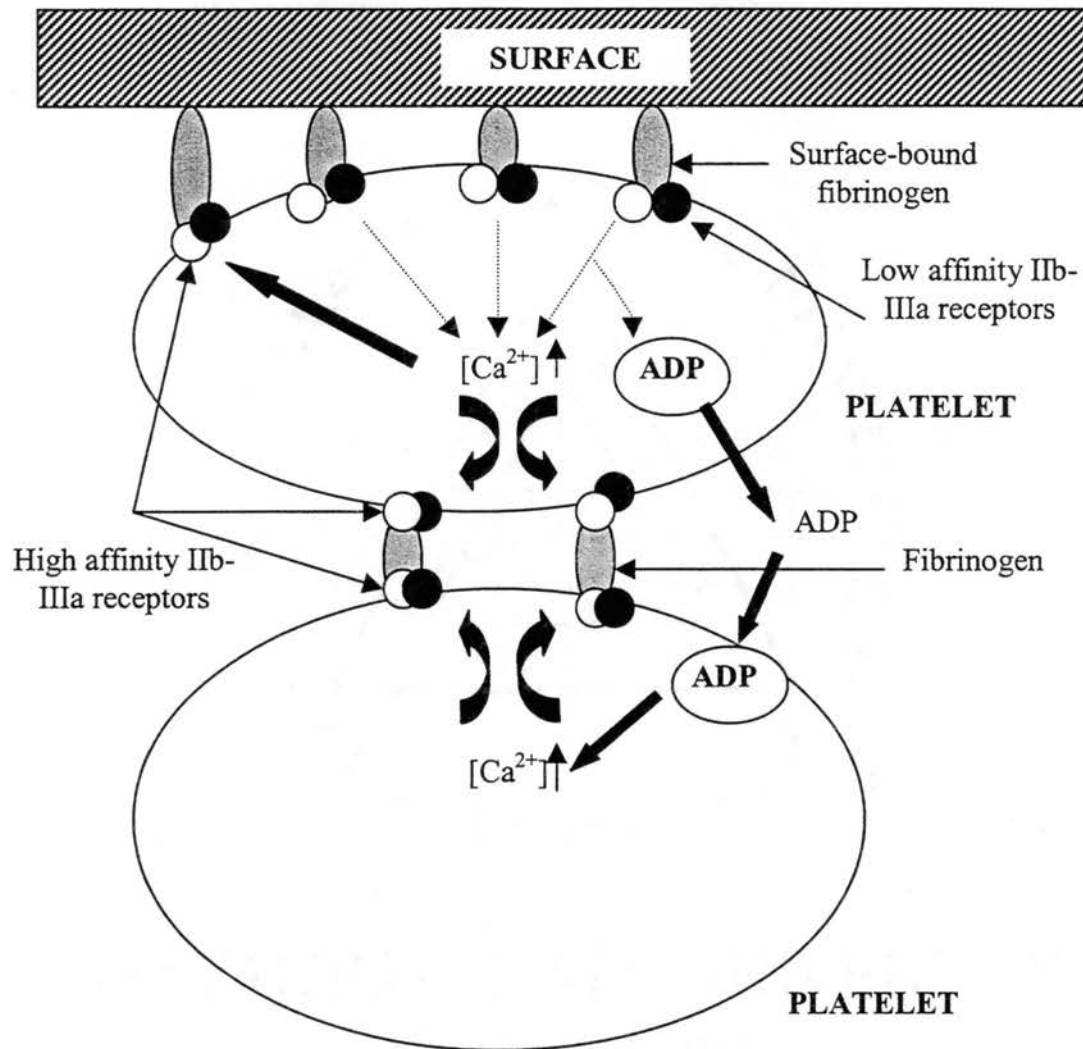


Figure 4.1. Scheme of platelet activation by adhesion to fibrinogen-coated surfaces. Surface-bound fibrinogen reacts with low affinity platelet GpIIa-IIIb receptors. High affinity receptor sites bind fibrinogen resulting in adherence to other platelets. A side-effect is the release of ADP from adherent platelets which further enhances calcium levels and activates adhesion/cohesion receptors. Figure adapted from Salzman *et al.*, 1987.

#### 4.2.1.2 Components of vessel wall.

Various thrombogenic plasma proteins described in the above section, in addition to several other fibrous proteins, are localized on the vessel wall [Rand *et al.*, 1980]. When immobilized on vessel wall surfaces, plasma proteins such as fibrinogen, fibronectin, and vWF contribute primarily to the initial adhesion process (and therefore to deposition of thrombi) rather than platelet-platelet cohesion. Collagen is the vascular protein that plays an important role in the development of platelet thrombus formation after initial platelet attachment. This is especially true *in vivo*, if the outer protective layer of endothelial cells is damaged, exposing blood to the collagen-rich extracellular matrix (ECM) (refer to section 1.1). Fibrillar collagen (types III and I) promotes extensive platelet deposition when exposed to flowing blood *in vitro or vivo* [Baumgartner, 1977; Muggli and Baumgartner, 1978]. Collagen acts through its ability to stimulate platelet release of ADP and other granular components or by direct alteration of receptor sites on the platelet surface. Collagen-stimulated platelet deposition is essentially limited to injured vascular tissues or bioartificial surfaces (*e.g.*, stents) in contact with or near the site of vascular damage. The most serious effect is the growth of platelet aggregates into the lumen, although collagenated surfaces such as ECM have been shown to be more resistant to embolus formation as compared to aggregates formed in response to other agonists [Turitto *et al.*, 1987].

#### 4.2.1.3 Selection of agonists.

In the current study, NO inhibition of agonist-induced platelet deposition was investigated. All experiments were performed *in vitro*. The selection of agonists for

this study was based on the following criteria:

- (a) *Source*. Platelet agonistic proteins were to be derived from plasma proteins and matrix proteins. To provide physiological relevance to the study, and in consideration of the specific application of results, tissue source from which the agonist was isolated was of particular interest.
- (b) *Abundance*. Selection of proteins was based on their relative importance as platelet agonists and their abundance in physiological tissues (*e.g.*, sub-endothelium, blood).
- (c) *Adsorption on surfaces*. Protein adsorption on biomaterial surfaces in significant concentrations was essential to attract platelets and ensure significant platelet deposition on surfaces.
- (d) *Economics*. Selected plasma- or matrix-proteins were to be available in a purified form and at low cost.

For this study, human fibrinogen and IgG (plasma proteins), and type I calfskin collagen (ECM component) were selected. Purified forms of these proteins are available at relatively low costs. The proteins were easily adsorbable on the biomaterial utilized for the study. Initial studies showed that platelet deposition stimulated by these adsorbed proteins were significant for detection.

#### 4.2.2 *Shear rate*.

Platelet-surface interactions are influenced strongly by wall shear rates [Turitto and Baumgartner, 1979]. In physiological systems, circulatory shear rates range from  $30 \text{ s}^{-1}$

in the large blood vessels to over  $4000 \text{ s}^{-1}$  in the smallest capillaries. Increased radial transport of platelets towards vessel/channel walls with increased shear has been confirmed experimentally. This phenomenon is especially enhanced in the presence of erythrocytes (RBCs) that drive platelets to the peripheral regions of the flow channel. Up to shear rates of  $650 \text{ s}^{-1}$ , platelet deposition is related to the shear rate but is mostly uninfluenced at higher shear rates [Turitto and Baumgartner, 1979]. Platelet adhesion is significantly transport controlled at shear rates lower than  $650 \text{ s}^{-1}$ , while at higher shear rates, the process is dictated more by platelet-surface kinetics. Accordingly, at shear rates greater than  $650 \text{ s}^{-1}$ , thrombus formation increases dramatically [Turitto *et al.*, 1980].

#### 4.2.2.3 Selection of shear rates.

In this study, shear rates were selected on the basis of the following criteria:

- (a) *Physiological relevance*: Shear rates were within the physiological range specified earlier. To avoid biasing results due to selection of shear rates at the limits of the range, shear rates were selected in the middle of the range.
- (b) *Thrombus formation*: The objective of the study was to evaluate NO as an agent for inhibition of platelet deposition on biomaterials. However, the emphasis for this study was on platelet-surface interactions (adhesion) relative to platelet-platelet interactions (aggregation). Adhesion is the primary and initiating step for the formation of surface aggregates. Therefore, NO inhibition of platelet adhesion was of primary interest. Since quantitative methods used in this study (see section 3.7.1) did not allow differentiation between platelet adhesion and aggregation, shear rates were maintained lower

than  $650 \text{ s}^{-1}$ , to minimize aggregation and thrombus formation [Baumgartner and Sakariassen, 1985].

(c) *Perfusion volumes*: The NO delivery device/perfusion chamber described in section 2.1 was designed for a wide range of perfusate wall shear rates (up to approx.  $1500 \text{ s}^{-1}$ ). In all experiments perfusates were not re-circulated.

Therefore, to obtain higher wall shear rates, higher flow rates and consequently greater volumes of platelet suspension were required.

Limitations imposed by blood supply restricted selection of wall shear rates to less than  $500 \text{ s}^{-1}$ .

In this section of the study, wall shear rates of  $250 \text{ s}^{-1}$  and  $500 \text{ s}^{-1}$  were adopted. For the designed device, the shear rates correspond to flow rates of  $1 \text{ cc min}^{-1}$  and  $2 \text{ cc min}^{-1}$ , respectively. For the short perfusion times adopted in this study ( $<15 \text{ min}$ ), the volume of platelet suspension was restricted to 30 cc. At the above shear rates, surface platelet aggregation does occur, although it is expected to be less extensive relative to that at higher shear rates.

#### 4.2.3 *Perfusion time and other parameters.*

The time course of platelet adhesion and thrombus formation has been studied in numerous *in vitro*, *ex-vivo* and *in vivo* experiments [Baumgartner *et al.*, 1980; Baumgartner and Sakariassen, 1985]. Experimental factors such as shear rate, temperature, and the nature of platelet agonists significantly affect time course profiles for platelet adhesion and thrombus formation. However, an overall assessment of trends indicates that at a given shear rate, surface coverage with platelets (signifying platelet



adhesion) increases with perfusion time and levels off to a maximum upon prolonged perfusion (>30 min). Surface thrombi (signifying platelet aggregation) increase in number and size with perfusion time, attaining a maximum at times less than 10 minutes. Subsequently, surface coverage with thrombi decreases continuously due to shearing off of surface aggregates. To minimize platelet aggregation relative to adhesion, while taking into account the shear rate requirements and the availability of a sufficient volume of platelet suspension, perfusion times were restricted to less than 15 minutes.

Lowering the temperature below 37 °C decreases platelet adhesion and subsequent thrombus formation. To avoid significant thrombosis on the biomaterial, all experiments were performed at 23 °C. However, the advantages of performing experiments at 23°C include reduced thrombosis and elimination of the requirement for incubators or temperature-controlled rooms.

#### **4.3 Objectives.**

As described in chapter 3, experiments demonstrated that at  $250 \text{ s}^{-1}$ , an aqueous NO concentration of 0.09 nM at the adhesion surface was effective in almost totally inhibiting platelet deposition on a collagen-coated surface. However, the generality of the determined threshold NO concentration and flux was not established. As described in earlier sections, platelet agonists can evoke very different responses in platelets and stimulate adhesion/aggregation by different mechanisms. Therefore, NO may or may not be as effective an inhibitory agent as in the case of collagen-induced platelet deposition. As shown in section 2.6.2, at a given NO exposure, spatial NO concentration and flux profiles within the flow slit are functions of shear rate. Therefore, at higher shear rates,

platelets may be exposed to lower NO concentrations over most of the slit height except very close to the adhesion surface. Thus, exposure of platelets to NO may be insufficient for significant inhibition even at the threshold NO exposures earlier determined. Additionally, prolonged exposure to NO may evoke pro-aggregatory responses in platelets or inhibit platelet deposition more effectively.

In the current study, the dependence of NO delivery requirements for effective platelet inhibition, as a function of platelet agonist, shear rate, and perfusion time was investigated. Establishment of generalized guidelines for delivery of NO at concentrations and fluxes identified in this study will provide design parameters for incorporating NO release at biomaterial surfaces. Toxicity and carcinogenicity due to excessive NO release may thus be avoided if minimal NO concentrations are utilized.

#### **4.4 Experimental methods.**

##### *4.4.1 Reagents.*

All gases (NO, N<sub>2</sub>) and chemicals (of appropriate grades) for preparation of perfusates, platelet counting, and platelet labeling were obtained from sources mentioned earlier in section 3.2.2. Collagen (Type I, from calfskin), human fibrinogen (Type I), and human IgG, were obtained from Sigma Chemicals (St. Louis, MO).

##### *4.4.2 Platelet perfusates.*

All experiments were performed with platelet suspensions prepared in BSGC buffer, pH 7.3, at a final platelet count of  $3.5 \times 10^8$  platelets/ml. Platelets were isolated from 30

cc of human blood drawn by venipuncture from consenting adult volunteers. Platelet suspensions were prepared as per the method described in section 3.2.3. Platelet deposition was monitored by labeling platelets with  $^{51}\text{CrO}_4$  as described in section 3.6.4. Platelet aggregation and activation during processing was reduced by addition of aspirin ( $1.2 \mu\text{g}/10^9$  platelets).

#### 4.4.3 *Experimental setup.*

The experimental setup for the platelet deposition studies was identical to that described earlier in section 3.3 and shown in Fig. 3.2. Results of previous quantitative platelet inhibition studies indicated that gaseous NO exposures should be less than 10 ppm. Accordingly, the NO source tank containing 1% (v/v) NO was used to obtain NO gas mixtures as low as 0.01 ppm. The porous/holed NO delivery device described in section 2.3 was used for all experiments. Perfusion through the flow slit was maintained using a syringe pump (Cole Parmer Instrument Company, Vernon Hills, IL).

#### 4.4.4 *Preparation and coating of agonists.*

Preparation of collagen was based on a method described by Cazenave *et al.* (1973). Specifically, 100 mg type I calf-skin collagen was dissolved in 1.2 ml glacial acetic acid and diluted with 19.8 ml of deionized water. The suspension was gently stirred over ice for ten minutes. Subsequently, the suspension was homogenized for 15 minutes in a Biospec Homogenizer (Biospec, Bartlesville, OK) and then centrifuged for ten minutes at  $2500 \times g$  at room temperature. The suspension was further diluted with 20 ml of deionized water and re-homogenized for ten minutes, followed by re-centrifugation at

1000 × g. The overlying white layer was skimmed off. The final suspension contained 0.8 mg collagen /ml in 0.522 M glacial acetic acid. Type I -human fibrinogen was prepared at a final concentration of 0.3 mg /ml, as recommended by Fry and Hoak (1989). Fibrinogen (30 mg) was allowed to slowly dissolve over time when layered on the surface of a 100 ml volume of 0.85% (v/v) saline solution at 37 °C to avoid protein-globulization that occurs upon agitation. Preparation of IgG (final concentration of 0.3 mg/ml) was similar to that described for fibrinogen, except that the saline solution was at 23 °C. Prior to each experiment, the membrane surface was incubated with a solution of the agonist in a humidified environment at 37 °C for two hours.

#### 4.4.5 *Experimental protocol.*

All experimental methods were approved by the *Institutional Review Board for Human Research* at Oklahoma State University, Stillwater, OK. Experiments were performed at 23 °C. All gas mixing was performed in a certified safety hood due to the potential toxicity of NO.

Two similar NO delivery chambers were used. Platelet suspension perfusing through one chamber was exposed to a gaseous mixture of NO /N<sub>2</sub>. Platelet suspension flowing through the other chamber, used as a control, was exposed to N<sub>2</sub> alone. Due to negligible back-diffusion, platelets in the upstream half of the flow slit were not exposed to the gas. In all experiments, the perfusion of platelet suspension was preceded and followed by a five-minute perfusion of 1% (v/v) PBS. Pre-perfusion with PBS was necessary to remove microbubbles at the liquid/gas interface at the membrane/adhesion that would otherwise alter normal platelet deposition characteristics. The influence of

agonist, perfusion time, and shear rate on NO inhibition of platelet deposition was assessed following perfusion of the platelet suspension.

*Agonist studies.* Previous quantitative experiments with collagen demonstrated that 0.1 ppm of NO was effective in inhibiting platelet deposition, at a wall shear rate of  $250 \text{ s}^{-1}$ . Thus, for agonist studies platelet inhibition was initially evaluated upon exposure to 0.1 ppm NO. Platelet suspension was perfused through the flow slit at a shear rate of  $250 \text{ s}^{-1}$  (1 cc/min) for 15 minutes to determine the minimal (threshold) surface NO concentration at which platelet inhibition occurs for each agonistic protein. Platelet suspension was exposed to gaseous NO concentrations of 0.02 or 0.1 ppm for experiments with collagen and IgG. When the membrane was coated with fibrinogen, platelet inhibition was evaluated subsequent to exposure to 0.01 or 0.1 ppm of NO.

*Time-dependency studies.* The influence of perfusion time was assessed using a collagen-coated membrane for times of 7.5 minutes and 15 minutes. The wall shear rate was  $250 \text{ s}^{-1}$  and platelets were exposed to either 0.02 ppm or 0.1 ppm of NO.

*Shear-rate studies.* The influence of wall shear rate on NO inhibition of platelet deposition was assessed at  $250 \text{ s}^{-1}$  and  $500 \text{ s}^{-1}$  for both collagen and fibrinogen. Platelet suspension was perfused through the flow slit for 7.5 minutes. Platelet inhibition was assessed upon exposure of platelets to 0.02 ppm of NO for collagen and 0.01 ppm of NO for fibrinogen.

Following each experiment, membranes were sectioned into upstream and downstream halves and the radioactivity due to adhered platelets was counted on an Autogamma Counter (Cobra II, Beckman Instruments, Downers Grove, IL). Calibration of radioactive counts in terms of platelet counts was performed as detailed in Eq. 3.2 in

section 3.7.1. Again, the concentration of agonist protein coated on the membrane was not assessed, since the proteins were not radiolabeled. Accordingly, to avoid biasing results due to potential differences in agonist concentrations on control and non-control surfaces, the total platelet counts in the upstream and downstream sections were quantified. The percentage inhibition due to NO was estimated using Eq. 3.3.

Aspirin is a potent antagonist of platelet aggregation, although its role in inhibiting platelet adhesion is ambiguous. Aspirin was added to both control (only N<sub>2</sub> exposure) and non-control (NO exposure) chambers. The percentage inhibition estimated using Eq. 3.3 is due to NO alone. However, in order to estimate inhibition due to aspirin alone, additional platelet experiments were performed. Platelet deposition on a membrane exposed to a platelet suspension with aspirin was compared with deposition on a control membrane (aspirin not added to perfusate). In these experiments, the wall shear rate was 250 s<sup>-1</sup> and perfusion was maintained for 15 minutes. Platelet deposition was induced by fibrinogen pre-adsorbed on the membrane for the aspirin studies.

#### **4.5 Results.**

*Platelet Counts.* The platelet counts per unit area of the upstream section for membranes exposed to N<sub>2</sub> alone are shown in Table 4.2. Platelet counts on the upstream membrane sections in both control and non-control experiments were mostly similar. Conforming to established trends, for a given platelet agonist, platelet deposition was enhanced at higher wall shear rates for similar perfusion times [Baumgartner and Sakariassen, 1985]. Also, as shown for both collagen and fibrinogen at 250 s<sup>-1</sup>, platelet deposition was enhanced upon perfusion for 7.5 minutes relative to 15 minutes. This

**Table 4.2****Platelet counts per unit area of upstream membrane section of control**

<b>Agonist</b>	<b>Wall Shear Rate (<math>\gamma</math>) (<math>s^{-1}</math>)</b>	<b>Perfusion Time (min)</b>	<b>Platelet Count (<math>10^6/cm^2</math>)</b>
Collagen	250	15	$5.3 \pm 2.4$ ( $n = 6$ )
		7.5	$9.9 \pm 1.5$ ( $n = 6$ )
	500	7.5	$12.1 \pm 5.2$ ( $n = 6$ )
Fibrinogen	250	15	$2.9 \pm 0.3$ ( $n = 6$ )
		7.5	$4.3 \pm 3.0$ ( $n = 3$ )
	500	7.5	$9.2 \pm 3.2$ ( $n = 3$ )
IgG	250	15	$8.7 \pm 2.4$ ( $n = 6$ )

may be due to the shearing off and break-up of surface platelet thrombi upon perfusion for prolonged time periods.

*Effect of Agonist.* Fig. 4.2, 4.3, and 4.4 show the percentage inhibition of platelet deposition following gaseous NO exposures of 0.1 ppm and 0.01/0.02 ppm (0.01 for fibrinogen, 0.02 for others) to collagen, fibrinogen, and IgG, respectively. An exposure of 0.1 ppm of NO resulted in complete or near complete inhibition of platelet deposition, regardless of the protein studied. However, platelet deposition was only partially inhibited following exposure to 0.02 (or 0.01) ppm of NO. For fibrinogen, platelet inhibition was still significant at 0.02 ppm, and as a result, radioactive counts in the downstream NO-exposed membrane section were too low for reliable measurements. Accordingly, for fibrinogen, 0.01 ppm NO exposure was studied to yield higher counts. Table 4.3 summarizes the results of the agonist studies. Inhibition values shown represent Mean  $\pm$  SD of  $n$  repeats. In this study, surface concentrations of agonists were not measured. Therefore, a quantitative comparison of percent inhibition for different agonists at the lower NO exposure levels is not feasible. To obtain this information, similar surface concentrations of all agonists must form a basis for evaluation.

*Effect of Perfusion Time.* Figure 4.5 shows the inhibition due to exposure of platelets to 0.02 ppm and 0.01 ppm of NO over 7.5 minutes and 15 minutes. For a NO exposure of 0.02 ppm and a flow wall-shear rate of  $250 \text{ s}^{-1}$ , percent platelet inhibition was  $8 \pm 5\%$  and  $10 \pm 8\%$  for 15 and 7.5-minute perfusion times, respectively. The corresponding levels of inhibition for 0.02 ppm NO exposure were  $99 \pm 3\%$  and  $97 \pm 3\%$ , respectively. Platelet deposition was induced by collagen.



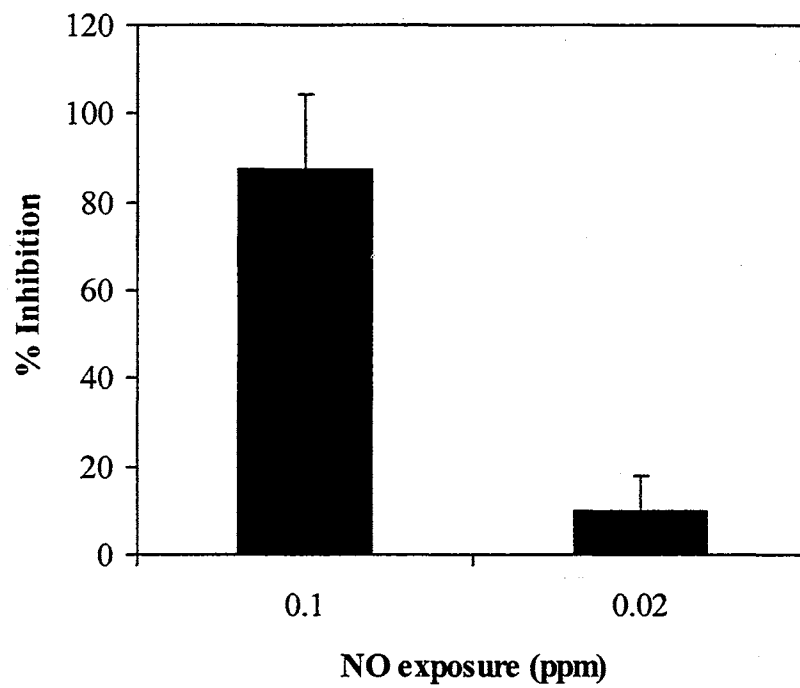


Figure 4.2. Percentage inhibition of collagen-stimulated platelet deposition upon exposure to 0.1 and 0.02 ppm of gaseous NO. Columns and bars represent Mean  $\pm$  SD for each exposure series ( $n = 3$ ).

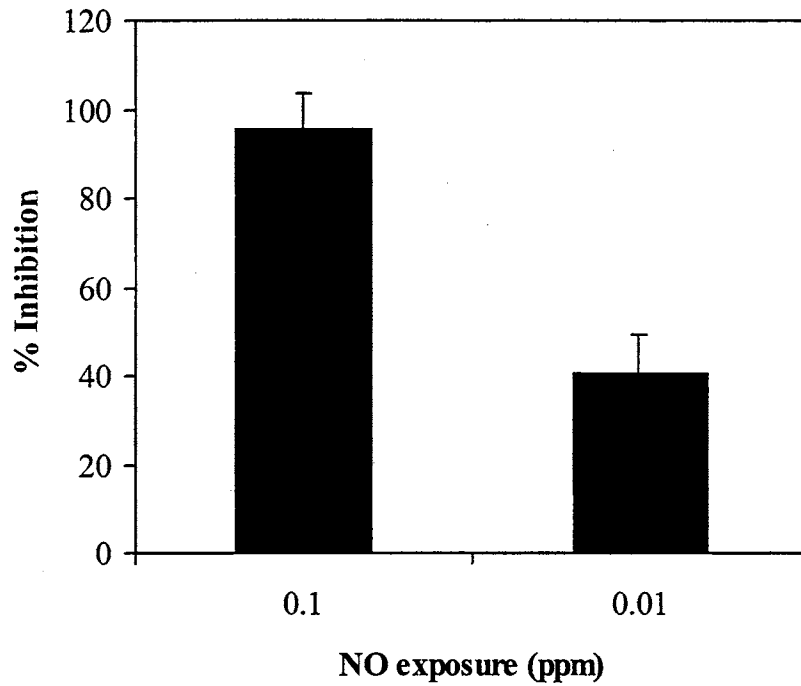


Figure 4.3. Percentage inhibition of fibrinogen-stimulated platelet deposition upon exposure to 0.1 and 0.01 ppm of gaseous NO. Columns and bars represent Mean  $\pm$  SD for each exposure series ( $n = 3$ ).

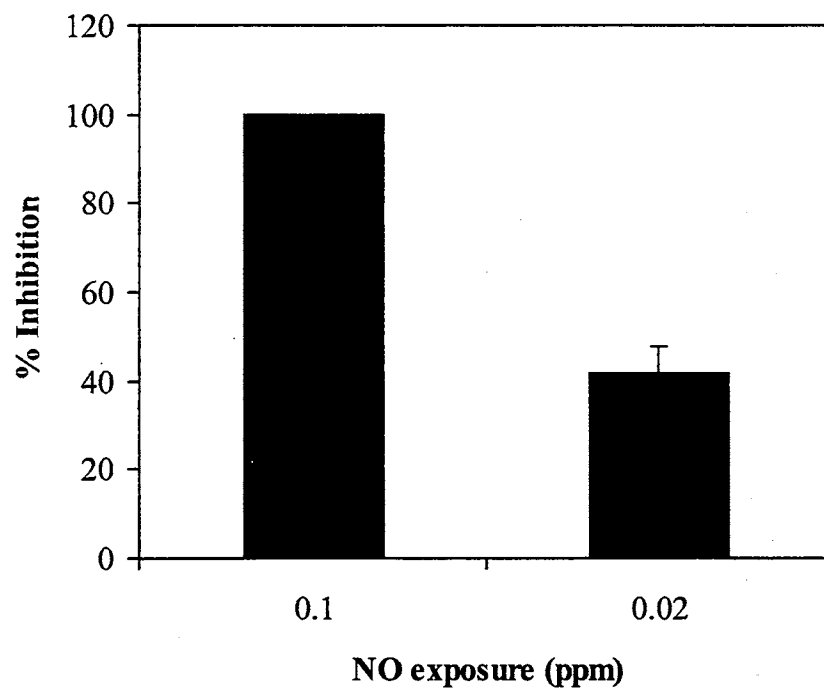


Figure 4.4. Percentage inhibition of IgG-stimulated platelet deposition upon exposure to 0.1 and 0.02 ppm of gaseous NO. Columns and bars represent Mean  $\pm$  SD for each exposure series ( $n = 3$ ).

**Table 4.3****Nitric oxide inhibition of agonist-induced platelet deposition**

<b>Agonist</b>	<b>NO Exposure (ppm)</b>	<b>Shear Rate (s<sup>-1</sup>)</b>	<b>Perfusion Time (min)</b>	<b>% Inhibition</b>	<b><i>n</i></b>
Collagen	0.1	250	15	87.5 ± 16.8	3
	0.02			9.7 ± 8.4	3
Fibrinogen	0.1	250	15	95.4 ± 7.9	3
	0.01			40.4 ± 8.9	3
IgG	0.1	250	15	100.0 ± 0.00	3
	0.02			41.7 ± 6.2	3

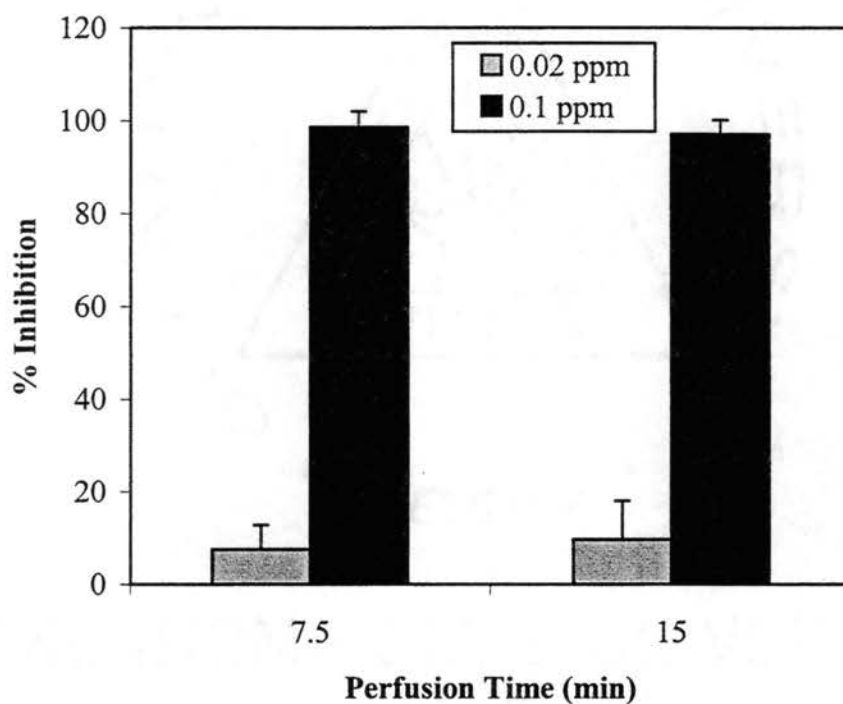


Figure 4.5 Percentage inhibition of platelet deposition on a collagen-coated membrane by 0.02 and 0.1 ppm of NO, as a function of perfusion time. Columns and bars represent Means  $\pm$  SD at each perfusion time ( $n = 3$ ).

*Effect of Shear Rate.* The anti-thrombogenic potency of NO appeared independent of the wall shear rate for the two shear rates studied. As shown for collagen in Fig.4.6, exposure to 0.02 ppm of NO resulted in inhibition of platelet deposition by  $8 \pm 6\%$  and  $5 \pm 6\%$ , at shear rates of  $250 \text{ s}^{-1}$  and  $500 \text{ s}^{-1}$ , respectively. A similar trend is exhibited for fibrinogen (see Fig. 4.7) for which platelet adherence was inhibited by  $41 \pm 9\%$  and  $34 \pm 12\%$  at shear rates of  $250 \text{ s}^{-1}$  and  $500 \text{ s}^{-1}$ , respectively, for a NO exposure of 0.01 ppm.

#### **4.6 Interpretation of results.**

In the study described in chapter 3, the minimal NO concentration and flux significantly inhibiting collagen-stimulated platelet deposition was predicted at the adhesion surface. Relating surface NO concentrations or fluxes to corresponding levels of platelet inhibition is helpful in assessing threshold aqueous NO concentrations required for significant anti-platelet deposition.

In the current study, experiments performed using the hole/porous delivery device, at  $250 \text{ s}^{-1}$ , showed complete inhibition at a surface NO concentration of 0.09 nM (0.1 ppm exposure) irrespective of the agonist employed. Thus, this study shows that a surface NO concentration of 0.09 nM is essentially effective in maintaining the membrane surface platelet-free, independent of the agonist (collagen, fibrinogen, or IgG) used to stimulate platelet-surface interactions. The comparable NO flux at the delivery surface ranges between 0.3 and 0.6 femtomoles  $\text{cm}^{-2} \text{ s}^{-1}$ , at  $250 \text{ s}^{-1}$ , when predicted using the model represented by Eq. 2.8. However, a NO concentration of 0.02 nM (0.02 ppm exposure) at the adhesion surface is only partially effective in inhibiting platelets. The different levels of inhibition by NO observed for different platelet agonists at NO

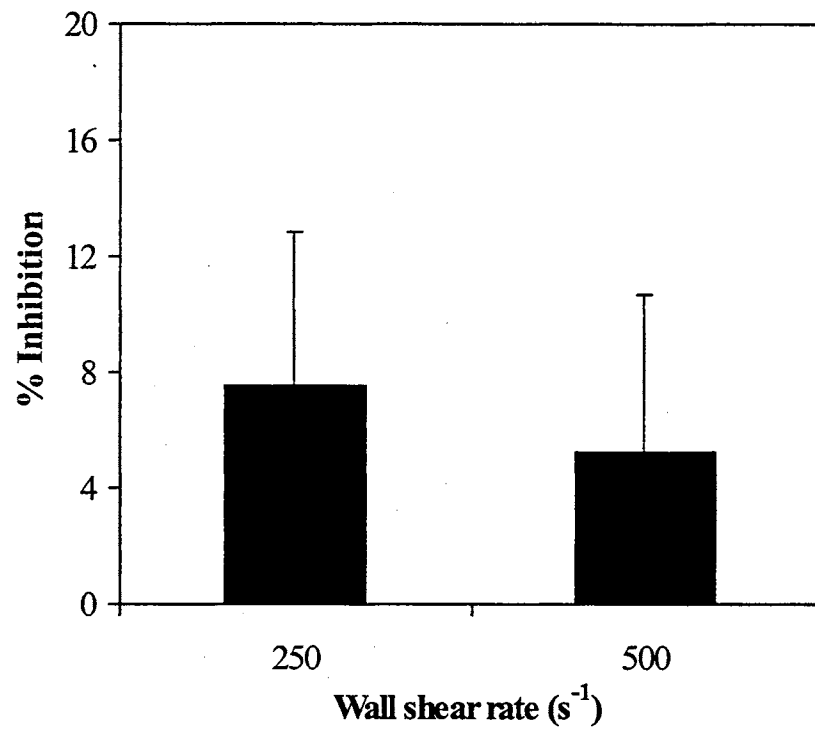


Figure 4.6. Nitric oxide inhibition of collagen-stimulated platelet deposition as a function of wall shear rate. NO exposure is 0.02 ppm. Columns and bars represent Means  $\pm$  SD of  $n = 3$  repeats at each shear rate.

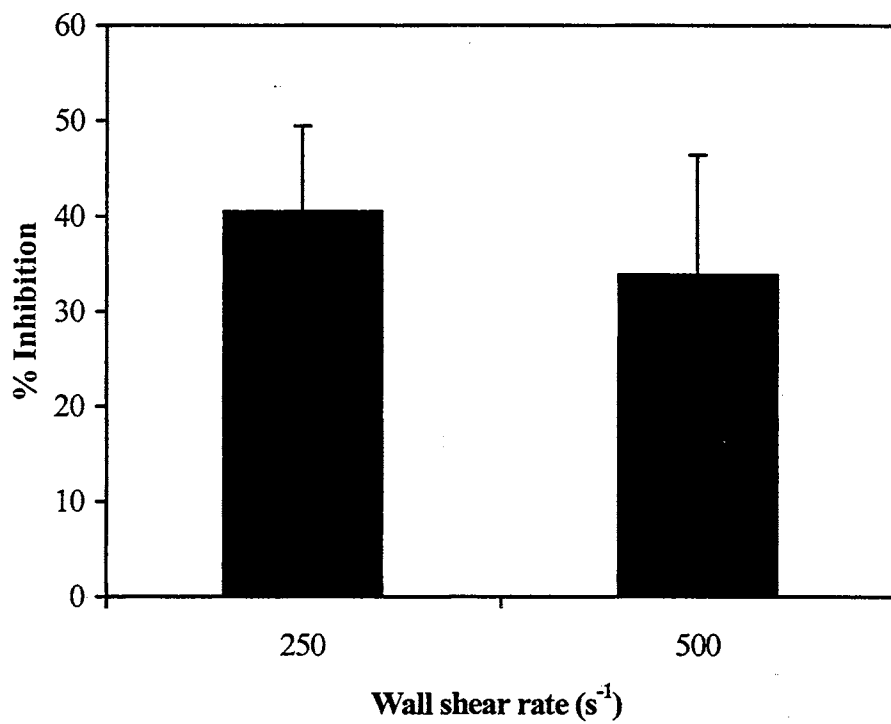


Figure 4.7. Nitric oxide inhibition of fibrinogen-stimulated platelet deposition as a function of wall shear rate. NO exposure was 0.01 ppm of NO. Columns and bars represent Means  $\pm$  SD of  $n = 3$  repeats at each shear rate.



exposures lower than 0.1 ppm suggests that multiple mechanisms of platelet inhibition may be involved. However, in the absence of data corroborating the actual surface protein concentration, such conclusions are premature. Radiolabeling of coated proteins would provide a better inter-agonist comparison of NO inhibitory action.

The current study shows that overall inhibition of platelet adhesion at the NO delivery surface is uninfluenced by duration of platelet exposure to NO, over at least 15 minutes. Although the platelet count per unit area varies with perfusion time (see Table 4.2), the percent inhibition does not. This is probably due to purely physical phenomena such as shearing, platelet migration, etc. Thus, for once-through flow systems prolonged exposure of surface-adhered platelets to NO does not appear to have a cumulative effect on platelet inhibition, as long as the NO exposure level and other flow parameters are maintained the same.

For a given NO exposure level, variation in wall shear rate does not significantly affect the platelet-inhibitory potency of NO. At shear rates of  $250 \text{ s}^{-1}$  and  $500 \text{ s}^{-1}$  and at a NO exposure of 0.1 ppm, the model predicts NO concentrations of 0.090 nM and 0.086 nM at the adhesion surface, respectively. Although values shown were predicted at the flow slit exit, they are representative of surface concentrations along a significant portion of the membrane length. Results of shear rate studies clearly indicate that such small differences in NO concentrations exposed to platelets do not cause any significant variation in inhibition trends. Even for a five-fold increase in shear rate to  $1000 \text{ s}^{-1}$ , the model predicts a slightly lower surface NO concentration of 0.082 nM, which is likely within the range for significantly inhibiting platelet deposition. However, at such high shear rates, platelet deposition on the membrane surface will be less transport controlled

and predominantly influenced by platelet-surface kinetics [Tschopp *et al.*, 1975]. Also, the NO concentration gradient from the NO delivery surface to the solution would be greater, resulting in a lower NO concentration in the bulk solution. Thus, platelets would likely need to be exposed for longer periods of time to the NO-delivery surface to achieve the degree of inhibition similar to that observed in this study at low shear rates.

In this study, platelet activation during resuspension was avoided by the addition of aspirin to platelet perfusates. A review of literature indicates that the inhibitory action of NO is aspirin-insensitive [Marcus *et al.*, 1995]. For this study, the addition of aspirin did not influence the reported NO inhibitory capacities. This was confirmed by synergy studies with aspirin and NO, discussed elaborately in chapter 5. However, aspirin by itself inhibited platelet deposition by 50% over 15 min at 250 s<sup>-1</sup>.

#### **4.7 Physiological relevance.**

The relevance of this study is enhanced by the general agreement of the results discussed above with previously estimated NO fluxes from endothelial cells lining blood vessels. The vascular endothelium inhibits vascular platelet deposition via three mechanisms, one of which is mediated by NO release [Marcus *et al.*, 1995]. Kelm *et al.* (1988) estimated the NO flux generated by endothelial cells obtained from porcine thoracic aorta as ~ 6 femtomoles cm<sup>-2</sup> s<sup>-1</sup>. Although these physiological fluxes are slightly higher than the threshold values determined in this study (0.3-0.6 femtomoles cm<sup>-2</sup> s<sup>-1</sup>), it is important to realize that the values determined are only the minimal fluxes required to effectively inhibit platelet deposition. In parallel, the 'free' NO concentration in blood was estimated as 3 nM [Stamler *et al.*, 1992]. The threshold surface NO

concentrations for significant platelet inhibition, determined in this study, are  $\sim 0.09$  nM. Again, this difference may be due to the fact that in blood NO is present in excess of the minimal requirement for anti-thrombotic action in order to compensate for significant consumption of NO due to reaction.

#### **4.8 Conclusions**

In conclusion, the novel NO delivery system developed previously was used to quantitatively compare the potency of NO inhibition of platelet adherence and thrombosis as a function of platelet agonist, shear rate, and perfusion time. Results clearly indicate that the minimal NO exposure significantly inhibiting platelet deposition is uninfluenced by the nature of the platelet agonist, shear rate, or perfusion time ( $< 15$  minutes). For each platelet-agonist studied, the minimal surface NO concentrations and fluxes significantly inhibiting platelet deposition were determined for a variety of shear rates and perfusion times. The results of this study are useful in establishing generalized guidelines for the design and development of suitable bioartificial surfaces incorporating NO to reduce surface thrombosis. Thus, controlled delivery of NO at the minimal rates determined in this study will minimize the potential for toxicity and mutagenicity associated with excessive NO exposures.

## CHAPTER 5

### SYNERGISTIC PLATELET INHIBITION BY APYRASE AND NITRIC OXIDE

#### 5.1 Introduction.

In chapters 3 and 4, the minimal surface NO concentrations or fluxes necessary for significant inhibition of platelets were determined. The studies demonstrated that the effective NO concentrations and fluxes were not influenced by factors such as time of exposure, shear rate, and nature of the platelet agonist. The gaseous NO exposure that minimized platelet deposition (0.1 ppm) is below NO toxicity limits set by OSHA (25 ppm).

The exposure of platelets to lower NO amounts than described above, without compromising the inhibitory effects, would be preferred to reduce the potential toxicity or carcinogenicity of NO. The investigation of agents that work in combination with NO in inhibiting platelet-biomaterial interactions is relevant in this context. The benefit of such agents is that significant inhibition of surface thrombosis may occur using lower NO exposure levels in combination with the agents.

Apyrases (or ectonucleotidases) are enzymes released by vascular endothelial cells as one of three primary *in vivo* mechanisms for inhibiting vascular thrombosis [Marcus *et al.*, 1995]. The other two anti-platelet agents released by endothelial cells are eicosanoids and nitric oxide. The mechanisms via which the above platelet antagonists effect their anti-platelet actions is detailed in section 1.1.2. Currently, it is unknown whether these

three mechanisms are synergistic or merely complementary. Synergistic inhibition would imply that if two inhibitory agents were to act in parallel, inhibition of platelet adhesion/aggregation would be greater than the sum of the inhibitory potencies due to either of the antagonists alone. This could be due to conformational changes in either or both platelet surface receptor sites, thereby enhancing the affinity for binding the antagonists. Alternately, the inhibitory potency of apyrase may be enhanced due to NO-induced conformational changes of apyrase.

This chapter describes results that show synergistic inhibition between apyrases and NO. The study yields information useful in establishing guidelines for synergistic platelet inhibition due to interactions between the two platelet antagonists released by vascular endothelia *in vivo*. The results of the study may also be used to design novel biomaterials incorporating apyrase and NO for enhancing hemocompatibility while reducing the NO release requirements for significant platelet inhibition determined earlier in chapters 3 and 4.

## **5.2 Objectives.**

The overall objectives of the study were to

- (a) Experimentally demonstrate or disprove synergy between NO and apyrase in inhibiting platelet deposition to a collagen-coated biomaterial in an *in vitro* flow environment. To realize this goal, platelet inhibition by apyrase was first determined as a function of apyrase dose. Further the inhibitory potency of apyrase and synergy between NO and apyrase was determined under various shear rate conditions.

- (b) Establish guidelines for delivery of apyrases in parallel with NO at biomaterial surfaces for significant inhibition of platelet deposition at NO exposures lower than the threshold values established previously for NO alone. Therefore, it was necessary to investigate dependence of synergy between apyrase and NO on their respective dosages/exposures at given flow conditions.
- (c) Examine the effect of aspirin addition on synergy between NO and apyrases.

### 5.3 Materials and Methods.

#### 5.3.1 Reagents.

All gases and reagents required for platelet counting, preparation of platelet suspensions, platelet labeling, and pre-perfusion were obtained from sources detailed earlier in chapters 2, 3, and 4.  $MgCl_2 \cdot 6H_2O$  was purchased from EM Science (Gibbstown, NJ). Acetyl salicylic acid (aspirin) and potato apyrase (Grade VII) containing a low ATPase/ADPase ratio were procured from Sigma Chemicals (St. Louis, MO).

#### 5.3.2 Selection of Enzyme.

Apyrase is a generic term applied to several classes of related enzymes that are characterized by significant capacity for degradation of ADP, and to a lesser extent, ATP into AMP and adenosine. Apyrases are thus classified as ADPases. Excessive platelet accumulation and recruitment at sites of vascular injury and exposure to collagenated basement membranes stimulate ADP release from platelets [Koyamada *et al.*, 1996; Robson *et al.*, 1997; Gayle *et al.*, 1998]. Extracellular ADP is a key mediator of platelet

thrombosis. Thus, the capacity of apyrases for scavenging ADP contributes to their importance as anti-thrombogenic agents.

ADPases are isolated from several different sources. Apyrases may be relatively easily isolated from plant sources such as potatoes [ Molnar and Lorand, 1961; Kinloch-Rathbone *et al.*, 1983; Mustard *et al.*, 1989]. Quiescent endothelial cells (ECs) also release ecto-nucleotidases, which are morphologically and functionally similar to potato apyrases. CD39 is a soluble form of the human ecto-enzyme (i.e., an enzyme released to outside the cell) which was previously demonstrated to show potential as a therapeutic agent for inhibition of platelet-mediated thrombosis *in vivo* [Koyamada *et al.*, 1996] or *in vitro* [Gayle *et al.*, 1998]. Although mechanisms of action of the apyrases are mostly similar, they may differ significantly in their activities, and hence in their effectiveness as platelet antagonists.

Several factors influenced the selection of the apyrase used in this study, including (a) ease of isolation, (b) quantities available, (c) activity, (d) ATPase/ADPase ratio, and (e) cost. Endothelial CD39 is considerably more difficult and expensive to isolate relative to potato apyrases, which may be easily obtained in relatively large amounts within a few hours. Furthermore, they are not commercially available. The endothelial enzymes may be obtained in a highly pure form or may be manipulated to obtain recombinant forms that may be obtained in larger quantities. The recombinant enzymes, however, rapidly lose their activity and may not show significant anti-platelet characteristics except under certain specified conditions. Potato apyrases are commercially available and have a wide range of activities and specificities for applications to different situations. Therefore, highly purified potato apyrase was used for this study. Grade VII apyrase containing a

low ratio of ATPase to ADPase activity (ATPase activity > 200 U/mg protein; ATPase/ADPase <2) was selected. The enzyme degrades both ATP and ADP. Similar to ADP, ATP is also constituent of dense granules within platelets, is also released upon stimulation with collagen [Reimers, H.J, 1985]. However, ATP is a known antagonist of platelet purinoreceptors (i.e., adhesion receptors activated by agents certain with purine moieties, such as ADP) involved in the aggregation process, while ADP is an agonist. Therefore, preferred degradation of ADP by ADPase predominance was desired.

### *5.3.3 Preparation of enzyme and platelet perfusate.*

A stock solution of soluble grade VII apyrase was prepared as per methods suggested by the manufacturers (Sigma Chemicals, St. Louis, MO). The volume of medium used for dissolution of the enzyme depended upon the initial activity of the enzyme and later the amount to be added to the platelet suspension. Apyrase used in this study contained either 100 U (0.8 mg) or 200 U (1.55 mg). Preparation guidelines by Sigma advise dissolution of apyrase in physiological saline (1% v/v) or deionized water when the concentration is greater than 1 mg/ml. When prepared at concentrations less than 1 mg/ml, apyrase is unstable and may degenerate in storage over short time periods. This may be reduced by preparation of apyrase in HEPES buffer pH 7.5 containing 1 mM MgCl<sub>2</sub>, 1 mM DTT, 1 mM EDTA, and 1 mM BSA. For this study, stock apyrase solutions containing 200 U/ml (~1.6 mg/ml) were prepared in deionized water for both reasons of enzyme stability, and economics.

Washed platelet suspensions containing  $3.5 \times 10^8$  platelets/ml were prepared, as described earlier in section 3.6.4., from 30 cc of human blood drawn from consenting



adult volunteers. However, in addition to the regular buffer components, BSGC buffer used for suspending platelets contained 4 mM MgCl<sub>2</sub>. Mg<sup>2+</sup> ions are necessary to avoid irreversible monophasic platelet aggregation, which results in platelet destruction. Further, the presence of divalent Mg<sup>2+</sup> or Ca<sup>2+</sup> ions is required to maintain apyrase activity [Luthje *et al.*, 1988]. Similar to earlier studies (see chapters 3 and 4), platelet deposition on the biomaterial was induced by a surface coat of Type I calfskin collagen (0.8 mg/ml v/v). Collagen was prepared by the method of Cazenave *et al.*, detailed in section 3.2.6. Platelet deposition was quantified by radiolabeling platelets with <sup>51</sup>CrO<sub>4</sub> as detailed in section 3.6.4. For apyrase studies, an appropriate micro-volume of the stock apyrase solution (200 U/ml) was added to the platelet suspension, which was then incubated at 37 °C for 15 minutes prior to the experiment. In this study, apyrase dosages ranged between 0.025 U/ml and 0.2 U/ml. The apyrase-dosed platelet suspension was allowed to cool to room temperature (23 °C) before perfusion.

All perusates were aspirin-free except for studies with aspirin where 1.2 µg aspirin/10<sup>9</sup> platelets was added to the platelet perfusate early in the preparative procedure (see section 3.6.4).

#### 5.3.4 *General experimental methods.*

All experiments were approved by *the Institutional Review Board for Human Research* at Oklahoma State University, Stillwater, OK. All experiments were performed at 23 °C. The experimental setup for the platelet deposition studies was identical to that described earlier in section 3.3 and shown in Fig. 3.2. The perfusion device incorporating parallel slots for delivery of NO (described previously in chapter 2), was used in this

study. The NO delivery/platelet adhesion surface was coated with collagen, a platelet agonist to induce platelet deposition. Based on the results of previous platelet inhibition studies with NO, gaseous NO exposures were restricted to less than 0.1 ppm. Accordingly, the NO source tank containing 1% (v/v) NO was used to obtain NO gas mixtures as low as 0.01 ppm. Flow shear rates were restricted between  $250 \text{ s}^{-1}$  and  $750 \text{ s}^{-1}$ . Gas exposure times were either 5 minutes or 7.5 minutes. . In all experiments, perfusion of platelets was preceded and followed by perfusion with PBS (1% v/v) for five minutes to remove microbubbles at the liquid-collagen surface.

### 5.3.5 *Non-synergistic studies.*

#### 5.3.5.1 *Nitric oxide.*

*Dosage studies.* Previously, inhibition of platelet deposition on a collagen-coated surface was assessed at NO exposures of 0.02 and 0.1 ppm. In these studies, aspirin was added to platelet perfusates in both control (only  $\text{N}_2$  exposure) and non-control (NO exposure) chambers. In the current study, platelet perfusates were aspirin-free. Hence, platelet inhibition by NO, in the absence of aspirin, was assessed at gaseous NO exposures of 0.02 ppm and 0.05 ppm, at  $250 \text{ s}^{-1}$ . Platelets were exposed to NO for 7.5 minutes. In the control chamber, platelets were only exposed to  $\text{N}_2$ .

*Shear rate studies.* Previous studies (see chapter 4) indicated that platelet inhibition at a given NO exposure was unaffected by perfusion time (less than 15 minutes) and shear rate (less than  $500 \text{ s}^{-1}$ ). Thus the percentage inhibition determined at  $250 \text{ s}^{-1}$ , would be similar to that at  $500 \text{ s}^{-1}$  for similar NO exposures. As will be described later, synergy studies between NO and apyrase were performed at  $750 \text{ s}^{-1}$ . NO exposure time was 5

minutes. Thus, both the shear rate and NO exposure time studies were beyond the range for which NO inhibitory potencies were previously determined. The inhibitory potency of NO was therefore evaluated at  $750\text{ s}^{-1}$  for a 5-minute exposure time period, in an aspirin-free environment. Platelets in the downstream half of the flow slit were exposed to 0.05 ppm of NO in one chamber and  $\text{N}_2$  alone in the other (control).

#### 5.3.5.2 *Apyrase.*

*Dosage studies.* The objective of this study was to determine apyrase inhibition of platelet deposition as a function of apyrase dosage. Platelet deposition on the collagen-coated membrane in a control chamber (no apyrase added) was compared with that in a similar chamber through which an apyrase dosed- platelet suspension was perfused. Platelet inhibition was assessed for apyrase dosages of 0.025, 0.05, 0.1, and 0.2 U/ml, respectively. Perfusion of platelets was maintained at  $250\text{ s}^{-1}$  (i.e., 1 cc/min) for 7.5 minutes

*Shear rate studies.* The inhibitory potency of apyrase, evaluated at shear rates of  $500\text{ s}^{-1}$  and  $750\text{ s}^{-1}$ , was compared to the value determined at  $250\text{ s}^{-1}$ . In all experiments, platelet deposition was assessed for a 7.5-minute perfusion time. In each case, platelet deposition in the presence of 0.025 U/ml apyrase was compared to platelet deposition in a control chamber perfused with an apyrase-free platelet suspension. In addition, at  $500\text{ s}^{-1}$ , platelet inhibition was determined for an apyrase dosage of 0.05 U/ml, and compared to the inhibition caused by a similar dose of apyrase at  $250\text{ s}^{-1}$ .

### 5.3.6 *Synergistic studies.*

#### 5.3.6.1 *Nitric oxide and aspirin.*

In all experiments,  $1.2 \mu\text{g aspirin}/10^9$  platelets was added to platelet perfusates as described earlier in section 5.3.3. Inhibition of platelet deposition in the absence of aspirin was compared to that observed when aspirin was added to a platelet suspension. For aspirin-free studies, platelets in the downstream half of the flow slit were exposed to 0.02 ppm of NO, in one chamber and  $\text{N}_2$  alone in the other (controls). Perfusion was maintained for 7.5 minutes at a shear rate of  $250 \text{ s}^{-1}$ . Upstream membrane sections in both control and non-control chambers were unexposed to gas. Platelet inhibition in the presence of aspirin was determined from previous experiments (0.02 ppm NO;  $250 \text{ s}^{-1}$ ; 15 minutes) described in section 3.7.

#### 5.3.6.2 *Apyrase and aspirin.*

The purpose of this study was to determine if addition of aspirin influenced the inhibitory capacity of apyrase. Platelet deposition on a membrane exposed to a platelet suspension containing 0.025 U/ml apyrase and aspirin was compared with deposition on a membrane exposed to a platelet perfusate containing aspirin alone (controls). Perfusion was maintained at a wall shear rate of  $250 \text{ s}^{-1}$  for 7.5 minutes.

#### 5.3.6.3 *Nitric oxide and apyrase.*

Initially, synergy between apyrase and NO in inhibiting platelet deposition was assessed at a shear rate of  $250 \text{ s}^{-1}$  over 7.5 minutes. All experiments were performed with aspirin-free perfusates. In the first set of experiments, platelet perfusates in both control

and non-control chambers contained 0.025 U/ml apyrase. However, platelets in the downstream porous block region of the non-control chamber were additionally exposed to 0.02 ppm of NO. Platelets in the upstream half of the flow slit in both chambers were unexposed to gas. Thus, deposition on upstream membrane sections in both chambers was expected to be similar.

*Dosage studies.* In order to assess the influence of apyrase dosage and NO exposure on the extent of synergy, further experiments were performed. In one set of experiments, platelets were exposed to higher gas NO concentrations (0.05 ppm) while the apyrase dosage was maintained at similar to the first set of experiments (0.025 U/ml). In the other set, the apyrase dosage was increased to 0.05 U/ml while the NO exposure was maintained the same at 0.05 ppm. In all experiments, platelet inhibition due to NO in the presence of apyrase was determined and compared with the inhibition due to NO in the absence of apyrase.

*Shear rate studies.* The influence of shear rate on synergistic platelet inhibition by NO and apyrase was determined by comparing platelet inhibition at higher shear rates of 500 s<sup>-1</sup>, and 750 s<sup>-1</sup> with that at 250 s<sup>-1</sup>. Perfusion of platelets was maintained for 7.5 minutes at 250 s<sup>-1</sup> and 500 s<sup>-1</sup>, and for 5 minutes at 750 s<sup>-1</sup> with 0.025 U/ml apyrase and 0.05 ppm NO. Again, platelets in the control chamber were exposed to apyrase alone. The effect of apyrase dose on the extent of synergy was evaluated at 500 s<sup>-1</sup> also. In these experiments, NO exposure was maintained at 0.05 ppm while the platelets were exposed to higher apyrase dosages (0.05 U/ml). Results were compared with that of similar experiments performed at 250 s<sup>-1</sup>.

#### *5.3.6.4 Nitric oxide, apyrase, and aspirin.*

These experiments evaluated the influence of aspirin on synergistic platelet inhibition by NO and apyrase. Platelets in one chamber were exposed to 0.025 U/ml apyrase, 0.02 ppm NO, and aspirin. In the other chamber (controls), platelets were exposed to aspirin and apyrase, but not NO. Platelet deposition on membranes in both chambers was compared to determine the inhibitory potency of NO in the simultaneous presence of both apyrase and aspirin. Inhibition due to NO in the presence of apyrase and aspirin was compared to that in the presence or absence of apyrase with no aspirin. This allowed assessment of the effect of apyrase/aspirin on platelet inhibition by NO.

#### *5.3.7 Methods of analysis.*

For studies involving NO, NO gas was exposed to platelets in the downstream half of the flow slit. In some cases, platelets were also exposed to aspirin and/or apyrase added to the platelet suspension. To determine the percentage inhibition due to NO, platelet deposition on the membrane in the non-control chamber was compared with that in a control chamber in which platelets were exposed to all species except NO. The upstream membrane sections in both the NO-exposure and control chambers were used as a basis for comparison. As mentioned earlier, the upstream membrane sections in both chambers are not exposed to any gas, and should accordingly have similar levels of platelet deposition if surface concentrations of collagen are similar.

The concentration of collagen coated on the membrane was not assessed since the collagen was not radiolabeled. To avoid biasing results due to potential differences in collagen concentrations on control and non-control surfaces, the total platelet counts in

the upstream and downstream sections were quantified. The percentage inhibition due to NO was estimated using Eq. 3.3 described previously.

Platelet inhibition due to apyrase was assessed differently. In these experiments, platelets in the control chamber were exposed to all species except the apyrase. However, unlike experiments with NO described above, platelets in the upstream half of the flow slit in both control and non-control chambers were not exposed to similar species and thus could not form a basis for comparison. In such experiments, platelet deposition on the entire membrane exposed to a platelet suspension with added apyrase was compared with deposition on the entire control (apyrase-free) membrane. A disadvantage of this method is that it assumes that the collagen concentrations on both membranes are similar. However, this has been shown to be true in most cases.

#### 5.3.8 *Statistical methods.*

Statistical analysis of data was performed with Statistica software (Statsoft, Tulsa, OK) utilizing a Student's *t* test. A *p* value less than 0.05 is considered to be statistically significant.

### 5.4 **Results.**

#### 5.4.1 *Non-synergistic studies.*

##### 5.4.1.1 *Nitric oxide.*

*Exposure studies.* Figure 5.1 shows percentage inhibition of platelet deposition on the NO-exposed membrane section, relative to controls. Platelet deposition was assessed at

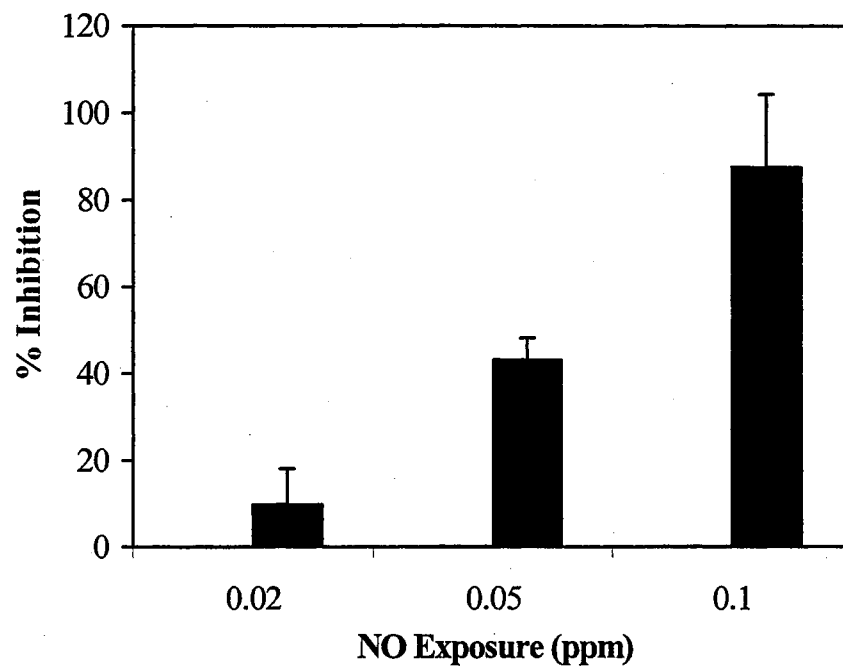


Figure 5.1. Platelet inhibition as a function of NO exposure. Perfusion was maintained at a wall shear rate of  $250 \text{ s}^{-1}$  for 7.5 minutes (15 minutes for 0.1 ppm exposure). Columns and bars represent Mean  $\pm$  SD of  $n = 3$  repeats.



NO exposures of 0.02, 0.05, and 0.1 ppm. The corresponding percentage inhibitions were  $10 \pm 8\%$ ,  $43 \pm 5\%$ , and  $89 \pm 16\%$  at  $250 \text{ s}^{-1}$ . NO exposure time was 7.5 minutes (15 minutes at 0.1 ppm NO). Platelet deposition at NO exposures of 0.02 and 0.05 ppm were assessed in the absence of aspirin while that at 0.1 ppm NO was determined for a platelet suspension containing aspirin. However, as will be discussed later (see section 5.4.2.1), the addition of aspirin does not influence the inhibitory potency of NO. As is evident, NO exposure less than 0.1 ppm results in incomplete inhibition.

*Shear rate studies.* Previously, platelet inhibitory potency of NO was shown to be uninfluenced by shear rate (at less than  $500 \text{ s}^{-1}$ ) and perfusion time (between 7.5 and 15 minutes). Hence, it was not deemed necessary to experimentally determine NO inhibition at  $500 \text{ s}^{-1}$ . Synergy studies between NO and apyrase were also performed at  $750 \text{ s}^{-1}$  with a 5-minute exposure time (see section 5.4.2.3). Thus, both the shear rate and the NO exposure time lie beyond the range studied earlier. Accordingly, the independence of NO inhibitory potency from shear rate and perfusion time was confirmed under these conditions. The percentage inhibition was  $39 \pm 12\%$  upon exposure to 0.05 ppm NO for 5 minutes at  $750 \text{ s}^{-1}$ . This value is similar to the percent inhibition upon exposure to 0.05 ppm NO determined previously, at  $250 \text{ s}^{-1}$ , for 7.5 minutes.

#### 5.4.1.2 Apyrase studies.

*Dosage studies.* Figure 5.2 shows the effect of dose on inhibition of platelet deposition by potato apyrase, at  $250 \text{ s}^{-1}$  for 7.5 minutes. As shown in the figure, platelet inhibition was  $22 \pm 7\%$ ,  $48 \pm 4\%$ ,  $65 \pm 4\%$ , and  $91 \pm 6\%$  at 0.025, 0.05, 0.1, and 0.2

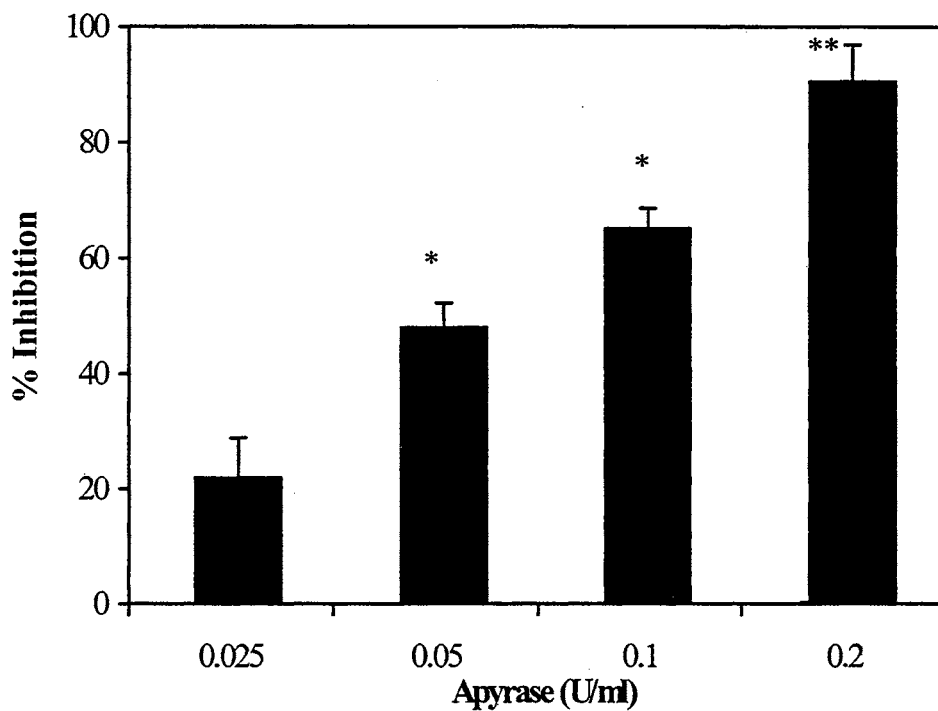


Figure 5.2. Inhibition of platelet deposition by potato apyrase. Perfusion was maintained for 7.5 minutes at a wall shear rate of  $250 \text{ s}^{-1}$ . Columns and bars represent Mean  $\pm$  SD of  $n = 3$  repeats ( $p < 0.01$  for \* and  $p < 0.001$  for \*\* vs. 0.025 U/ml).

U/ml respectively. Thus, almost total inhibition was observed at 0.2 U/ml ( $p < 0.001$  vs. inhibition at 0.025 U/ml).

*Shear rate studies.* Figure 5.3 illustrates the effect of shear rate on the inhibitory potency of apyrase. Inhibition of platelet deposition following exposure of platelets to 0.025 U/ml apyrase was assessed at shear rates of 250, 500, and 750  $s^{-1}$ . The corresponding levels of inhibition observed were  $22 \pm 7\%$ ,  $15 \pm 2\%$ , and 14.6% for 7.5 minutes of exposure (5 minutes at 750  $s^{-1}$ ). Statistical analysis indicated that differences in inhibition between shear rates were statistically insignificant ( $p > 0.2$  vs 250  $s^{-1}$ ).

#### 5.4.2 Synergy studies.

##### 5.4.2.1 Nitric oxide and aspirin studies.

Figure 5.4 compares the percentage inhibition of platelet deposition following exposure to aspirin and aspirin-free platelet suspensions in the presence of 0.02 ppm of NO. At 250  $s^{-1}$ , and for 7.5 minutes of NO exposure (15 minutes in the presence of aspirin), platelet deposition was inhibited by  $10 \pm 8\%$  both in the presence and absence of aspirin. Thus, addition of aspirin does not influence the platelet inhibitory potency of NO.

##### 5.4.2.2 Apyrase and aspirin.

Differences in inhibition of platelet deposition by apyrase in the presence or absence of aspirin was determined to be statistically insignificant as shown in Fig. 5.5. 0.025 U/ml apyrase inhibited platelet deposition by  $15 \pm 2\%$  and  $22 \pm 7\%$  in the absence and

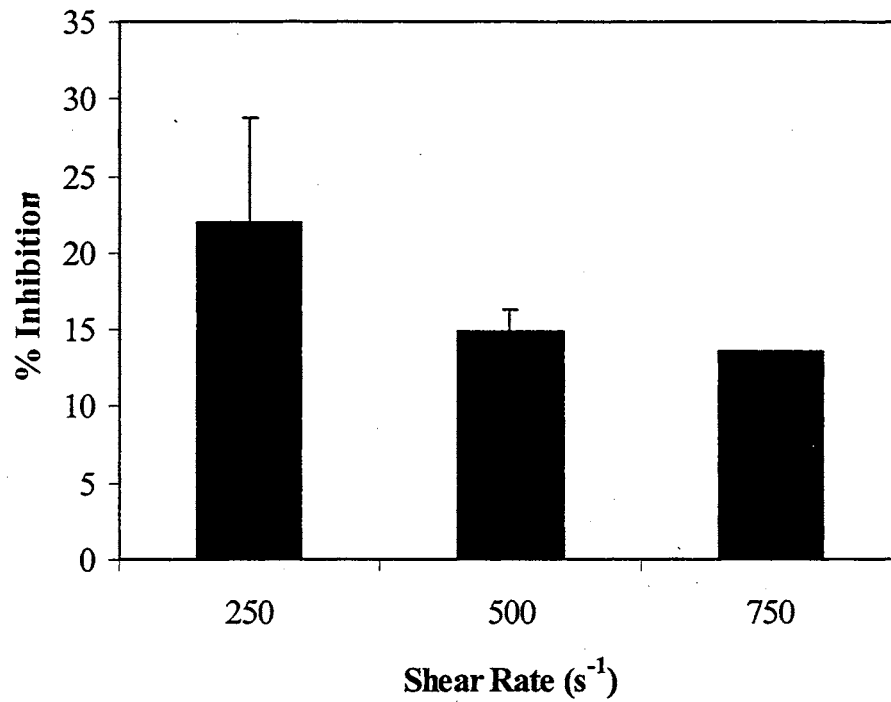


Figure 5.3. Effect of shear rate on apyrase inhibitory potency. Platelets were exposed to 0.025 U/ml of potato apyrase for 7.5 minutes (5 minutes at 750 s<sup>-1</sup>). Columns and bars represent Mean  $\pm$  SD of  $n = 3$  repeats ( $n = 2$  at 750 s<sup>-1</sup>).

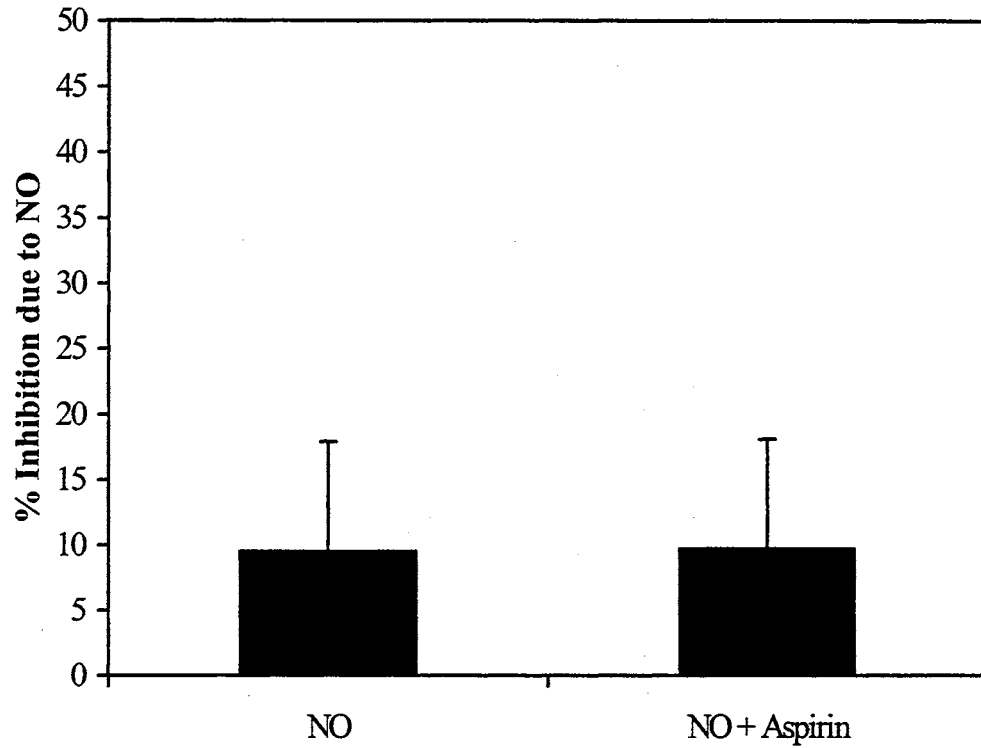


Figure 5.4. Effect of aspirin on platelet inhibitory potency of nitric oxide. Columns and bars represent Mean  $\pm$  SD of inhibition at  $250 \text{ s}^{-1}$  for  $0.02 \text{ ppm NO}$  exposure ( $n = 3$ ). Exposure time is 7.5 minutes in the absence of aspirin and 15 minutes in the presence of aspirin.

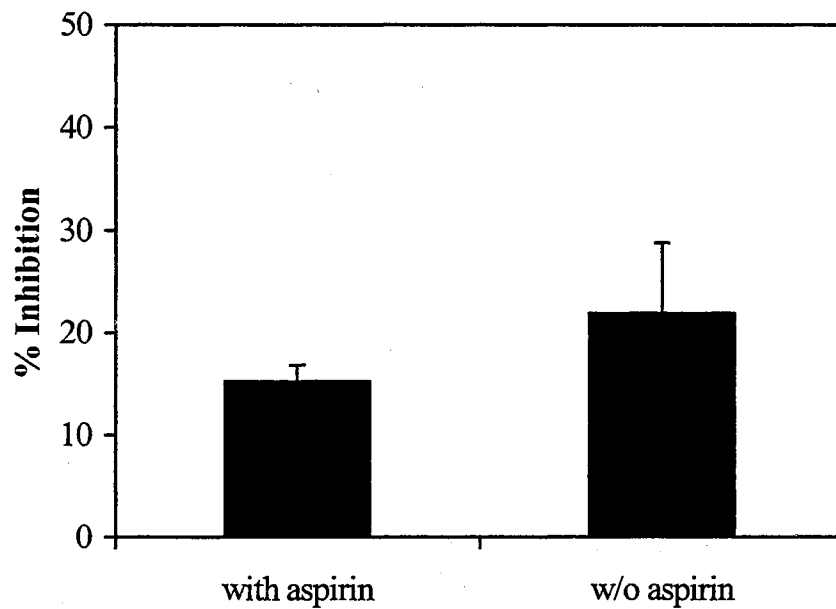


Figure 5.5. Effect of aspirin on platelet inhibition by potato apyrase. 1.2  $\mu\text{g}$  aspirin/ $10^9$  platelets was added. Apyrase dosage was 0.025 U/ml. Perfusion was maintained for 7.5 minutes at  $250 \text{ s}^{-1}$ . Columns and bars represent Mean  $\pm$  SD of  $n = 3$  repeats.

presence of aspirin, respectively. Platelets were exposed to the membrane for 7.5 minutes at  $250 \text{ s}^{-1}$ .

#### 5.4.2.3 Nitric oxide and apyrase.

*Dosage studies.* At  $250 \text{ s}^{-1}$  following NO exposure for 7.5 minutes, apyrase enhanced platelet inhibition due to NO as shown in Figure 5.6. In experiments with apyrase, platelet suspensions perfused through both control and non-control chambers contained apyrase. Therefore, the platelet inhibition shown is due to NO alone. At 0.02 ppm NO exposure, addition of 0.025 U/ml apyrase enhanced platelet inhibition from  $10 \pm 8\%$  (for NO alone) to  $28 \pm 6\%$ . Similarly, dosing the platelet suspension with 0.025 U/ml apyrase enhanced platelet inhibition upon exposure to 0.05 ppm NO from  $43 \pm 5\%$  to  $62 \pm 6\%$ . Experiments also indicated that for a given NO exposure (0.05 ppm), platelet inhibitory potency of NO was enhanced by apyrase in a dose-dependent manner. The effective inhibition by NO was  $89 \pm 9\%$  for addition of 0.05 U/ml of apyrase compared to an inhibition of  $62 \pm 6\%$  observed on addition of 0.025 U/ml apyrase.

*Shear rate studies.* Synergy in platelet inhibition between apyrase and NO was evaluated at wall shear rates of 250, 500, and  $750 \text{ s}^{-1}$  (see Fig. 5.7). In each case, 0.05 ppm of NO was exposed to platelets for 7.5 minutes except at  $750 \text{ s}^{-1}$ , where exposure was for 5 minutes. At shear rates of  $250 \text{ s}^{-1}$  and  $750 \text{ s}^{-1}$ , NO inhibited platelet deposition by  $43 \pm 5\%$  and  $39 \pm 12\%$ , respectively, when no apyrase was added. The similarity of the inhibitions confirmed earlier observations that the inhibitory potency of NO is independent of shear rate. Hence, inhibition due to NO in the absence of apyrase was not determined at  $500 \text{ s}^{-1}$ .

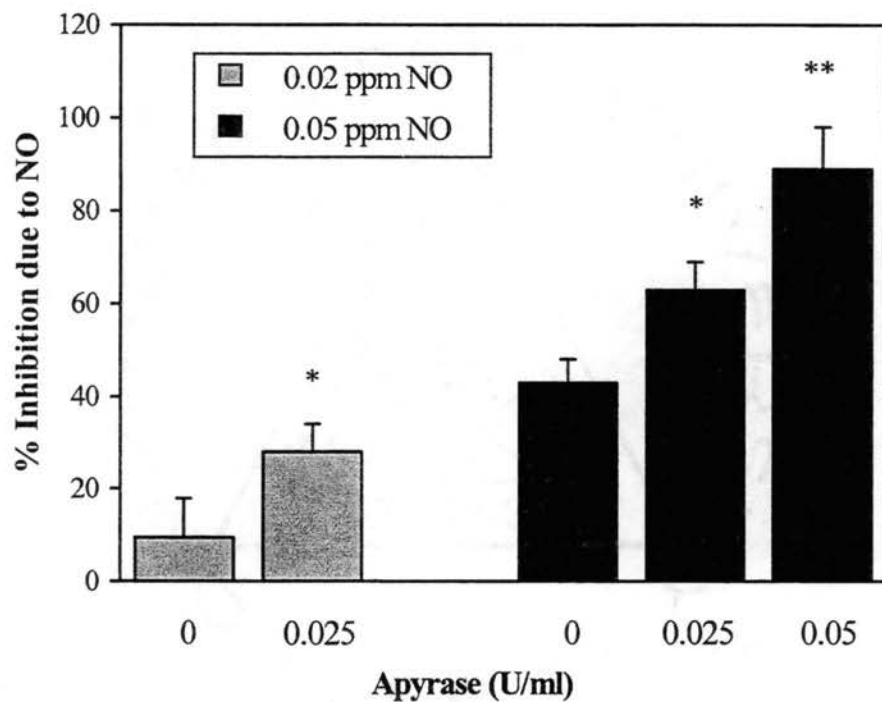


Figure 5.6. Synergy between NO and apyrase. Columns and bars represent Mean  $\pm$  SD of  $n = 3$  runs at  $250 \text{ s}^{-1}$  and 7.5 minutes exposure. ( $p < 0.05$  for \* and  $p < 0.005$  for \*\* vs. 0 U/ml apyrase).



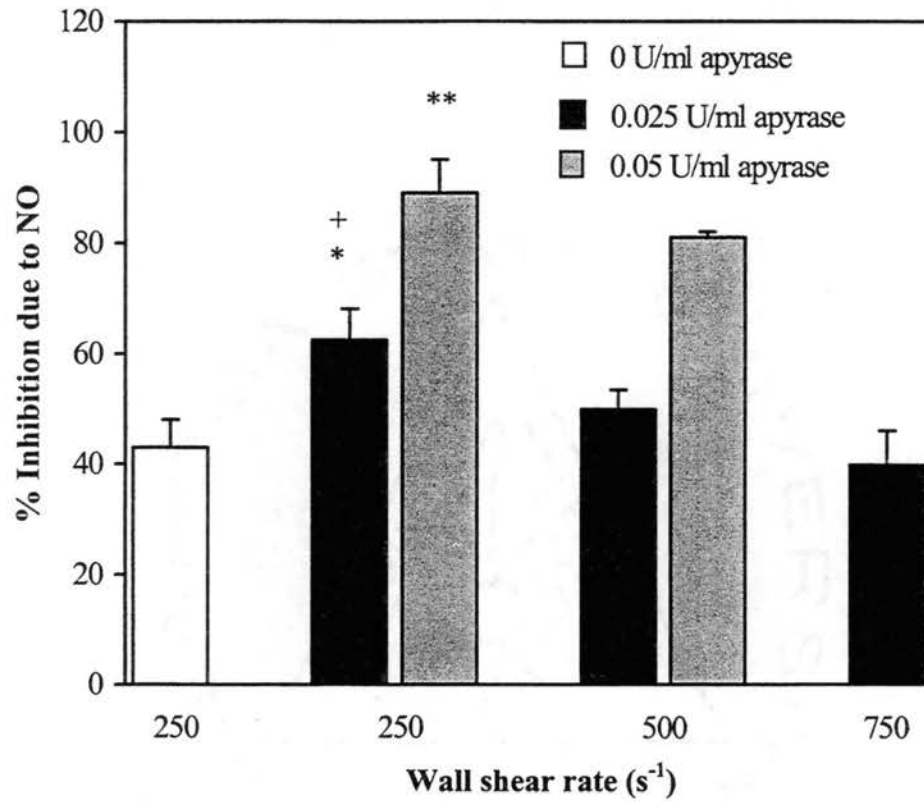


Figure 5.7. Synergy between apyrase and NO as a function of shear rate. Columns and bars represent Mean  $\pm$  SD of  $n = 3$  repeats. (\* $p < 0.01$  and \*\*  $p < 0.005$  vs. 0 U/ml apyrase at  $250 \text{ s}^{-1}$ ; +  $p < 0.05$  vs. 0.025 U/ml apyrase at  $500 \text{ s}^{-1}$ ). NO exposure is 0.05 ppm.

Apyrase synergistically enhanced NO inhibition of platelet deposition, but to a lesser extent as shear rate increased. Apyrase (0.025 U/ml) enhanced the inhibitory potency of 0.05 ppm of NO from a shear rate-independent value of  $43 \pm 5\%$  to  $62 \pm 6\%$  at  $250 \text{ s}^{-1}$ , and  $50 \pm 4\%$  at  $500 \text{ s}^{-1}$ . At  $750 \text{ s}^{-1}$ , inhibition decreased to  $40 \pm 6\%$  similar to NO in the absence of apyrase. Similarly, at an apyrase dosage of 0.05 U/ml, NO inhibited platelet deposition by  $89 \pm 6\%$  and  $81 \pm 1\%$ , respectively, at  $250 \text{ s}^{-1}$ , and  $500 \text{ s}^{-1}$ . However, the decrease in inhibition at  $500 \text{ s}^{-1}$  relative to  $250 \text{ s}^{-1}$ , was determined to be statistically insignificant.

Figure 5.7 also shows the effect of apyrase dosage on platelet inhibition due to NO at wall shear rates of  $250 \text{ s}^{-1}$  and  $500 \text{ s}^{-1}$ . Within each shear rate group, increased apyrase dosages induced higher levels of synergy, which confirmed earlier observations at  $250 \text{ s}^{-1}$  (see Figure 5.6). At  $250 \text{ s}^{-1}$ , inhibition due to NO upon addition of 0.05 U/ml apyrase was  $89 \pm 6\%$  compared to  $62 \pm 6\%$  inhibition obtained with 0.025 U/ml apyrase. The corresponding values at  $500 \text{ s}^{-1}$  were  $81 \pm 1\%$ , and  $50 \pm 3\%$ , respectively.

#### 5.4.2.4 Nitric oxide, apyrase and aspirin.

*Synergy studies.* Figure 5.8 shows the effect of aspirin addition on synergistic platelet inhibition by NO and apyrase. For NO alone, NO and aspirin, NO and apyrase, and NO with both aspirin and apyrase, inhibition due to NO was  $10 \pm 8\%$ ,  $10 \pm 8\%$ ,  $29 \pm 6\%$ , and  $8 \pm 6\%$ , respectively. The results clearly indicate that addition of apyrase enhances the inhibitory potency of NO significantly as previously shown ( $p < 0.05$  vs. NO alone). More interestingly, the exposure of platelets to aspirin in addition to apyrase and NO

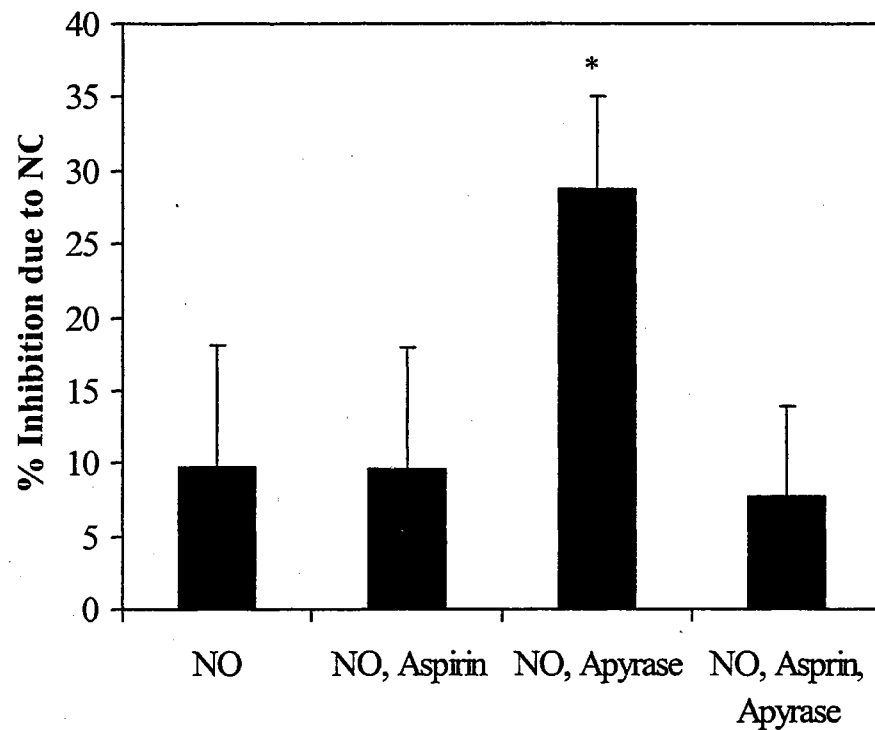


Figure 5.8. Effect of aspirin on synergy between NO and apyrase. NO exposure and apyrase dosage were 0.02 ppm and 0.025 U/ml respectively. Perfusion was maintained for 7.5 minutes at  $250 \text{ s}^{-1}$ . Columns and bars represent Mean  $\pm$  SD of % inhibition by NO ( $n = 3$ ). Addition of apyrase (without aspirin) enhanced inhibition by NO significantly (\*  $p < 0.05$  vs. NO alone).

negates this increase. Thus, inhibition by NO in the presence of apyrase and aspirin was similar to that in the presence of NO alone or NO with aspirin.

## 5.5 Discussion.

Results of platelet inhibition studies performed with NO and apyrases conclusively showed that apyrase enhanced inhibition of platelet deposition by NO in a dose-dependent manner. Therefore, apyrase synergistically inhibits platelet deposition in the presence of NO. Two possible scenarios are hypothesized below, which may at least partly justify the trend of results described in the previous sections.

*Hypothesis I.* NO may induce functional changes in the apyrase enzyme resulting in enhanced enzyme activity. This may result in decreased ADP availability. Thus, platelet deposition will be inhibited to greater levels than that caused only by action of NO on platelets. Addition of aspirin may not affect action sites of NO or adenosine on platelets. However, aspirin may possibly block the site of NO attachment/action on the apyrase enzyme, reducing the reactivity of the enzyme to normal (pre-NO addition) levels.

*Hypothesis II.* The presence of apyrase results in conversion of ADP (an agonist) to adenosine (an antagonist), resulting in reduced platelet adhesion. As shear rate increases, leading to a greater ADP production, the amount of ADP converted decreases resulting in reduced platelet inhibition.

NO by itself may affect the expression or the affinity of adhesion receptor sites on the platelet surface (different from the sites acted upon by adenosine), thereby inhibiting platelet deposition. However, when adenosine is formed in the presence of apyrase, the

simultaneous NO and adenosine actions on the platelet may result in greater inhibition of receptor site expression or binding affinity, leading to enhanced platelet inhibition. This may explain the synergistic increase in platelet inhibition due to NO in the presence of apyrase.

This study showed that addition of aspirin did not affect inhibition due to apyrase or NO alone, but significantly reduced synergy when both species were present. This suggests that aspirin does not affect the platelet when acted upon by either NO or adenosine. However, in the presence of both NO and apyrase, the addition of aspirin may interfere with the synergistic mechanisms described above, negating any synergy. Thus, platelet inhibition due to NO with apyrase will not be enhanced as earlier, but will remain at levels observed due to the action of NO alone.

## **5.6 Conclusions.**

This study experimentally demonstrated synergy between NO and apyrase in inhibiting platelet deposition to a collagen-coated biomaterial in an *in vitro* flow environment. Apyrase was shown to enhance the effectiveness of NO as an antagonist of platelet adhesion and recruitment in a dose-dependent manner. Further work is required to assess the effect of NO on the inhibitory potency of apyrase and also clarify the biochemical inhibitory mechanisms involved at the molecular level.

However, the study yields information useful for understanding interactions between NO and apyrases as anti-thrombogenic agents released by vascular endothelial cells *in vivo*. The results of the study may also be used to design novel biomaterials

incorporating apyrase and NO for enhancing hemocompatibility while reducing the NO release requirements for significant platelet inhibition determined in chapters 3 and 4.

## CHAPTER 6

### CONCLUSIONS

This study investigated the applicability of nitric oxide (NO) and ecto-nucleotidases as agents for inhibiting platelet-biomaterial interactions. The deleterious long-term effects of conventional anti-platelet aggregative agents such as heparin and aspirin motivated the investigation of the feasibility of use of these anti-thrombogenic agents. The NO exposures adopted in previous anti-platelet studies [Keh *et al.*, 1996, Konishi *et al.*, 1996] were above normal toxic limits (25 ppm) established by OSHA. Also, aqueous *in situ* NO concentrations and fluxes at the biomaterial surface were not quantified. Knowledge of minimal effective NO exposures and surface NO concentrations and fluxes is essential for the development of surfaces incorporating NO to minimize the potential toxicity and mutagenicity of NO. Thus, the overall objective of this study was to establish valid guidelines for the local delivery of NO to reduce platelet deposition on biomaterials.

#### 6.1 Summary of study.

In this study, a novel NO delivery/perfusion device was designed and developed to quantitatively study NO inhibition of platelet deposition on biomaterials. A salient feature of this device is that controlled delivery of gaseous NO is possible via a semi-permeable membrane that also serves as a test biomaterial for platelet deposition. A mathematical model was solved to predict aqueous NO concentration and flux profiles

within the flow slit. The model assumed negligible reaction of NO with O<sub>2</sub>, due to low concentrations of NO, and a short residence time within the flow slit. Model predictions were validated experimentally with excellent agreement.

Quantitative platelet studies were performed to determine the minimal NO exposures required for significant inhibition of platelet deposition on the biomaterial. The biomaterial surface was coated with an agonist protein to simulate the deposition of thrombogenic plasma protein on biomaterial surfaces in contact with whole blood.

## 6.2 Inferences.

The study essentially showed that gaseous NO exposures as low as 0.1 ppm could completely inhibit platelet deposition on the biomaterial. The surface NO concentration (0.09 nM) and fluxes (0.3-0.6 femtomoles cm<sup>-2</sup>s<sup>-1</sup>) at the NO delivery/platelet adhesion surface compared well with estimated free NO concentrations (3 nM) and fluxes (6 femtomoles cm<sup>-2</sup>s<sup>-1</sup>) from endothelial cells *in vivo*. The importance of this study lies in the establishment of guidelines for the development of novel biomaterial surfaces incorporating NO release. Platelet inhibition studies with NO alone showed that

- (a) The minimal effective NO concentrations or fluxes required for significant anti-thrombogenesis of biomaterial surfaces lie between 0.3 and 0.6 femtomoles cm<sup>2</sup> s<sup>-1</sup> delivered at the adhesion surface.
- (b) Surface NO concentrations of ~0.09 nM are effective in significantly inhibiting platelet deposition on biomaterials.



- (c) The determined NO delivery requirements are valid irrespective of the nature of platelet agonists inducing platelet deposition, shear rates and NO exposure/perfusion times.

The physiological relevance of the study supports the application of results to real applications. This information is likely to be useful for the development of NO releasing compounds applied to platelet-exposed surfaces. With the knowledge gained from this study, biomaterials incorporating NO or NO donors may be designed which incorporate controlled release of NO so as to obtain the minimal effective surface NO concentrations or fluxes determined in this study. Potential toxicity and/or mutagenicity associated with excessive or rapid NO exposure to cells may thus be avoided.

The synergy studies between apyrase and NO indicated that

- (a) Apyrase synergistically enhances platelet inhibition due to NO.
- (b) At a given shear rate, increased apyrase dosages induce higher levels of synergy.
- (c) Synergy between apyrase and NO decreases with increase in shear rate.
- (d) The addition of aspirin negates synergy between apyrase and NO.

This work demonstrates that almost complete inhibition of platelet deposition may be achieved even at sub-threshold NO exposures by simultaneous exposure of platelets to both apyrase (or related enzymes) and NO. Thus, lower NO exposures may be delivered to biomaterial surfaces and yet obtain significant platelet inhibition. Risk of toxicity due to NO may therefore be further reduced. This information may be used in the

development of novel bio-surfaces incorporating NO and apyrases, which have enhanced hemocompatibility.

### **6.3 Further Studies.**

In the current study, NO was delivered to washed platelet suspensions rather than plasma or whole blood. The surface NO concentrations and fluxes determined in this study are the values that would be effective in significantly inhibiting platelet deposition on biomaterials. However, in practical applications, platelet deposition from whole blood or plasma is more relevant. Blood and plasma contain numerous thiols and proteins, some of which bind NO or undergo complex reactions with NO. In addition, blood also contains heme as a component of the red blood cells, which has a high affinity for NO. Therefore, in the presence of heme, NO is rapidly consumed by reaction. The mathematical model used to predict NO profiles in the current study is only applicable to non-heme containing platelet suspensions. A logical extension of this work would be to model, predict, and validate NO concentration and flux profiles in a more physiologically relevant medium containing heme, which scavenges NO. The proposed study would determine the equivalent minimal surface NO concentrations and fluxes that would need to be delivered to obtain significant platelet inhibition in the presence of heme. This study will also shed light on the rapidity of the inhibitory action relative to transport of platelets and depletion of NO.

The establishment of suitable guidelines for delivery of NO at biomaterial surfaces in contact with plasma or whole blood would allow the design of suitable biomaterials incorporating NO. Suitable polymeric coatings on biomaterials or NO donors

incorporated in the biomaterials structure itself could be designed to release NO at desired rates to keep biomaterial surfaces platelet-free. Regeneration of surface NO with time is also an aspect that could be addressed which would have tremendous bearing on the long-term use of NO-releasing biomaterials.

The current study demonstrated that apyrase enhanced the inhibitory potency of NO. The future engineering of biomaterials incorporating simultaneous NO and apyrase release holds good promise as a means of enhancing hemocompatibility of biomaterials. In the current study the apyrase used was isolated from potatoes. Morphologically similar apyrases may be isolated from endothelial cells in highly purified forms. An excellent study would be to compare the synergistic capacities of plant and endothelium-derived apyrases. The viability of endothelial apyrases for *in vitro* or *ex-vivo* inhibition of thrombosis on biomaterial surfaces would provide reason for the inexpensive large-scale production of these enzymes using recombinant techniques. Biomaterial surfaces can then be engineered for attachment of these recombinant enzymes and their slow release under specified conditions. In another approach, cells releasing apyrases may themselves be attached to surfaces thereby keeping the biomaterials platelet-free via apyrase release (with or without concomitant NO delivery).

The overall objective of each of the above-proposed studies is to develop suitable means to prevent platelet adhesion and aggregation on biomaterial surfaces in a minimally invasive and safe manner.

## REFERENCES

- Adams, G.A. and Feuerstein, I.A., How much fibrinogen or fibronectin is enough for platelet adhesion?, *Trans. Am. Soc. Artif. Intern. Organs*, **27**, 219-224 (1981b).
- Adams, G.A. and Feuerstein, I.A., Platelet adhesion and release: interfacial concentration of released materials, *Am. J. Physiol.*, **240**(1), H99-108 (1981a).
- Adams, G.A. and Feuerstein, I.A., Visual fluorescent and radio-isotopic evaluation of platelet accumulation and embolization, *Trans. Am. Soc. Artif. Intern. Organs*, **26**, 17-23 (1980).
- Adams, G.A., Platelet aggregation, in *The Platelets: Physiology and Pharmacology* (Longenecker, G.L., Ed.), Academic Press, Orlando, FL, (1985a), pp 1-11.
- Adnot, S., Raffestin, B., and Eddahibi, S., NO in the lung, *Respir. Physiol.*, **101**(2), 109-120 (1995).
- Adnot, S., Raffestin, B., Eddahibi, S., Braquet, P., and Chabrier, P.E., Loss of endothelium-dependent relaxant activity in the pulmonary circulation of rats exposed to chronic hypoxia, *J. Clin. Invest.*, **87**(1), 155-162 (1991).
- Andersson, K.E. and Persson, K., Nitric oxide synthase and nitric oxide-mediated effects in lower urinary tract smooth muscles, *World J. Urol.*, **12**(5), 274-280 (1994).
- Andrade, J.D., and Hlady, V., Plasma protein adsorption, *Ann. N.Y. Acad. Sci.*, **516**, 158-172 (1987).
- Antiplatelet trialists collaboration. Collaborative overview of randomised trials of antiplatelet therapy- I: Prevention of death, myocardial infarction, and stroke by prolonged antiplatelet therapy in various categories of patients, *BMJ*, **308**, 81-106 (1994a).
- Antiplatelet trialists collaboration. Collaborative overview of randomised trials of antiplatelet therapy- II: Maintenance of vascular graft or arterial patency by antiplatelet therapy, *BMJ*, **308**, 159-168 (1994b).
- Bartlett, R.H., and Anderson, J.C., in *Biologic and synthetic vascular prostheses* (Stanley, J.C., Ed.), Grune and Stratton, New York, NY, (1982), pp 63.

- Bassenge, E., Clinical relevance of endothelium-derived relaxing factor (EDRF), *Br. J. Clin. Pharmacol.*, **34** (Suppl 1), 37S-42S (1992).
- Baumgartner, H.R. and Sakariassen, K.S., Factors controlling thrombus formation on arterial lesions, *Ann. N. Y. Acad. Sci.*, **454**, 162-177 (1985).
- Baumgartner, H.R., Haudenschild, C., Adhesion of platelets to subendothelium, *Ann. N.Y. Acad. Sci.*, **201**, 22-36 (1972).
- Baumgartner, H.R., Tschopp, T.B., and Weiss, H.J., Platelet interaction with collagen fibrils in flowing blood. II. Impaired adhesion-aggregation in bleeding disorders. A comparison with subendothelium, *Thromb. Haemost.*, **37**(1), 17-28 (1977).
- Baumgartner, H.R., Turitto, V., and Weiss, H.J., Effect of shear rate on platelet interaction with subendothelium in citrated and native blood. II. Relationships among platelet adhesion, thrombus dimensions, and fibrin formation, *J. Lab. Clin. Med.*, **95**(2), 208-221 (1980).
- Beckman, J.S., Beckman, T.W., Chen, J., Marshall, P.A., and Freeman, B.A., Apparent hydroxyl radical production by peroxynitrite: implications for endothelial injury from nitric oxide and superoxide, *Proc. Natl. Acad. Sci. USA*, **87**(4), 1620-1624 (1990).
- Bendtzen, K., Mandrup-Poulsen, T., Nerup, J., Nielsen, J.H., Dinarello, C.A., and Svenson, M., Cytotoxicity of human pI 7 interleukin-1 for pancreatic islets of Langerhans, *Science* **232**(4757), 1545-1547 (1986).
- Brash, J.L., in *Interaction of the blood with natural and artificial surfaces* (Salzman, E.W., Ed.), 2<sup>nd</sup> Edition, Dekker, New York, NY, (1981), pp 37.
- Bredt, D.S. and Snyder, S.H., Nitric oxide: a physiologic messenger molecule, *Annu. Rev. Biochem.*, **63**, 175-195 (1994).
- Busse, R., Fleming, I., and Hecker, M., Signal transduction in endothelium-dependent vasodilatation, *Eur. Heart J.*, **14**(Suppl I), 2-9 (1993).
- Butler, A.R. and Williams, D.L.H., The physiological role of nitric oxide, *Chem. Soc. Rev.*, 233-241, 1994.
- Calver, A., Collier, J., and Vallance, P., Nitric oxide and cardiovascular control., *Exper. Phys.*, **78**, 303-326 (1993).
- Cannon, R.O., III, Role of nitric oxide in cardiovascular disease: focus on the endothelium, *Clin. Chem.*, **44**(8), 1809-1819 (1998).

- Carville, C., Raffestin, B., Eddahibi, S., Blouquit, Y., and Adnot, S., Loss of endothelium-dependent relaxation in proximal pulmonary arteries from rats exposed to chronic hypoxia: effects of in vivo and in vitro supplementation with L-arginine, *J. Cardiovasc. Pharmacol.*, **22**(6), 889-896 (1993).
- Cazenave, J.P., Packham, M.A., and J.F. Mustard, Adherence of platelets to a collagen-coated surface: development of a qualitative method. *J. Lab. Clin. Med.*, **82** (6), 978-990 (1973).
- Coade, S.B. and Pearson, J.D., Metabolism of adenine nucleotides in human blood, *Circ. Res.*, **65**(3), 531-537 (1989).
- Coleman, D.L., Gregonis, D.E., and Andrade, J.D., Blood-materials interactions: the minimum interfacial free energy and the optimum polar/apolar ratio hypotheses, *J. Biomed. Mater. Res.*, **16**(4), 381-398 (1982).
- Comens, P.G., Wolf, B.A., Unanue, E.R., Lacy, P.E., and McDaniel, M.L., Interleukin 1 is potent modulator of insulin secretion from isolated rat islets of Langerhans, *Diabetes*, **36**(8), 963-970 (1987).
- Corbett, J.A., Lancaster, J.R., Jr., Sweetland, M.A., and McDaniel, M.L., Interleukin-1 beta-induced formation of EPR-detectable iron-nitrosyl complexes in islets of Langerhans. Role of nitric oxide in interleukin-1 beta-induced inhibition of insulin secretion, *J. Biol. Chem.*, **266**(32), 21351-21354 (1991).
- Corbett, J.A., Sweetland, M.A., Wang, J.L., Lancaster, J.R., Jr., and McDaniel, M.L., Nitric oxide mediates cytokine-induced inhibition of insulin secretion by human islets of Langerhans, *Proc. Natl. Acad. Sci. USA*, **90**(5), 1731-1735 (1993).
- Cox, R.D., Determination of nitrate and nitrite at the parts per billion level by chemiluminescence. *Anal. Chem.*, **52**, 332-335 (1980).
- de Graaf, J.C., Banga, J.D., Moncada, S., Palmer, R.M.J., de Groot, P.G., and Sixma, J.J., Nitric oxide functions as an inhibitor of platelet adhesion under flow conditions., *Circulation*, **85**(6), 2284-90 (1992).
- Deboer, J.H., Dynamical character of adsorption, 2<sup>nd</sup> Edition, Clarendon press, Oxford, U.K. (1968).
- Didisheim, P., Tirrell, M.V., Lyons, C.S., Stropp, J.Q., and Dewanjee, M.K., Relative role of surface chemistry and surface texture in blood-material interactions, *Trans. Am. Soc. Artif. Intern. Organs*, **29**, 169-76 (1983).

- Evans, C.H., Stefanovic-Racic, M., and Lancaster, J., Nitric oxide and its role in orthopaedic disease, *Clin. Orthop.*, **312**, 275-294 (1995).
- Feuerstein, I.A., and Kush, J., Measurements of platelet collision efficiency upon virgin and platelet-primed (foot-printed) fibrinogen with fluorescent video-microscopy, *Trans. Am. Soc. Artif. Intern. Organs*, **29**, 430-435 (1983).
- Finder, J., Stark, W.W. Jr., Nakayama, D.K., Geller, D., Wasserloos, K., Pitt, and B.R., Davies, P., TGF-beta regulates production of NO in pulmonary artery smooth muscle cells by inhibiting expression of NOS, *Am. J. Physiol.*, **268**(5 Pt 1), L862-867 (1995).
- Fostermann, U., Pollock, J.S., Schmidt, H.H.H.W., Heller, M., and Murad, F., Calmodulin-dependent endothelium-derived relaxing factor/nitric oxide synthase activity is present in the particulate and cytosolic fractions of bovine aortic endothelial cells, *Proc. Natl. Acad. Sci. USA*, **88**, 1788-1792 (1991).
- Fry, G.L., and Hoak, J.C., Measurement of platelet interaction with endothelial monolayers., *Methods Enzymol.*, **169**, 71-76 (1989).
- Gaboury, J., R.C. Woodman, D.N. Granger, P. Reinhardt, and P. Kubes., Nitric oxide prevents leukocyte adherence: role of superoxide, *Am. J. Physiol.*, **265**, H862 - H867 (1993).
- Garthwaite, J., Glutamate, nitric oxide and cell-cell signaling in the nervous system, *Trends Neurosci.*, **14**(2), 60-67 (1991).
- Garthwaite, J., and Boulton C.L., Nitric oxide signaling in the central nervous system, *Annu. Rev. Physiol.*, **57**, 683-706 (1995).
- Gayle, R.B. 3rd, Maliszewski, C.R., Gimpel, S.D., Schoenborn, M.A., Caspary, R.G., Richards, C., Brasel, K., Price, V., Drosopoulos, J.H., Islam, N., Alyonycheva, T.N., Broekman, M.J., and Marcus, A.J., Inhibition of platelet function by recombinant soluble ecto-ADPase/CD39, *J. Clin. Invest.*, **101**(9), 1851-1859 (1998).
- Gibbons, G., and Dzau, V., The emerging concept of vascular remodeling, *N. Engl. J. Med.*, **330**, 1431-1438 (1994).
- Gordon, E.L., Pearson, J.D., Dickinson, E.S., Moreau, D., and Slakey, L.L., The hydrolysis of extracellular adenine nucleotides by arterial smooth muscle cells. Regulation of adenosine production at the cell surface, *J. Biol. Chem.*, **264**(32), 18986-18995 (1989).

- Gries, A., Bode, C., Peter, K., Herr, A., Bohrer, H., Motsch, J., and Martin, E., Inhaled nitric oxide inhibits human platelet aggregation, P-selectin expression, and fibrinogen binding *in vitro* and *in vivo*, *Circulation*, **97**(15), 1481-1487 (1998).
- Hackman, A., Abe, Y., Insull, W., Pownall, H., Smith, L., and Dunn, K., Levels of soluble cell adhesion molecules in patients with dyslipidemia, *Circulation*, **93**, 1334-1338 (1996).
- Hall, A.V., Antoniou, H., Wang, Y., Cheung, A.H., Arbus, A.M., Olson, S.L., Lu, W.C., Kau, C.L., and Marsden, P.A., Structural organization of the neuronal nitric oxide synthase gene (NOS1), *J. Biol. Chem.*, **269**, 33082-33090 (1994).
- Herman, B., *Fluorescence microscopy*, 2<sup>nd</sup> Edition, BIOS Scientific Publishers Limited, Guildford, U.K., (1998), pp 1-37.
- Herzlinger, G.A., Bing, D.H., Stein, R., and Cumming, R.D., Quantitative measurement of C3 activation at polymer surfaces, *Blood*, **57**(4), 764-770 (1981).
- Hoffman, A.S., Blood-biomaterial interactions: An overview, in *Biomaterials: Interfacial Phenomena and Applications* (Cooper, S.L., and Peppas, N.A., Ed.) Washington, D.C, 3-8 (1980).
- Hogg, N., Darley-Usmar, V.M., Wilson, M.T., and Moncada, S., Production of hydroxyl radicals from the simultaneous generation of superoxide and nitric oxide, *Biochem. J.*, **281**(2), 419-424 (1992).
- Hudson, E.M., Ramsey, R.B., and Evatt, B.L., Subcellular localization of indium-111 in indium-111-labeled platelets, *J. Lab. Clin. Med.*, **97**, 577-582 (1981).
- Ignarro, L.J., Nitric oxide-mediated vasorelaxation, *Thromb. Haemost.*, **70**(1):148-151 (1993).
- Ischiropoulos, H., Zhu, L., Chen, J., Tsai, M., Martin, J.C., Smith, C.D., and Beckman, J.S., Peroxynitrite-mediated tyrosine nitration catalyzed by superoxide dismutase, *Arch. Biochem. Biophys.*, **298**(2), 431-437 (1992).
- Joist, J.H., Baker, R.K., Welch, M.J., Methodologic and basic aspects of indium-111 platelets, *Semin. Thromb. Hemost.*, **9**(2), 86-99 (1983).
- Kavdia, M., Nagarajan, S., and Lewis, R.S., Novel devices for the predictable delivery of nitric oxide to aqueous solutions, *Chem. Res. Toxicol.*, **11**(11), 1346-1351 (1998).
- Keefer, L.K., and Wink, D.A., DNA damage and nitric oxide, *Adv. Exp. Med. Biol.*, **387**, 177-185 (1996).



- Keh, D., Gerlach, M., Kurer, I., Falke, K.J., and Gerlach, H., Reduction of platelet trapping in membrane oxygenators by transmembrane application of gaseous nitric oxide., *Int. J Artif. Organs*, **19**(5), 291-293 (1996).
- Kelly, R.A. and Smith T.W., Nitric oxide and nitrovasodilators: similarities, differences, and interactions, *Am. J. Cardiol.*, **77**(13), 2C-7C (1996).
- Kerwin, J.F. Jr., Lancaster, J.R. Jr., and Feldman, P.L., Nitric oxide: A new paradigm for second messengers., *J. Med. Chem.*, **38**, 4333-4362 (1995).
- Kinlough-Rathbone, R.L., Packham, M.A., and Mustard, J.F., in *Methods in hematology: Measurements of platelet function* (Harker, L.A., and Zimmerman, T.S., Ed.), Churchill-Livingstone, Edinburgh, Scotland, 1983, pp 64.
- Konishi, R., Shimizu, R., Firestone, L., Walters, F.R., Wagner, W.R., Federspiel, W.J., Konishi, H., and Hattler, B.G., Nitric oxide prevents human platelet adhesion to fiber membranes in whole blood., *ASAIO J.*, **42**(5), M850-853 (1996).
- Koppenol, W.H., The basic chemistry of nitrogen monoxide and peroxy nitrite, *Free Radic. Biol. Med.*, **25**(4-5), 385-391 (1998).
- Koyamada, N., Miyatake, T., Candinas, D., Hechenleitner, P., Siegel, J., Hancock, W.W., Bach, F.H., and Robson, S.C., Apyrase administration prolongs discordant xenograft survival., *Transplantation*, **62**(12), 1739-1743 (1996).
- Ku, D.N., and Allen, R.C., Vascular graft, in *The Biomedical Engineering Handbook* (Bronzino, J.D., Ed.), CRC, Boca Raton, FL, (1995), pp 1871-1978.
- Lange, N.A, Ed., *Lange's Handbook of Chemistry*, rev. 10<sup>th</sup> ed., McGraw-Hill, New York, NY, (1967), pp 1101.
- Larm, O., Larsson, R., and Olsson, P., A new non-thrombogenic surface prepared by selective covalent binding of heparin via a reducing terminal residue., *Biomater. Med. Devices. Artif. Organs.*, **11**, 161-174 (1983).
- Larsson, R., Larm, O., and Olsson, P., The search for thromboresistance using immobilized heparin., *Ann. NY. Acad. Sci.*, **516**, 102-108 (1987).
- Laskin, D.L., Heck, D.E., Gardner, C.R., Feder, L.S., and Laskin, J.D., Distinct patterns of nitric oxide production in hepatic macrophages and endothelial cells following acute exposure of rats to endotoxin, *J. Leukoc. Biol.*, **56**(6), 751-758 (1994).
- Lewis, R.S., and Deen, W.M., Kinetics of the reaction of nitric oxide with oxygen in aqueous solutions., *Chem. Res. Toxicol.* **7**, 568-574 (1994).

Lindon, J.N., Kushner, L., and Salzman, E.W., Platelet interaction with artificial surfaces: *In vitro* evaluation, *Meth. Enzymol.*, **169**, 104-117 (1989).

Luscher, T.F., Biology of the endothelium., *Clin. Cardiol.*, **11** (Suppl 2):II, 3-10 (1997).

Luthje, J., Schomburg, A., and Ogilvie, A., Demonstration of a novel ecto-enzyme on human erythrocytes, capable of degrading ADP and of inhibiting ADP-induced platelet aggregation, *Eur. J. Biochem.*, **175**(2), 285-289 (1988).

Lyman, D.J., Metcalf, L.C., Albo, D. Jr., Richards, K.F., and Lalmb, J., The effect of chemical structure and surface properties of synthetic polymers on the coagulation of blood. III. In vivo adsorption of proteins on polymer surfaces. *Trans. Am. Soc. Artif. Int. Organs.*, **20**, 474-478 (1974).

Lyons, D., Impairment and restoration of nitric oxide-dependent vasodilation in cardiovascular disease, *Int. J. Cardiol.*, **62**(Suppl. 2), S101-109 (1997).

Makita, K., Shimoyama, T., Sakurai, Y., Yagi, H., Matsumoto, M., Narita, N., Sakamoto, Y., Saito, S., Ikeda, Y., Suzuki, M., Titani, K., and Fujimura, Y., Placental ecto-ATP diphosphohydrolase: its structural feature distinct from CD39, localization and inhibition on shear-induced platelet aggregation., *Int. J. Hematol.*, **68**, 297-310 (1998).

Marcus, A.J., and Safier, L.B., Thromboregulation: Multicellular modulation of platelet reactivity in hemostasis and thrombosis, *FASEB J.*, **7**, 516-522 (1993).

Marcus, A.J., Eicosanoid interactions between platelets, endothelial cells, and neutrophils, *Meth. Enzymol.*, **187**, 585-598 (1990).

Marcus, A.J., Safier, L.B., Broekman, M.J., Islam, N., Fliessbach, J.H., Hajjar, K.A., Kaminski, W.E., Jendraschak, E., Silverstein, R.L., and von Schacky, C., Thrombosis and inflammation as multicellular processes: significance of cell-cell interactions., *Thromb. Haemost.*, **74**(1), 213-217 (1995).

Marcus, A.J., Safier, L.B., Hajjar, K.A., Ullman, H.L., Islam, N., Broekman, M.J., and Eiroa, A.M., Inhibition of platelet function by an aspirin-insensitive endothelial ADPase. Thromboregulation by endothelial cells, *J. Clin. Invest.*, **88**, 1690-1696 (1991).

McCollum, C.N., Crow, M.J., Rajah, S.M., Kester, R.C., Antithrombotic therapy for vascular prosthesis: an experimental model testing platelet inhibitory drugs, *Surgery*, **87**(6), 668-676 (1980).

McNicol, A., Platelet preparation and estimation of functional responses, in *Platelets: A practical approach* (Watson, S.P., and Authi, K.S., Ed.), Oxford University Press, New York, NY, (1996), pp 1-25.

Mehta, J.L., Lawson, D.L., Nicolini, F.A., Cain, D.A., Mehta, P., and Schreier, H., Evidence for generation of a large amount of nitric oxide-like vascular smooth muscle

relaxant by cholesterol-rich neutrophils, *Biochem. Biophys. Res. Commun.*, **173**, 438-442 (1990).

Mellgren, K., Skogby, M., Jarnas, A., Friberg, L.G., Wadenvik, H., and Mellgren, G., Platelet activation and degradation in an experimental extracorporeal system. A comparison between a silicone membrane and a hollow-fibre oxygenator, *Perfusion*, **11**(5), 383-388 (1996).

Minor, R.L.J., Myers, P.R., Guerra, R.J., Bates, J.N., and Harrison, D.G., Diet-induced atherosclerosis increases the release of nitrogen oxides from rabbit aorta, *J.Clin. Invest.*, **86**, 2109-2116 (1990).

Mohammad, S.F., Hardison, M.D., Chuang, H.Y., and Mason, R.G., Adhesion of human blood platelets to glass polymer surfaces. II. Demonstration of the presence of a natural platelet adhesion inhibitor in plasma and serum, *Haemostasis*, **5**(2), 96-114 (1976).

Molnar, J. and Lorand, L., *Arch.Biochem. Biophys.*, **93**, 353 (1961).

Moncada, S. and Higgs, A., The L-arginine-nitric oxide pathway, *N. Engl. J. Med.*, **329**(27), 2002-2012 (1993).

Moncada, S., Nitric oxide, *J. Hypertens. Suppl.*, **12**(10), S35-39 (1994).

Moncada, S., Palmer, R.M.J., and Higgs, E.A. Nitric oxide: Physiology, pathophysiology and pharmacology, *Pharmacol. Rev.*, **43**, 109-142 (1991).

Mueller, A.R., Platz, K.P., Langrehr, J.M., Hoffman, R.A., Nussler, A.K., Nalesnik, M., Billiar, T.R., and Schraut, W.H., The effects of administration of nitric oxide inhibitors during small bowel preservation and reperfusion, *Transplantation*, **58**(12), 1309-1316 (1994).

Muggli, R. and Baumgartner, H.R., Platelet interactions with collagenous substrates in the presence of flowing blood, *Suppl. Thromb. Haemost.*, **63**, 289-300 (1978).

Mustard, J.F., Kinlough-Rathbone, R.L., and Packham, M.A., Isolation of human platelets from plasma by centrifugation and washing, *Meth. Enzymol.*, **169**, 3-11 (1989).

Nakai, K., Itoh, C., Kawazoe, K., Miura, Y., Sotoyanagi, H., and Hotfa, K., Concentration of soluble vascular cell adhesion molecule-1 (VCAM-1) correlated with expression of VCAM-1 mRNA in the human atherosclerotic aorta. *Coronary Art. Dis.*, **6**, 497-502 (1995).

Nakashima, S., Tohmatsu, T., Hattori, H., Okano, Y., and Nozawa, Y., Inhibitory action of cyclic GMP on secretion, polyphosphoinositide hydrolysis and calcium mobilization in

thrombin-stimulated human platelets, *Biochem. Biophys. Res. Commun.*, **135**(3), 1099-1104 (1986).

Neumann, A.W., Hum, O.S., Francis, D.W., Zingg, W., and van Oss, C.J., Kinetic and thermodynamic aspects of platelet adhesion from suspension to various substrates, *J Biomed. Mater. Res.*, **14**(4), 499-509 (1980).

Nguyen, T., Brunson, D., Crespi, C.L., Penman, B.W., Wishnok, J.S., and Tannenbaum, S.R., DNA damage and mutation in human cells exposed to nitric oxide *in vitro*, *Proc. Natl. Acad. Sci. USA*, **89**(7), 3030-3034 (1992).

Nose, Y., Ohashi, Y., Tasai, K., and DeBakey, M.E., Biomaterial considerations for cardiac prosthesis, in *Human Biomaterial Applications*. (Wise *et al.*, Ed.), Humana Press, Totowa, NJ, 205-214 (1996).

Ohashi, Y., Kawashima, S., Hirata, K., and Yokoyama, M., Nitric oxide inhibits neutrophil adhesion to cytokine-activated cardiac myocytes., *Am. J. Physiol.*, **41**(6), H2807-H2814 (1991).

O'Sullivan, A.J. and Burgoyne, R.D., Cyclic GMP regulates nicotine-induced secretion from cultured bovine adrenal chromaffin cells: effects of 8-bromo-cyclic GMP, atrial natriuretic peptide, and nitroprusside (nitric oxide), *J. Neurochem.*, **54**(5), 1805-1808 (1990).

Pabla, R., Buda, A.J., Flynn, D.M., Blesse, S.A., Shin, A.M., Curtis, M.J., and Lefer, D.J., Nitric oxide attenuates neutrophil-mediated myocardial contractile dysfunction after ischemia and reperfusion, *Circ. Res.*, **78**(1), 65-72 (1996).

Page, R.L. and Mitchell, J.R., Platelet adhesiveness to glass, *Thromb. Haemost.*, **42**(2) 705-725 (1979).

Palacios, M., Knowles, R.G., Palmer, R.M., and Moncada, S., Nitric oxide from L-arginine stimulates the soluble guanylate cyclase in adrenal glands, *Biochem. Biophys. Res. Commun.*, **165**(2), 802-809 (1989).

Patrono, C., Aspirin and human platelets: from clinical trials to acetylation of cyclooxygenase and back, *Trends Pharmacol. Sci.*, **10**(11), 453-458 (1989).

Polanowska-Grabowska, R., and Gear, A.R., Role of cyclic nucleotides in rapid platelet adhesion to collagen., *Blood*, **83**(9), 2508-2515 (1994).

- Pryor, W.A. and Squadrito, G.L., The chemistry of peroxynitrite: a product from the reaction of nitric oxide with superoxide, *Am. J. Physiol.*, **268**(5 Pt 1), L699-722 (1995).
- Radi, R., Reactions of nitric oxide with metalloproteins., *Chem. Res. Toxicol.*, **9**(5), 828-835 (1996).
- Radomski, M.W., Palmer, R.M., and Moncada, S., The role of nitric oxide and cGMP in platelet adhesion to vascular endothelium., *Biochem. Biophys. Res. Commun.*, **148**(3), 1482-1489 (1987).
- Radomski, M.W., Zakar, T., and Salas, E., Nitric oxide in Platelets, in *Methods Enzymol.*, **269**, 88-107 (1996).
- Ramamurthi, A., and Lewis, R.S. Design of a novel apparatus to study nitric oxide (NO) inhibition of platelet adhesion. (Erratum) *Ann. Biomed. Engg.* **27**(3), 1036-1043 (1999)(In print).
- Ramamurthi, A., and Lewis, R.S., Design of a novel apparatus to study nitric oxide (NO) inhibition of platelet adhesion, *Ann. Biomed. Engg.*, **26**(6), 1036-1043 (1998).
- Rand, J.H., Sussman, I.I., Gordon, R.E., Chu S.V., and Solomon, V., Localization of factor-VIII-related antigen in human vascular subendothelium, *Blood*, **55**(5), 752-756 (1980).
- Rand, M.J., Nitrergic transmission: nitric oxide as a mediator of non-adrenergic, non-cholinergic neuro-effector transmission, *Clin. Exp. Pharmacol. Physiol.*, **19**(3), 147-169 (1992).
- Raulli, R., Inhibition of human platelet aggregation by diazeniumdiolates: extent of inhibition correlates with nitric oxide load delivered, *J. Pharm. Pharmacol.*, **50**(1), 75-82 (1998).
- Reimers, H.J., Adenine nucleotides in blood platelets, in *The platelets: physiology and pharmacology* (Longnecker, G.L., Ed.), Academic Press, Orlando, FL, (1985), pp 85-106.
- Robson, S.C., Kaczmarek, E., Siegel, J.B., Candinas, D., Koziak, K., Millan, M., Hancock, W.W., and Bach, F.H. Loss of ATP diphosphohydrolase activity with endothelial cell activation, *J. Exp. Med.*, **185** (1), 153-163 (1997).
- Rosenberg, J.C., and Sell, T.L., In vitro evaluation of inhibitors of platelet release and aggregation., *Arch. Surg.*, **110**(8), 980-983 (1975).

- Rubanyi, G.M., Endothelium-derived relaxing and contracting factors, *J. Cell. Biochem.* **46**(1), 27-36 (1991).
- Ruggeri, Z.M., Mechanisms of shear induced platelet adhesion and aggregation, *Thromb. Haemost.*, **70**, 119-123 (1993).
- Sakariassen, K.S., Aarts, P.A., de Groot, P.G., Houdijk, W.P., and Sixma, J.J., A perfusion chamber developed to investigate platelet interaction in flowing blood with human vessel wall cells, their extracellular matrix, and purified components, *J. Lab. Clin. Med.*, **102**(4), 522-535 (1983).
- Sakariassen, K.S., Muggli, R., and Baumgartner, H.R., Measurements of platelet interaction with components of the vessel wall in flowing blood, *Meth. Enzymol.*, **169** (A), 37-70 (1989).
- Salas, E., Moro, M.A., Askew, S., Hodson, H.F., Butler, A.R., Radomski, M.W., and Moncada, S., Comparative pharmacology of analogues of S-nitroso-N-acetyl-DL-penicillamine on human platelets, *Br. J. Pharmacol.*, **112**(4), 1071-1076 (1994).
- Salzman, E.W., Harris, W.H., and DeSanctis, R.W., Reduction in venous thromboembolism by agents affecting platelet function., *New Engl. J. Med.*, **284**, 1287-1292 (1971).
- Salzman, E.W., *J. Lab. Clin. Med.*, **62**, 724 (1963).
- Salzman, E.W., Lindon, J., McManama, G., and Ware, J.A., Role of fibrinogen in activation of platelets by artificial surfaces, *Ann. N.Y. Acad. Sci.*, **516**, 184-195 (1987).
- Salzman, E.W., Merrill, E.W., Interaction of blood with artificial surfaces, in *Haemostasis and Thrombosis*, 2<sup>nd</sup> Edition (Colman, R.W., Hirsh, J., Marder, V.J., and Salzman E.W., Ed.), J.B. Lippincott, Philadelphia, PA., (1987), pp 1335-1347.
- Samama, C.M., Diaby, M., Fellahi, J.L., Mdhafar, A., Eyraud, D., Arock, M., Guillosson, J.J., Coriat, P., and Rouby, J.J., Inhibition of platelet aggregation by inhaled nitric oxide in patients with acute respiratory distress syndrome, *Anesthesiology*, **83**(1), 56-65 (1995).
- Scheffel, U., McIntyre, P.A., Evatt, B., Dvornicky, J.A., Natarajan, T.K., Bolling, D.R., and Murphy, E.A., Evaluation of indium-111 as a new high photon yield gamma-emitting "physiological" platelet label, *Johns Hopkins Med. J.*, **140**, 285-293 (1977).
- Serhan, C.N., Lipoxins: eicosanoids carrying intra- and intercellular messages, *J. Bioenerg. Biomembr.*, **23**(1), 105-122 (1991).

- Sixma, J.J., Nievelstein, P.F., Zwaginga, J.J., and de Groot, P.G., Adhesion of blood platelets to the extracellular matrix of cultured human endothelial cells, *Ann. N.Y. Acad. Sci.*, **516**, 39-51 (1987).
- Smith, D.J., Chakravarthy, D., Pulfer, S., Simmons, M.L., Hrabie, J.A., Citro, M.L., Saavedra, J.E., Davies, K.M., Hutsell, T.C., Mooradian, D.L., Hanson, S.R., and Keefer, L.K., Nitric oxide-releasing polymers containing the [N(O)NO]- group, *J Med. Chem.*, **39**(5), 1148-1156 (1996).
- Stamler J.S., Jia L., Eu J.P., McMahon T.J., Demchenko I.T., Bonaventura J., Gernert K., Piantadosi C.A. Blood flow regulation by S-nitrosohemoglobin in the physiological oxygen gradient, *Science*, **276**(5321), 2034-2037 (1997).
- Steiner, M., and Baldini, M., Subcellular distribution of <sup>51</sup>Cr and characterization of its binding sites in human platelets, *Blood*, **25**(5), 727-739 (1970).
- Tamir, S., deRojas-Walker, T., Wishnok, J.S., and Tannenbaum, S.R., DNA damage and genotoxicity by nitric oxide, *Methods Enzymol.*, **269**, 230-243 (1996).
- Thakur, M.L., Radioisotopic labeling of platelets: a historical perspective, *Semin Thromb. Hemost.*, **9**(2), 79-85 (1983).
- Toda, N., Mediation by nitric oxide of neurally-induced human cerebral artery relaxation, *Experientia*, **49**(1), 51-53 (1993).
- Tottrup, A., Svane, D., and Forman, A., Nitric oxide mediating NANC inhibition in opossum lower esophageal sphincter, *Am. J. Physiol.*, **260**(3 Pt 1), G385-389 (1991).
- Tschopp, T.B., Aspirin inhibits platelet aggregation on, but not adhesion to, collagen fibrils: An assessment of platelet adhesion and deposited platelet mass by morphometry and <sup>51</sup>Cr-labeling, *Thromb. Res.*, **11**, 619-632 (1977).
- Tschopp, T.B., Weiss, H.J., and Baumgartner, H.R., Decreased adhesion of platelets to subendothelium in von Willebrand's disease, *J. Lab. Clin. Med.*, **83**(2), 296-300 (1974).
- Turitto, V.T. and Baumgartner, H.R., Platelet interaction with subendothelium in a perfusion system: physical role of red blood cells, *Microvasc. Res.*, **9**(3), 335-344 (1975).
- Turitto, V.T. and Baumgartner, H.R., Platelet interaction with subendothelium in flowing rabbit blood: effect of blood shear rate, *Microvasc. Res.*, **17**(1), 38-54 (1979).
- Turitto, V.T., Weiss, H.J., and Baumgartner, H.R., *Haemostasis and Thrombosis Research: Basic Principles and Clinical Practice* (Colman, R.W., Hirsh J., Marder, V.J., and Salzman, E.W., Ed.), Lippincott, Philadelphia, PA, (1982), pp 364.

- Turitto, V.T., Weiss, H.J., and Baumgartner, H.R., The effect of shear rate on platelet interaction with subendothelium exposed to citrated human blood, *Microvasc. Res.*, **19**(3), 352-365 (1980).
- Turitto, V.T., Weiss, H.J., Baumgartner, H.R., Badimon, L., and Fuster, V., Cells and aggregates at surfaces, *Ann. N.Y. Acad. Sci.*, **516**, 453-467 (1987).
- Turitto, V.T., Weiss, H.J., Zimmerman, T.S., and Sussman, I.I., Factor VIII/von Willebrand factor in subendothelium mediates platelet adhesion, *Blood*, **65**(4), 823-831 (1985).
- Vallance, P. and Collier, J., Biology and clinical relevance of nitric oxide, *BMJ*, **309**(6952), 453-457 (1994).
- Vallance, P. and Moncada, S., Hyperdynamic circulation in cirrhosis: a role for nitric oxide?, *Lancet*, **337**(8744), 776-778 (1991).
- Valles, J., Aznar, J., Santos, T., Marcus, A.J., Safier, L.B., and Broekman, M.J., Effects of different doses of aspirin on 'ex-vivo' platelet recruitment. Modulatory role of erythrocytes, *Thromb. Haemost.*, **69**(4), 212-218 (1993).
- Weiss, H.J., Tschopp, T.B., Baumgartner, H.R., Sussman, I.I., Johnson, M.M., and Egan, J.J., Decreased adhesion of giant (Bernard-Soulier) platelets to subendothelium. Further implications on the role of the von Willebrand factor in hemostasis, *Am. J. Med.*, **57**(6), 920-925 (1974).
- Wink, D.A., and Mitchell, J.B., Chemical biology of nitric oxide: Insights into regulatory, cytotoxic, and cytoprotective mechanisms of nitric oxide, *Free Rad. Bio. Med.*, **25**(4-5): 434-456 (1998).
- Wise, D.L. and Houghton, G., Diffusion coefficients of neon, krypton, xenon, carbon monoxide, and nitric oxide in water at 10-60 °C, *Chem. Eng. Sci.*, **23**, 1211-1216 (1968).
- Wood, J., and Garthwaite, Models for the diffusional spread of nitric oxide: Implications for neural nitric oxide signalling and its pharmacological properties, *Neuropharmacol.*, **33**(11), 1235-1244 (1994).
- Wright, C.E., Rees, D.D., and Moncada, S., Protective and pathological roles of nitric oxide in endotoxin shock, *Cardiovasc. Res.*, **26**(1), 48-57 (1992).



OKLAHOMA STATE UNIVERSITY  
INSTITUTIONAL REVIEW BOARD  
HUMAN SUBJECTS REVIEW

Date: 04-21-97

IRB#: EG-97-003

Proposal Title: NITRIC OXIDE EFFECTS ON PLATELET ADHESION

Principal Investigator(s): Randy Lewis, Anand Ramamurthi

Reviewed and Processed as: Expedited

Approval Status Recommended by Reviewer(s): Approved

ALL APPROVALS MAY BE SUBJECT TO REVIEW BY FULL INSTITUTIONAL REVIEW BOARD AT NEXT MEETING, AS WELL AS ARE SUBJECT TO MONITORING AT ANY TIME DURING THE APPROVAL PERIOD.  
APPROVAL STATUS PERIOD VALID FOR DATA COLLECTION FOR A ONE CALENDAR YEAR PERIOD AFTER WHICH A CONTINUATION OR RENEWAL REQUEST IS REQUIRED TO BE SUBMITTED FOR BOARD APPROVAL.  
ANY MODIFICATIONS TO APPROVED PROJECT MUST ALSO BE SUBMITTED FOR APPROVAL.

---

Comments, Modifications/Conditions for Approval or Disapproval are as follows:

Signature:

  
\_\_\_\_\_  
Chair of Institutional Review Board

Date: April 30, 1997

cc: Anand Ramamurthi

✓  
VITA

Anand Ramamurthi

Candidate for the Degree of

Doctor of Philosophy

Thesis: NITRIC OXIDE INHIBITION OF PLATELET DEPOSITION ON  
BIOMATERIALS

Major field: Chemical Engineering

Biographical:

Personal Data: Born in Bombay, India, On January 6, 1972, the son of Meenakshi and V.Ramamurthi.

Education: Graduated from Vidya Mandir, Madras, June 1990; received Bachelor of Engineering (Hons.) degree in Chemical Engineering from Bangalore University, Bangalore, India, and a completed Master of Science degree in Chemical Engineering at Oklahoma State University in August 1994 and December 1996, respectively. Completed the requirements for the Doctor of Philosophy degree with a major in Chemical Engineering at Oklahoma State University in July 1999.

Experience: Summer Intern, NitroMed, Inc., Bedford, MA, from May to August 1998. Intern at ICI (India) Ltd., Madras India, from December 1992 to February 1993. Graduate Research Assistant, Department of Chemical Engineering, Oklahoma State University, May 1995 to August 1995 and May 1996 to August 1996. Teaching Assistant, Department of Chemical Engineering, Oklahoma State University, August 1995 to May 1996.

Professional Memberships: American Institute of Chemical Engineers, Tau Beta Pi Engineering Honor Society.